ICLLT 2021

2nd International Conference on Light and Light-Based Technologies

26 – 28 MAY

Ankara, Turkey

Abstract and Proceeding Book

ABSTRACT AND PROCEEDING BOOK

2nd International Conference on Light and Light-Based Technologies (2nd ICLLT 2021)

26th-28th May, 2021, Gazi University, Ankara, Turkey

Edited by

Prof. Dr. Süleyman ÖZÇELİK

Second Published, August 04, 2021

ISBN: 978-975-507-294-4

This book is available on the ICLLT website: *http://icllt-2.gazi.edu.tr*

ORGANISERS

- Photonics Application & Research Center (Gazi Photonics), Gazi University
- Photonics Department of Applied Science Faculty, Gazi University

Welcome to the 2nd ICLLT-2021

Dear Distinguished Participants and Colleagues

"International Day of Light" has been declared on 16 May at UNESCO 39th General Conference held in Paris between 30 October and 14 November 2017. UNESCO aims with this precious day to raise awareness of people in all United Nations countries in light and light-based technologies. The goal of sharing knowledge and increasing cooperation from R&D studies on photonics, nanotechnology, microtechnology and semiconductor technology of Gazi University Photonics Application and Research Center is in line with UNESCO's goal of creating Light Science awareness. With this aim, "2nd International Conference on Light and Light-based Technologies (2nd ICLLT-2021)" was held at the Gazi University (Ankara, Turkey), from 26 to 28 May 2021 as virtually due to Covid-19 pandemic. The ICLLT will be held annually from 2021.

The 2nd ICLLT-2021 conference targets guests from various branches and disciplines related to Optics and Photonics Technologies**.** Its interdisciplinary approach is the key to maximizing the potential and development of light-based technologies and tools for various applications. The purpose of the conference is to explore new ideas, effective solutions and collaborative partnerships for business growth by catalyzing the creation of a beneficial synergy between researchers, engineers, manufacturers, suppliers, and end-users of all sectors and making full use of this potential. At this event, the world's leading scientists in Optical and Photonic technologies discussed the latest developments in related technologies. 100 oral presentations were made, including 10 keynote speakers, 31 invited speakers and 59 oral presentations from 26 different countries. While 61 of the presented papers were presented by researchers from abroad, 39 papers were presented by researchers from Turkey. The event was held with 254 registered participants.

On behalf of the organizing committee, we would like to thank all participated academics, research institutions and organizations and especially young students from around the world for exchange of ideas and experiences at ICLLT-2021.

We are honored to invite you to the 3rd ICLLT conference will be held face to face and virtual in May 2022!

Prof. Dr. Süleyman ÖZÇELİK
Conference Chair

COMMITTEES

Organizing Committee

Prof. Süleyman Özçelik, *Gazi Univ., Turkey*
Assoc. Prof. Nihan Akın Sönmez, *Gazi Univ., Turkey*
Assoc. Prof. Yashar Azizian Kalandaragh, *Gazi Univ., Turkey*
Dr. Buse Cömert Sertel, *Gazi Univ., Turkey*
Dr. Meltem Dönmez Kaya, *Gazi Univ., Turkey*
Gökhan Gözlekçi, *Gazi Univ., Turkey*

Scientific Committee

Prof. Şemsettin Altındal, *Gazi Univ., Turkey*
Prof. Aytunç Ateş, *Yıldırım Beyazit Univ., Turkey*
Prof. Bülent Çakmak, *Erzurum Technical Univ., Turkey*
Prof. Sezai Elagöz, *Vice President of R&D at ASELSAN, Turkey*
Prof. Andrew Forbes, *Witsatersrand Univ, South Africa*
Prof. Leonid Golovan, *Moscow State Univ., Russia*
Prof. Valery Gremenok, *National Academy of Science of Belarus*
Prof. Rasim Jabbarov, *Azerbaijan National Academy of Sciences, Azerbaijan*
Prof. Victor Kotlyar, *Samara Univ., Russia*
Prof. Oliver Martin, *EPFL, Lausanne, Switzerland*
Prof. Mohammed Missous, *University of Manchester, UK*
Prof. Nahida Musayeva, *Azerbaijan National Academy of Sciences, Azerbaijan*
Prof. Sermin Onaygil, *İstanbul Tecnicak Univ., Turkey*
Prof. Ekmel Özbay, *Bilkent Univ., Turkey*
Prof. Süleyman Özçelik, *Gazi Univ., Turkey*
Prof. Raşit Turan, *Middle East Technical Univ., Turkey*
Prof. Canan Varlıklı, *İzmir Institute of Technology, Turkey*
Prof. Jian Wang, *Huazhong University of Science and Technology, China*
Prof. Halime Gül Yağlıoğlu, *Ankara Univ., Turkey*
Prof. Fahrettin Yakuphanoğlu, *Elazığ Fırat Univ., Turkey*
Prof. Ellen Petrovna Zaretskaya, *Belarus Bilimler Akademisi, Belarus*
Assoc. Prof. Yashar Azizian Kalandaragh, *Gazi Univ., Turkey*
Assoc. Prof. Barış Kınacı, *İstanbul Univ., Turkey*
Assoc. Prof. Viktor Kisel, *Belarusian National Technical University, Belarus*
Assoc. Prof. Nihan Akın Sönmez, *Gazi Univ., Turkey*
Dr. Raul Arenal, *University of Zaragoza, Spain*
Dr. Matteo Bosi, *IMEM-The National Research Council (CNR), Italy*
Dr. Benedetta Marmiroli, *Graz University of Technology, Austria*

PARTNERS & SPONSORS

The Best Presentation Awards for top three presenter were supported by Optical Society of America (OSA) and ASENTEK Company.

PROGRAM

Wednesday 26th May

09:00 – 09:30	**Opening Ceremony** (Zoom webinar and Youtube-Stream) Prof. Süleyman Özçelik *Chair of Photonics Department, Faculty of Applied Sciences, Gazi University, Ankara, Turkey* *Director of Photonics Application and Research Center, Gazi University, Ankara, Turkey* Prof. M. Öcal Oğuz *President of Turkish National Commission for UNESCO* Prof. Musa Yıldız *Rector of Gazi University, Ankara, Turkey*
Session I	**Chair:** Assoc. Prof. Yashar Azizian-Kalandaragh *Department of Photonics, Faculty of Applied Sciences, Gazi University, Ankara, Turkey*
09:30 – 10:20	Plenary Speaker / Prof. Andrew Forbes *School of Physics, University of the Witwatersrand, Johannesburg, South Africa* **Structured light: from fundamentals to applications**
10:20 – 10:50	Invited Speaker / Prof. Costas Balas *Department of Electrical and Computer Engineering, Technical University of Crete, Chania, Greece* **Transforming hyperspectral imaging into artificial spectral vision for advancing the diagnostic power of medical endoscopy and clinical/surgical microscopy**
10:50 – 11:20	Invited Speaker / Prof. Yu-Faye Chao *Retired Honorary Professor, Department of Photonics, National Chiao Tung University, Taiwan* **Zeros in polarimetry and ellipsometry**
11:20 – 11:30	**Coffee Break**
Session II	**HALL I** **Chair:** Prof. Şemsettin Altındal *Department of Physics, Gazi University, Ankara, Turkey*
11:30 – 11:45	Speaker / Prof. Rasim Mamedov *Department of Physics, Baku State University, Baku, Azerbaijan* **Photoeffect in Schottky diodes with an additional electric field**
11:45 – 12:00	**Dimension dependence of the I-V characteristic of illuminated Au-nGaAs Schottky diodes with an additional electric field**
12:00 – 12:15	Speaker / Dr. Yosef Badali *Department of Electrical and Electronics Engineering, Antalya Bilim University, Antalya, Turkey* **Electrical characteristics and photoconduction behaviour of the Au/Er_2O_3-PVC/n-Si structure**
12:15 – 12:30	Speaker / Dr. Mehmet Fidan *Department of Physics, İYTE, İzmir, Turkey* **Junction area dependent performance of graphene/n-Si based near-infrared Schottky photodetectors**
12:30 – 12:45	Speaker / Dr. Esra Erbilen Tanrıkulu *Department of Physics, Gazi University, Ankara, Turkey* **Investigation on the negative capacitance of the Au/ZnO/n-GaAs structures for 1 MHz at room temperature**
12:45 – 13:00	Speaker / Murat Ulusoy *Department of Physics, Gazi University, Ankara, Turkey* **Illumination effects on the capacitance/conductance-voltage characteristics of Au/(PVC:Er_2O_3)/n-Si (MPS) type structure for 0.5 MHz at room temperature**

13:00 – 13:15	Speaker / Philipp Aldo Wieser *Institute of Inorganic Chemistry, Graz University of Technology, Graz, Austria* **In operando Synchrotron GISAXS studies of nanostructured Pt films show preferential alignment during templated electrodeposition**
Session II	**HALL II** **Chair:** Prof. Canan Varlıklı *Department of Photonics, İYTE, İzmir, Turkey*
11:30 – 11:45	Speaker / Prof. Nikolai Staskov *A.A. Kuleshov Mogilev State University,, Mogilev, Republic of Belarus* **Incoherent spectrophotometry of soda-lime glass (SLG) substrates**
11:45 – 12:00	Speaker / Dr. Neslihan Akçay *Faculty of Engineering, Department of Mechanical Engineering, Baskent University, Ankara, Turkey* **Structural and optical characterization of Cu_2SnS_3 thin films prepared by sulfurization of sputtered Cu/Sn/Cu stack layers**
12:00 – 12:15	Speaker / Dr. Hasan Kurt *School of Engineering and Natural Sciences, Istanbul Medipol University, İstanbul, Turkey* **Plasmonic light management in PBDB-T:ITIC-M inverted organic photovoltaics**
12:15 – 12:30	Speaker / Giovanni Pica *Department of Physical Chemistry, University of Pavia, Pavia, Italy* **Accelerated Thermal Aging Effects on carbon-based perovskite solar cells: A joint experimental and theoretical analysis**
12:30 – 12:45	Speaker / Sumea Klokic *Institute of Inorganic Chemistry, Graz University of Technology, Graz, Austria* **Revealing the photo-triggered structural dynamics of photo-responsive MOFs grown on oriented ceramic thin films**
12:45 – 13:00	Speaker / Aytaç Onur *Department of Electrical and Electronics Engineering, Erciyes University, Kayseri, Turkey* **Effects of dielectric spacer on absorbance characteristics of a dual-band large-H shaped perfect absorber**
13:00 – 13:15	Speaker / Esra Koç *Electrical and Electronics Engineering, TOBB University of Economics and Technology, Ankara* **Optical system design in LED Lighting Luminaires**
13:15 – 14:00	**Lunch Break**
Session III	**Chair:** Prof. Mehmet Çakmak *Department of Photonics, Faculty of Applied Sciences, Gazi University, Ankara, Turkey*
14:00 – 14:50	Plenary Speaker / Prof. Ekmel Özbay *Department of Electrical and Electronics Engineering, İhsan Doğramacı Bilkent University, Ankara, Turkey* **Centimeter scale nanostructures: Lithograpgy-free metamaterials for photoconversion, photodetection, light emission, sensing, and filtering**
14:50 – 15:20	Invited Speaker / Prof. Martin Booth *Department of Engineering Science, University of Oxford, UK* **Three-dimensional super-resolution microscopy deeper in specimens using adaptive optics**
15:20 – 15:50	Invited Speaker / Dr. Christos Tserkezis *Center of Nano Optics, University of Southern Denmark, Denmark* **Quantum-informed plasmonics for extreme light-matter interaction**
15:50 – 16:20	Invited Speaker / Prof. Canan Varlıklı *Department of Photonics, İYTE, İzmir, Turkey* **White light generation from perylenediimide derivatives: frequency down-conversion and electroluminescence**
16:20 – 16:30	**Coffee Break**

Session IV	**Chair:** Prof. Sezai Elagöz *ASELSAN Vice President R&D Management, Turkey*
16:30 – 17:30	Plenary Speaker / Prof. Manijeh Razeghi *Director, Center for Quantum Devices, Department of Electrical and Computer Engineering, Northwestern University, USA* **Light and light-based technology**
17:30 – 18:00	Invited Speaker / Dr. Bhavin J. Shastri *Department of Physics, Engineering Physics and Astronomy, Queen's University, Canada* **Silicon photonics for machine learning and neuromorphic computing**
18:00 – 18:30	Invited Speaker / Prof. Leonid Golovan *Department of Physics, Moscow State University, Moscow, Russia* **Third-harmonic generation in silicon nanowire arrays: Effect of light scattering and nanowire orientation**
18:30 – 18:45	Speaker / Prof. Nahida Musayeva *Institute of Physics, Azerbaijan National Academy of Sciences, Azerbaijan* **Development of sensors based on functionalized carbon nanotubes**
18:45 – 19:00	**Coffee Break**
Session V	**Chair:** Assoc. Prof. İlkay Demir *Department of Nanotechnology Engineering, Sivas Cumhuriyet University, Sivas, Turkey*
19:00 – 19:30	Invited Speaker / Prof. Sabino Chavez-Cerda *Department of Optics, Instituto Nacional De Astrofisica Optica y Electronica, Mexico* **In pursue of understanding the physical nature of scalar structured beam**
19:30 – 20:00	Invited Speaker / Dr. Ana Predojevic *Department of Physics, Stockholm University, Sweden* **Entanglement generation in semiconductor nanostructures**
20:00 – 20:30	Invited Speaker / Prof. Sezai Elagöz *ASELSAN Vice President R&D Management, Turkey* **Optics Touches to our lives**
20:30 – 21:00	Invited Speaker / Prof. Deepa Venkitesh *Department of Electrical Engineering, Indian Institute of Technology Madras, India* **Phase manipulation with semiconductor optical amplifiers**
21:00 – 21:15	Speaker / Hakan Bozkurt *Department of Photonics, İYTE, İzmir, Turkey* **Design and fabrication of passive matrix quantum dot red-light emitting diode via spin coating or ink-jet printing technique**

Thursday 27th May

Session I	**Chair:** Assoc. Prof. Alpan Bek *Department of Physics, METU, Ankara, Turkey*
09:00 – 09:50	Plenary Speaker / Prof. Victor Kotlyar *Department of Technical Cybernetics, Samara University, Russia* **Topological charge of a superposition of optical vortices**
09:50 – 10:20	Invited Speaker / Prof. Hümeyra Çağlayan *Faculty of Engineering and Natural Sciences, Tempere University, Finland* **Light-matter interaction control with multilayer epsilon-near-zero metamaterials**
10:20 – 10:50	Invited Speaker / Dr. Matteo Degani *Department of Physical Chemistry, University of Pavia, Pavia, Italy* **Efficient inverted perovskite solar cells by dual interfacial modification**
10:50 – 11:00	**Coffee Break**
Session II	**Chair:** Prof. Hasan Efeoğlu *Department of Electronic, Ataturk University, Erzurum, Turkey*
11:00 – 11:50	Plenary Speaker / Prof. Mohamed Missous *Semiconductor Materials and Devices at the University of Manchester, UK* **Challenges in vertical cavity surface emitting lasers (VCSEL) manufacturing for quantum applications**
11:50 – 12:20	Invited Speaker / Dr. Beatriz Olmos Sanchez *Institute for Theoretical Physics, University of Tübingen, Germany* **Collective coupling of an array of atoms near a nanofiber**
12:20 – 12:50	Invited Speaker / Prof. Alexander Vladimirovich Volyar *Head of the General Physics Department in the Crimean Federal University named after V.I. Vernadsky, Ukraine* **Geometry of structured and spiral beams: structural stability and energy flows**
12:50 – 13:05	Speaker / Assoc. Prof. Alpan Bek *Department of Physics, METU, Ankara, Turkey* **Pulsed infrared laser crystallized silicon and germanium thin-films**
13.05 – 13:20	Speaker / Dr. Erkan Aksoy *Department of Photonics, İYTE, İzmir, Turkey* **Perylene Based Efficient TADF Downconversion WOLEDs**
13:20 – 14:00	**Lunch Break**
Session III	**Chair:** Prof. Andrew Forbes *School of Physics, University of the Witwatersrand, Johannesburg, South Africa*
14:00 – 14:50	Plenary Speaker / Prof. Miguel A. Alonso *Aix Marseille Univ., Centrale Marseille, Institute Fresnel, University of Rochester, USA* **The poincaré sphere, its generalizations, and their several applications in optics**
14:50 – 15:20	Invited Speaker / Prof. Frank Koppens *Group Leader, Quantum Nano-Optoelectronics group, ICFO, Spain* **Broadband image sensors based on 2D materials, integrated with silicon technology**
15:20 – 15:50	Invited Speaker / Dr. Benedetta Marmiroli *Institute of Inorganic Chemistry, Graz University of Technology, Graz, Austria* **Interdisciplinary research by combining small angle X-ray scattering and deep X-ray lithography**
15:50 – 16:20	Invited Speaker / Prof. Fahrettin Yakuphanoğlu *Physics Department, Elazığ Fırat University, Elazığ, Turkey* **Integrating nanostructured electrodes in photoresponse devices for enhancing UV-VIS-IR photoresponse**

16:20 – 16:30	**Coffee Break**
Session IV	**Chair:** Prof. Fahrettin Yakuphanoğlu *Physics Department, Elazığ Fırat University, Elazığ, Turkey*
16:30 – 17:30	Plenary Speaker / Prof. Olivier Martin *Nanophotonics and Metrology Laboratory, EPFL, Lausanne, Switzerland* **Controlling light with plasmonic and hybrid metasurfaces**
17:30 – 18:00	Invited Speaker / Assoc. Prof. Nejeh Hamdaoui *Institute of Computer Sciences and Communication Techniques, Sousse University, Tunisia* **New concept in ultraviolet photodetectors**
18:00 – 18:30	Invited Speaker / Assoc. Prof. Raul Arenal *The Institute of Nanoscience of Aragon, University of Zaragoza, Spain* **Optoelectronic properties of low-dimensional materials investigated by TEM-EELS**
18:30 – 18:45	Speaker / Assoc. Prof. Mehdi Mahmudov *Department of Physics, Baku State University, Baku, Azerbaijan* **Interband and intraband scattering of conduction electrons by phonons in superlattices in a strong magnetic field**
18:45 – 19:00	**Coffee Break**
Session V	**Chair:** Prof. Halit Altuntaş *Department of Physics, Çankırı Karatekin University, Çankırı, Turkey*
19:00 – 19:30	Invited Speaker / Prof. Halime Gül Yağlıoğlu *Physics Eng. Department, Ankara University, Ankara, Turkey* **Ultrafast dynamics in solutions and thin films**
19:30 – 20:00	Invited Speaker / Dr. Hadiseh Alaeian *Assistant Professor of ECE and Physics and Astronomy, Purdue University, USA* **Dipolar interaction in low-dimensional atom-photonics platforms**
20:00 – 20:30	Invited Speaker / Prof. Raşit Turan *Department of Physics, METU, Ankara, Turkey* **Light management strategies for high efficiency Si solar cells**
20:30 – 21:00	Invited Speaker / Prof. Mustafa Muradov Bayram *Nano Research Center, Baku, Azerbaijan* **Some features of the growth and optical properties of nanomaterials**
21:00 – 21:15	Speaker / Assoc. Prof. Merdan Amirov *Faculty of Physics, Baku State University, Baku, Azerbaijan* **Effect of refractive inhomogeneity on the efficiency of SHG in optical fiber**
21:15 – 21:30	Speaker / Assoc. Prof. Evren Mutlugün *Department of Electrical-Electronics Engineering, Abdullah Gül University, Kayseri, Turkey* **0D and 2D Nanocrystals for efficient electroluminescent devices**

Friday 28th May

Session I	**Chair:** Prof. Ali Teke *Department of Physics, Balıkesir University, Balıkesir, Turkey*
09:00 – 09:50	Plenary Speaker / Prof. Jian Wang *Wuhan National Laboratory for Optoelectronics, Huazhong University of Science and Technology, China* **Multi-dimensional entanglement transport in conventional single-mode fiber**
09:50 – 10:20	Invited Speaker / Assoc. Prof. Alexander Fuerbach *Department of Physics and Astronomy, Macquarie University, Australia* **Ultra-compact actively Q-switched waveguide lasers based on liquid crystal modulators**
10:20 – 10:50	Invited Speaker / Prof. Warwick Bowen *Australian Institute for Bioengineering and Nanotechnology, The University of Queensland, Australia* **Absolute quantum advantage in biological imaging**
10:50 – 11:00	**Coffee Break**
Session II	**Chair:** Prof. Ramazan Koç *Optic and Acoustical Engineering Gaziantep University, Gaziantep, Turkey*
11:00 – 11:50	Plenary Speaker / Prof. Sile Nic Chormaic *Light-Matter Interactions for Quantum Technologies Unit, Okinawa Institute of Science and Technology (OIST) Graduate University, Japan* **Ultrathin optical fibers and whispering gallery resonators - basics, particle trapping, and beyond**
11:50 – 12:20	Invited Speaker / Dr. Matteo Bosi *IMEM-The National Research Council (CNR), Italy* **UV-C solar blind photoresistors based on e-Ga_2O_3 polymorph**
12:20 – 12:50	Invited Speaker / Prof. Prasanta K. Panigrahi *Department of Physical Sciences, Indian Institute of Science Education and Research Kolkata, India* **Photon added cat state: phase space structure and statistics**
12:50 – 13:05	Speaker / Prof. Rasim Jabbarov *Institute of Physics, Azerbaijan National Academy of Sciences, Baku, Azerbaijan* **Factors affecting the efficiency of the LED**
13:05 – 13:20	Speaker / Dr. Özgür Selimoğlu *Department of Energy Engineering, Faculty of Engineering, Ankara University, Ankara, Turkey* **Design and analysis of 3x continuous zoom SWIR Lens**
13:20 – 14:00	**Lunch Break**
Session III	**HALL I** **Chair:** Prof. Halime Gül Yağlıoğlu *Physics Eng. Department, Ankara University, Ankara, Turkey*
14:00 – 14:15	Speaker / Dr. Nezaket Kerimli *Faculty of Physics, Baku State University, Baku, Azerbaijan* **The action of losses at three-wave mixing in metamaterials**
14:15 – 14:30	Speaker / Hakan Yergin *Department of Electrical and Electronics Eng., TOBB University of Economics and Technology, Ankara, Turkey* **Simulation of a semiconductor laser using AWR design environment**
14:30 – 14:45	Speaker / Fariba Lotfi *Faculty of Physics, Tabriz University, Tabriz, Iran* **A tunable plasmonic sensor-based metamaterial and graphene with high sensitivity**

14:45 – 15:00	Speaker / Serhat Çakır *Middle East Technical University, Physics Department, Ankara, Turkey* **Numerical modeling of plasma antennas, application areas, investigation of the effect of nano - phase materials on plasma antenna**
15:00 – 15:15	Speaker / Ali Khodayari *Department of Chemistry, Faculty of Science, University of Guilan, Iran* **Ag/AgBr/MIL-53(Al) plasmonic nanocomposite as an enhanced visible light photocatalyst for decomposition of RhB dye**
15:15 – 15:30	Speaker / Alpaslan Bayrakdar *Vocational School of Higher Education for Healthcare Services, Iğdır University, Iğdır, Turkey* **Investigation of structural and electronic properties of Bromineazocalix [4] arene Molecule using DFT Method**
15:30 – 15:45	Speaker / Cenk Ceylan *GÖKTÜRK Bilgi Teknolojiler Ltd. 5G RF Laboratory and ASIC R&D Center, İstanbul, Turkey* **The VCSEL solid state laser, its photonic MEMS and their several applications in 3D ToF Lidar**
15:45 – 16:00	Speaker / Atta ur Rehman Sherwani *Department of Physics, Istanbul University, Istanbul, Turkey* **Optical sense of anticancer drug doxorubicin (DOX) on PANI nanostructures**
16:00 – 16:15	Speaker / Sima Alilou *Faculty of Physics, University of Tabriz, Tabriz, Iran* **FDTD simulation of propagation of hermite - cosh gaussian high intensity laser beam in inhomogeneous plasma and modeling of ponderomotive force and magnetic field**
Session III	**HALL II** **Chair:** Prof. Musa Mutlu Can *Department of Physics, İstanbul University, İstanbul, Turkey*
14:00 – 14:15	Speaker / Dr. Yana Akimova *Physics Department in the Crimean Federal University named after V.I. Vernadsky, Ukraine* **Intensity moments technique as a simple and reliable tool for measuring 3D vortex spectra of structured beams**
14:15 – 14:30	Speaker / Dr. Angela Dudley *School of Physics, University of the Witwatersrand, South Africa* **Reconstructing polarisation with a digital micro-mirror device**
14:30 – 14:45	Speaker / Dr. Wagner Tavares Buono *School of Physics, University of the Witwatersrand, Johannesburg, South Africa* **Accelerated polarization structures with bessel beams**
14:45 – 15:00	Speaker / Chane Simone Moodley *School of Physics, University of the Witwatersrand, South Africa* **Approaching real-time non-degenerate ghost imaging by deep learning**
15:00 – 15:15	Speaker / Bereneice Sephton *Physics Department, University of the Witwatersrand, South Africa* **Exploiting up-conversion for spatial mode detection**
15:15 – 15:30	Speaker / Fatemeh Nourani *Department of Physics, University of Mohaghegh Ardabili, Ardabil, Iran* **Investigation of the effects of vortex beam propagation through a medium including nanostructures**
15:30 – 15:45	Speaker / Neda Rashidfarrokhian *Department of Photonics, Shahid Bahonar University of Kerman, Kerman, Iran* **Numerical investigation of self-healing characteristic of generalized parabolic beams**
15:45 – 16:00	Speaker / Atefe Emadoleslami *Department of Photonics, Shahid Bahonar University of Kerman, Kerman, Iran* **The investigation of self-healing feature of vortex Hermite-Gaussian beams**

16:00 – 16:15	Speaker / Zohreh Hashemi *Department of Photonics, Shahid Bahonar University of Kerman, Kerman, Iran* **A comparative study on self-healing property of elliptical and circular Airy beam**
16:15 – 16:30	**Coffee Break**
Session IV	**Chair:** Assoc. Prof. Evren Mutlugün *Department of Electrical-Electronics Engineering, Abdullah Gül University, Kayseri, Turkey*
16:30 – 17:30	Plenary Speaker / Prof. Kevin Eliceiri *Medical Physics and Biomedical Engineering, University of Wisconsin-Madison, USA* **Computational optics of the tumor microenvironment**
17:30 – 18:00	Invited Speaker / Prof. Bülent Çakmak *Department of Electrical and Electronic Engineering, Erzurum Technical University, Turkey* **Chalcogenide based two dimensional (2D) structures: New quantum materials**
18:00 – 18:30	Invited Speaker / Dr. Viktor Kisel *Research Centre for Optical Materials and Technologies, Belarusian National Technical University, Belarus* **Ultrafast solid-state lasers**
18:30 – 19:00	Invited Speaker / Dr. Alka Swanson *Kelvin Nanotechnology, Glasgow, UK* **Kelvin Nanotechnology Ltd: Provider of nanofabrication services for over two decades**
19:00 – 19:15	**Coffee Break**
Session V	**HALL I** **Chair:** Prof. Mustafa Sarısaman *Department of Physics, İstanbul University, İstanbul, Turkey*
19:15 – 19:30	Speaker / Dr. Atilla Eren Mamuk *Department of Physics, Muğla Sıtkı Koçman University, Muğla, Turkey* **Determination of the presence and molecular orientation of the liquid crystal in the core - sheath structure of the electrospun fiber by optical method**
19:30 – 19:45	Speaker / Lala Gahramanli *Nano Research Center Baku State Unversity, Baku, Azerbaijan* **Influence of various technological factors on the optical properties of $Cd_xZn_{1-x}S$ nanoparticles**
19:45 – 20:00	Speaker / Sevinj Mammadyarova *Department of Physics, Baku State University, Baku, Azerbaijan* **The effect of magnetic field on structural and optical properties of Ni/NiO nanochains**
20:00 – 20:15	Speaker / Mudathir F. O. Yahya *Department of Physics, Bursa Uludağ University, Bursa, Turkey* **Influence of Electron Incidence Angle on Position Resolution in Crystal Calorimeters**
20:15 – 20:30	Speaker / Huriye Gencal *Electrical-Electronics Engineering, Bursa Technical University, Bursa, Turkey* **A new approach to enhance the bandwidth value of UTC-PD**
20:30 – 20:45	Speaker / Şamil Şirin *Department of Electrical and Electronics Engineering, İYTE, Izmir, Turkey* **Distributed current sensing via optical reflectometry**
20:45 – 21:00	Speaker / Ertunga Burak Koçal *Department of Electrical and Electronics Engineering, İYTE, Izmir, Turkey* **Simulation tool development for FBG-Aided Φ-OTDR vibration sensors**
21:00 – 21:15	Speaker / Yusuf Mert Gümüşay *Department of Advanced Technologies, Gazi University, Ankara, Turkey* **Development of IR optical chopper disk by thermally evaporated ZnS thin films**

21:00 – 21:15	Speaker / Ofeliya Balayeva *Nano Research Center, Baku State University, Baku, Azerbaijan* **Controllable synthesis of $Ni_xZn_{1-x}S$ nanoparticles on the base of NiZnAl Layered Double Hydroxide/PVA composite matrix**
Session V	**HALL II** **Chair:** Assoc. Prof. Nihan Akın Sönmez *Department of Photonics, Gazi University, Ankara, Turkey*
19:15 – 19:30	Speaker / Hafize Seda Aydınoğlu *Department of Medical Services and Techniques, Program of Opticianry, Vocational School of Healthcare, Sivas Cumhuriyet University, Sivas, Turkey* **Structural and morpholojical characterization of Nitrogen doped ZnO thin films**
19:30 – 19:45	**Structural and electrical properties of p-type NiO thin films produced by thermal evaporation on different substrates**
19:45 – 20:00	Speaker / Hüda Akkaya Kömürcü *Department of Physics, Gazi University, Ankara, Turkey* **Sol-gel Spin Coated Nb_2O_5 Thin Films with Different Thicknesses**
20:00 – 20:15	Speaker / Gökhan Gözlekçi *Department of Advanced Technologies, Gazi University, Ankara, Turkey* **Investigation of quantum confinement effect in ultrathin TiO_2 films**
20:15 – 20:30	Speaker / Hicret Hopoğlu *Faculty of Technology, Department of Optical Engineering, Sivas Cumhuriyet University, Sivas, Turkey* **Optical Properties of Nitrogen doped ZnO thin films grown on n-Si and glass substrate**
20:30 – 20:45	**Thickness dependence of structural and optical properties of nitrogen doped ZnO thin films on glass**
20:45 – 21:00	Speaker / Esra Balcı *Department of Physics, Ankara Hacı Bayram Veli University, Ankara, Turkey* **Synthesis and optical characterization of $Gd_3Ga_{5-x}Al_xO_{12}$:Nd,Cr persistent phosphors**
21:00 – 21:15	Speaker / Berkcan Erenler *Department of Metallurgy and Materials Engineering, Gazi University, Ankara, Turkey* **Structural and optical properties of SnS thin films deposited with sputtering method**
21:15 – 21:30	Speaker / Nadezhda Lubochko *Scientific and Practical Materials Research Center NAS Belarus, Minsk, Belarus* **Tm^{3+}:$KY(WO_4)_2$ single crystals prepared by the modified Czochralski method: growth and optical properties**
21:30 – 21:45	**Closing Ceremony and Best Presentation Awards** (Zoom webinar and Youtube-Stream)

TABLE OF CONTENTS

PLENARY SPEAKERS

PS1

Structured light: from fundamentals to applications

Andrew Forbes

School of Physics, University of the Witwatersrand, Johannesburg, South Africa
andrew.forbes@wits.ac.za

Structured light is a term used to describe optical fields that have been tailored in their spatial intensity, phase and polarisation distributions, and may even be extended to include tailored light in the time and frequency domain too. Structured light has found many applications, including optical manipulation in biological systems, laser materials processing for better resolution, quality and efficacy, seeing smaller objects in microscopy, and new approaches to designing lasers, to name a few, spanning both fundamental science and applications alike. In this Plenary, I will explore how to create and manipulate exotically structured light fields with a modern optics toolkit, and cover some example applications in classical, laser and quantum optics. It will be a tutorial style talk that covers the basics of the field while highlighting the benefits that such control could bring to the user.

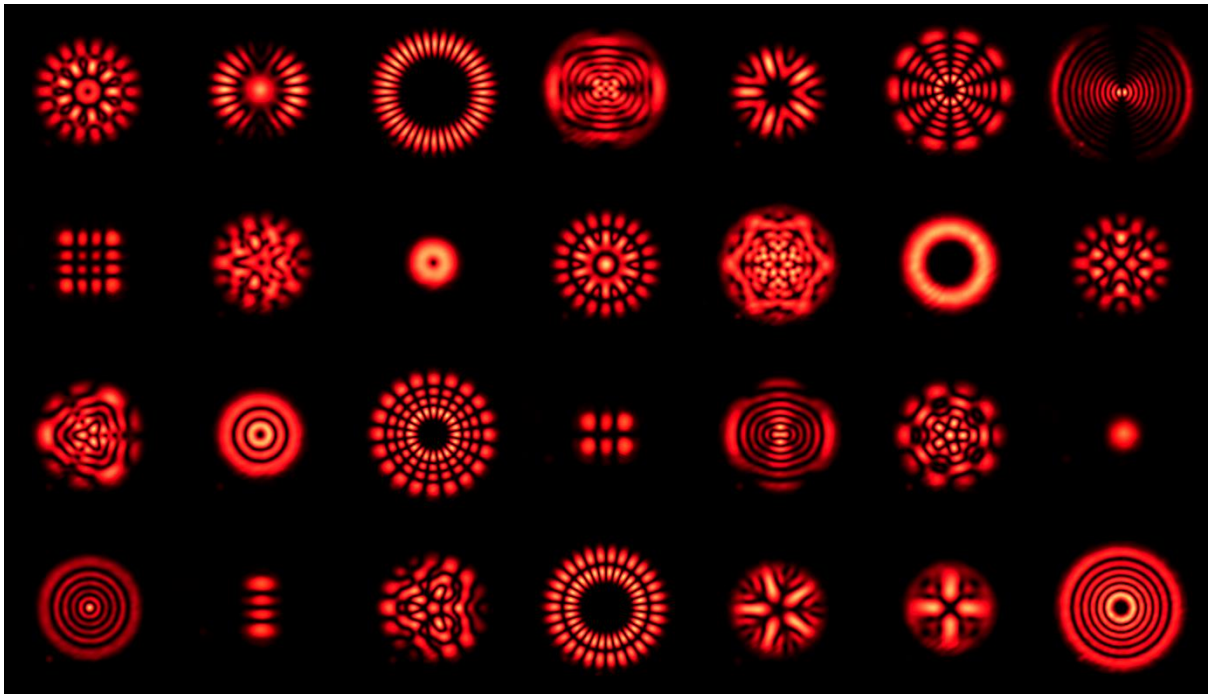

PS2

Centimeter scale nanostructures: Lithograpgy-free metamaterials for photoconversion, photodetection, light emission, sensing, and filtering

Ekmel Ozbay

NANOTAM-Nanotechnology Research Center, Bilkent University, 06800 Ankara, Turkey
ozbay@bilkent.edu.tr

The efficient harvesting of electromagnetic (EM) waves by subwavelength nanostructures can result in perfect light absorption in the narrow or broad frequency range. These metamaterial-based perfect light absorbers are of particular interest in many applications. Although advances in nanofabrication have provided the opportunity to observe strong light–matter interaction in various optical nanostructures, the repeatability and upscaling of these nano units have remained a challenge for their use in large scale applications. Thus, in recent years, the concept of lithography-free planar light perfect absorbers has attracted much attention in different parts of the EM spectrum, owing to their ease of fabrication and high functionality. In this presentation, we will explore the material and architecture requirements for the realization of light perfect absorption using these multilayer metamaterial designs from ultraviolet (UV) to far-infrared (FIR) wavelength regimes. We show that, by the use of proper material and design configuration, it is possible to realize these lithography-free light perfect absorbers in every portion of the EM spectrum [1]. This, in turn, opens up the opportunity of the practical application of these perfect absorbers in large scale dimensions. In last couple of years, we adopted these lithography-free techniques in many applications including photoconversion, photodetection, light emission, sensing, filtering and thermal camouflage [2-9]. This presentation will summarize our recent accomplishments in this field.

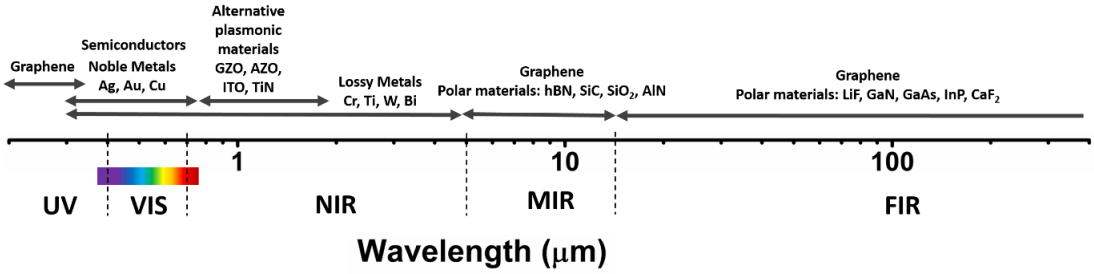

Figure 1. A graph summarizing the proper choice of materials to realize light perfect absorption in different parts of EM spectrum.

References:

[1] A. Ghobadi, H. Hajian, B. Butun, and E. Ozbay, ACS Photonics 5, 4203 (2018).
[2] T.G.U. Ghobadi, A. Ghobadi, M.C. Soydan, M.B. Vishlaghi, S. Kaya, F. Karadas, and E. Ozbay, ChemSusChem 13, 2577 (2020).

[3] A. Ghobadi, Y. Demirag, H. Hajian, A. Toprak, B. Butun, and E. Ozbay, IEEE Electron Device Lett. 40, 1 (2019).
[4] M.C. Soydan, A. Ghobadi, D.U. Yildirim, E.S. Duman, A. Bek, V.B. Erturk, and E. Ozbay, Adv. Opt. Mater. 8, 1 (2020).
[5] D.U. Yildirim, A. Ghobadi, M.C. Soydan, O. Atesal, A. Toprak, M.D. Caliskan, and E. Ozbay, ACS Photonics 6, 1812 (2019).
[6] Z. Eftekhari, A. Ghobadi, M.C. Soydan, D.U. Yildirim, N. Cinel, and E. Ozbay, Opt. Lett. 46, 1664 (2021).
[7] Z. Eftekhari, A. Ghobadi, and E. Ozbay, Opt. Lett. 45, 6719 (2020).
[8] A. Ghobadi, H. Hajian, M. Gokbayrak, B. Butun, and E. Ozbay, Nanophotonics 8, 823 (2019).
[9] M.C. Soydan, A. Ghobadi, D.U. Yildirim, E. Duman, A. Bek, V.B. Erturk, and E. Ozbay, Adv. Opt. Mater. 8, (2020).

PS3

Light and Light-Based Technology

Manijeh Razeghi

Walter P. Murphy Professor, Department of Electrical Engineering and Computer Science
Director, Center for Quantum Devices
Northwestern University, Evanston, IL 60208
razeghi@northwestern.edu

The Discovery of electronics and artificial light 130 years ago revolutionized human Civilization perhaps more than any other discovery before it. Today thanks to semiconductor Quantum Optoelectronic devices light waves flashing along glass fiber or atmosphere is connecting up the global information into ever bigger networks. Could you imagine a world without semiconductor? Your are probably picturing life without your cellphone and computer. If I say light based Semiconductor technology is the main fuel for the modern Society and without it we would go back to stone age! Light is the foundation of the universe!! Nature offers us a full assortment of atoms, but Quantum engineering is required to put them together in an elegant way to realize functional structures not found in nature. A particular rich playground for Quantum era, is the so-called III-V semiconductors, made of atoms from columns III and V of the periodic table, and constituting compounds with many useful optical and electronic properties. Guided by highly accurate simulations of the electronic structure, modern semiconductor quantum devices are literally made atom by atom using advanced growth technology to combine these materials in ways to give them new proprieties that neither material has on its own. Modern mastery of atomic engineering allows high-power and highly efficient functional devices to be made, such as those that convert electrical energy into coherent light or detect light of any wavelength and convert it into an electrical signal. This talk will present the future trends and latest world-class research breakthroughs that have brought semiconductor quantum engineering to an unprecedented level, creating IR light detectors and emitters over an extremely wide spectral range from 0.2 to 300 microns. As well as their integration with Si photonics.

PS4

Topological charge of a superposion of optical vortices

Kotlyar V.V.*[1,2], Kovalev A.A.[1,2]

[1]*Image Processing Systems Institute of RAS – Branch of the FSRC "Crystallography and Photonics" RAS, 151 Molodogvardeyskaya St., Samara 443001, Russia*
[2]*Samara National Research University, 34 Moskovskoye Shosse, Samara 443086, Russia*
kotlyar@ipsiras.ru

While orbital angular momentum (OAM) of paraxial vortex beams has been known to be preserved upon free-space propagation [1], the same cannot so far be said of the topological charge (TC) of optical vortices (OV). All radially symmetric OVs (e.g. Laguerre-Gaussian and Bessel-Gaussian beams), as well as some asymmetric OVs, preserve their TC upon free-space propagation [2]. No general proof of TC conservation has so far been offered, however some publications discussed examples of OVs whose TC was not preserved upon propagation. M. Soskin et al. were the first to demonstrate this effect in 1997 [3]. Their study looked into a simple superposition of a Gaussian beam and a Laguerre-Gaussian (LG) mode (0,n), with the Gaussian beams waists having different radii. With the constituent components of the combined beam diverging differently, TC was shown to change upon free-space propagation. If in the original plane, the Gaussian beam waist was larger than the LG mode waist, at first, TC of the combined beam was zero. Upon propagation, the beams radii were getting closer, with the LG mode radius becoming larger than that of the Gaussian beam after passing through the same-radius plane. From that plane onwards, TC of the combined beam was shown to get equal to *n*.
In this work we show that in the superposition of two different-waist LG beams, TC does not conserve during propagation because phase singularities partly either 'go to' or 'come from' infinity. Interestingly, the phase singularities 'go to and come from' infinity with a higher-than-light speed.

The work was partly funded by the Russian Foundation for Basic Research under RFBR grant # 18-29-20003.

References:

[1] Allen L, Beijersbergen M, Spreeuw R, Woerdman J. Orbital angular momentum of light and the transformation of Laguerre-Gaussian laser modes. Phys. Rev. A 1992; 45: 8185.
[2] Kotlyar VV, Kovalev AA. Topological charge of asymmetric optical vortices. Opt. Express, 2020; 28(14): 20449-60.
[3] Soskin MS, Gorshkov VN, Vastnetsov MV, Malos JT, Heckenberg NR. Topological charge and angular momentum of light beams carring optical vortex. Phys. Rev. A, 1997; 56(5): 4064-4075.

PS5

Challenges in Vertical Cavity Surface emitting lasers (VCSEL) manufacturing for Quantum applications

Mohamed Missous

Department of Electrical and Electronic Engineering,
University of Manchester, Sackville Street Building, Manchester M13 9PL, UK
m.missous@manchester.ac.uk

Vertical Cavity Surface emitting lasers (VCSEL) have become dominant components in a range of applications spanning high-speed data communication, laser printers, mobile communications, 3D sensing (face recognition), LIDAR and industrial manufacturing to name a few. Compared with their edge emitting counterparts, they are relatively easy to manufacture, and above all, are able to be tested on-wafers for wavelength, modes, power and beam shape greatly helping in reducing costs. Their success in all these applications derives largely from the fact that a small shift in wavelengths (few nm) due to wafer non-uniformities does not hinder the intended applications and as consequence higher device yields are readily attainable.

Modern Quantum applications in sensing, timing or magnetometry all use VCSELs as convenient low power components drivers for excitation of certain gases (Cs and Rubidium for example). However, the requirements for single mode frequency, linear polarization and precise output wavelength (to within 0.1nm) at operating temperatures (which can vary from ambient to 80 C) places stringent requirements on VCSEL device design and fabrication/testing yields.

In this talk I will illustrate how full 4” wafer mapping of > 100,000 devices is needed to sort out and bin VCSEL devices according to spectral wavelength, Mode, power. The precise requirements of an exact wavelength, power and mode stability lead to significant drops in VCSEL device yields in common MOCVD grown VCSEL wafers.

PS6

The Poincaré sphere, its generalizations, and their several applications in optics

Miguel A. Alonso

Aix Marseille Univ., Centrale Marseille, Institute Fresnel, France - The Institute of Optics, University of Rochester, USA
alonso@optics.rochester.edu

In this talk, I discuss the concept of the Poincaré sphere and its applications in optics, not only for describing paraxial polarization but also the spatial structure of optical beams, both within the ray and wave models. Also discussed are generalizations of the Poincaré sphere for the case of non-paraxial polarization (where all three field components are important), and their application in a novel technique for fluorescent microscopy.

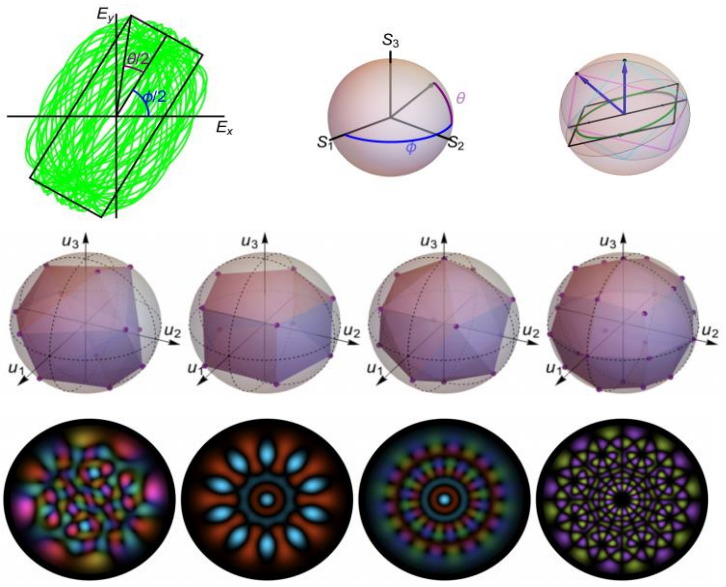

PS7

Controlling light with plasmonic and hybrid metasurfaces

Olivier J.F. Martin

Nanophotonics and Metrology Laboratory, Swiss Federal Institute of Technology Lausanne (EPFL)
www.nanophotonics.ch

After a general introduction to plasmonics, the optics of metal nanostructures, I will describe different technologies used for the fabrication of metal nanostructures with well-controlled features down to about 10 nm. Only a few plasmonic metals, such as gold, silver or aluminum, produce strong optical resonances, thus limiting the spectral range where plasmonics can be used. To extend that range, we recently developed a technology for the fabrication of Au-Ag alloyed nanostructures with well-controlled shapes that can be combined into metasurfaces to produce lenses or holograms. The working principle of these metasurfaces consists in engineering the phase associated with light scattered from metallic nanostructures to mimic the effects of gratings, lenses or phase plates.

While the metal dictates the wavelength range where plasmonic effects can occur, the dimensions and the shape of the nanostructures control the type of optical resonances that can be supported by a given nanostructure assembly. These optical resonances can be divided in essentially two families: electrical and magnetic modes. At optical frequencies, it is believed that electrical resonances

always dominate the response of the system, which has led to some confusion on the so-called magnetism at optical frequencies. I will however demonstrate that it is possible to produce plasmonic systems that radiate purely magnetic light. Finally, I will share some recent results on hybrid nanostructures that combine plasmonic elements with dielectric resonators and show how they can be utilized for sensing.

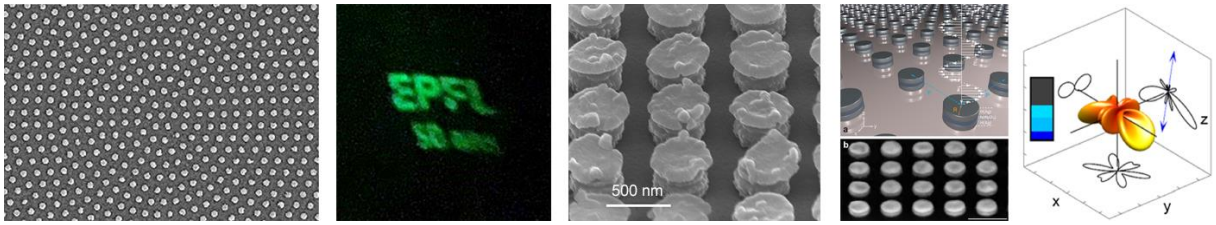

PS8

Multi-dimensional entanglement transport in conventional single-mode fiber

Jian Wang

Wuhan National Laboratory for Optoelectronics and School of Optical and Electronic Information, Huazhong University of Science and Technology, Wuhan 430074, Hubei, China.
jwang@hust.edu.cn

The orbital angular momentum (OAM) that accesses the space domain of photons has attracted increasing interest in many applications ranging from optical communications to quantum information processing. In this talk, we first show our recent works in optical communications employing OAM multiplexing, including basic concepts, key devices and technologies and system-level demonstrations in different application scenarios (free space, fiber, underwater). Then we present our recent research process in quantum information processing with OAM. In particular, we propose and demonstrate the transport of multidimensional entangled states down conventional single-mode fiber (SMF) by exploiting hybrid entangled states. We combine polarization qubits with high-dimensional spatial modes by entangling the spin-orbit degrees of freedom of a biphoton pair, passing the polarization (spin) photon down the SMF while accessing multidimensional OAM subspaces with the other photon in free space. We show high-fidelity hybrid entanglement preservation down 250 m of SMF across 2 two-dimensional subspaces (2 × 2 dimensions) in what we refer to as multidimensional entanglement. We quantify our one-sided channel by means of quantum state tomography, Bell inequality, and quantum eraser experiments. It offers an alternative approach to spatial mode entanglement transport in fiber, with the telling advantage of deployment over legacy optical networks with conventional SMF. After that, we also show a proof-of-concept demonstration on High-dimensional quantum cryptography with hybrid OAM states through 25 km of ring-core fiber. Finally, future challenges and perspectives are discussed.

PS9

Ultrathin optical Fibers and whispering gallery resonators-basics, particle trapping and beyond

Sile Nic Chormaic

Okinawa Institute of Science and Technology (OIST) Graduate University, Japan
sile.nicchormaic@oist.jp

Ultrathin optical fibres, with diameters on the order of the propagating light wavelength, have already proven their versatility across a variety of different areas, such as sensing, particle manipulation, cold atom physics, and as optical couplers for photonic resonators. The intense evanescent field at the fibre waist is one of the main advantages offered by these systems as it allows us to achieve ultrahigh light intensities that may otherwise not be attainable in a standard laboratory. In this talk, I will present work conducted at OIST related to the fields of particle trapping and manipulation where we exploit some of the unique properties of the non-paraxial light fields. For example, we use the evanescent field of ultrathin fibres to study particle trapping and optical binding in 1D arrays. We also use the fibres to couple light into hollow whispering gallery cavities for nanoparticle detection. Overall, the versatility of these fibres for many different experimental platforms will be promoted.

PS10

Computational optics of the collagen rich tumor microenvironment

Kevin Eliceiri

University of Wisconsin-Madison, Madison, Wisconsin, United States
eliceiri@wisc.edu

Collagen forms the structural network of the extracellular matrix (ECM) in biological tissues, and is the most abundant protein in vertebrates. The amount, distribution, and structural organization of fibrillar collagen are all important factors underlying the properties of tissues and play an integral role in many diseases. In cancer, we discovered Tumor Associated Collagen Signatures (TACS), where highly aligned collagen fibers are oriented perpendicular to the tumor boundary, was negatively prognostic in human breast cancer. We and other have found similar changes in other cancer types such as ovarian, prostate, pancreas and others. All these collagen fiber based studies either used specialized imaging approaches, such as specific stains or advanced and costly imaging modalities that are not currently in the clinical workflow. Although pathologists use special staining techniques when fibrosis is of clinical concern, these are not sufficient to fully characterize stromal biomarkers as described in research studies. To facilitate analysis of stromal biomarkers in clinical workflows, it would be ideal to have technical approaches that can characterize fibrillar collagen on standard H&E stained slides produced during routine diagnostic work. In this talk, we present a machine learning- based stromal collagen image synthesis algorithm that can be incorporated into existing H&E- based histopathology workflow. Specifically, this solution applies a convolutional neural network (CNN) directly onto clinically standard H&E bright field images to extract information about collagen fiber arrangement and alignment, without requiring additional specialized imaging stains, systems or equipment. We validated the methods by retrospectively analyzing samples previously used for identifying the negatively prognostic Tumor Associated Collagen Signatures (TACS) biomarker in breast and pancreatic cancers. This proposed solution has great promise to overcome the main technical barriers of transferring collagen image based prognostic stromal biomarkers to clinical practice and research.

INVITED SPEAKERS

IS1

Transforming hyperspectral imaging into artificial spectral vision for advancing the diagnostic power of medical endoscopy and clinical/surgical microscopy

Costas Balas

Department of Electrical and Computer Engineering, Technical University of Crete, 73100 Chania, Greece
QCELL PC 73132 Chania, Greece
balas@electronics.tuc.gr

Hyperspectral imagers can measure the spectral content of light energy at every point in an image. As such, they in principle comprise a unique tool for seeking spectral signatures of tissue lesions, depicting their altered structure and function. State of the art technologies are limited in the sense that they require prolonged scanning times often exciding one minute, which makes them suboptimal solutions for clinical live inspections through endoscopes and microscopes. Our work focuses on developing video rate spectral imagers or, in other words, spectral artificial vision systems. We present our patented “hybrid spectral imaging” technology offering dual, snapshot and scanning, modes of operation. In the snapshot operation mode, the system is autoconfigured to acquire critical spectral bands and to estimate the rest, both comprising a complete spectral cube. This way, the acquired spatial-spectral data set is displayed in video rate and at full sensor’s spatial resolution, making it suitable for live spectral inspections and for monitoring dynamic optical effects associated with the pharmacokinetics of contrast agents. The hybrid spectral imager can be trained to correlate spectral profiles with either chemical or pathology identifies. In these cases, the system outputs chemical or pathology maps respectively in real time, with undisputable analytical and diagnostic value. Results from its clinical applications in developing optical biopsy methods in endoscopy, colposcopy and dermoscopy are presented and discussed.

IS2

Zeros in polarimetry and ellipsometry

Yu-Faye Chao

Department of Photonics, National Chiao Tung University, Taiwan
yfchao@mail.nctu.edu.tw

The deviations of the azimuth angles of polarizer and analyzer are analytically solved. The ellipsometric parameters Ψ and Δ can be measured by three intensity measurements at P =45°; A=0°, 60° and 120°, respectively. Using CCD as detector, we obtain the refractive index of the surface of glass, water, fiber (radial distribution) and plano-convex lens. Because the mechanical rotation and slow imaging process, one can only apply this to measure the surface of a medium which is almost static. For speeding up, one has to remove the rotation and introduce a photoelastic modulator in the ellipsometric system. After aligning the optical axis of the photoelastic modulator, one can measure Ψ and Δ in real time. A plasma etching and the photo-induced process of a PQ-doped PMMA thick plate are used to demonstrate the concept. Furthermore, we introduce a stroboscopic illumination technique to lock four temporal phases by a programmable short pulse laser. The photoelastic modulated imaging ellipsometry was applied to measure a drainage process of oil drop. By two incident angles and post flight analysis technique, one can measure the refractive indices of uniaxial crystals within 20μs. All these achievements come from well aligned azimuth angles and calibrated phase retardation.

IS3

Three-dimensional super-resolution microscopy in thicker specimens using adaptive optics

Martin J. Booth

Department of Engineering Science, University of Oxford, United Kingdom
martin.booth@eng.ox.ac.uk

Adaptive optics (AO) is used to correct aberrations when focussing deep into specimens and is particularly important in super-resolution nanoscopy methods, whose performance is particularly sensitive to aberration effects. Novel AO methods have been developed to deal with the particular challenges posed by super-resolution microscopes. We show how various three-dimensional nanoscopy applications can be facilitated using new approaches to AO. Specifically, this includes whole cell and tissue imaging using a 4Pi single molecule localisation microscope. This uses an optical system with dual opposing objective lenses and two deformable mirrors, which require new approaches to AO control to facilitate correction of specimen aberrations in both paths. We show further results from structured illumination microscopy, with adaptive illumination and aberration correction permit sub-resolution imaging in multiple fluorescence channels. We have also developed methods to combine AO stimulated emission depletion (STED) microscopy with fluorescence correlation spectroscopy (FCS) to provide higher precision measurements inside living cells.

IS4

Quantum-informed plasmonics for extreme light-matter interactions

Christos Tserkezis

Center for Nano Optics, University of Southern Denmark, Campusvej 55, DK-5230 Odense M, Denmark
ct@mci.sdu.dk

Research in plasmonics is rapidly heading towards the quantum regime, allowing one to classify many of the ongoing theoretical and experimental activities under the label of Quantum Plasmonics. By this term, one usually refers to either the necessity to include information related to the microscopic —even atomistic— details of the metallic component in order to accurately describe the optical response of plasmonic nanostructures, or the interaction of plasmonic architectures with quantum emitters [1]. In this talk I will discuss our recent efforts to merge these two directions and describe quantum emitters weakly- or strongly-coupled to plasmonic systems described by some quantum-informed (but otherwise based on macroscopic electrodynamics) model. After a brief introduction to the main approaches employed in current theoretical studies [2,3], I will first focus on the weak-coupling regime, and describe how the fluorescence rates of emitters near plasmonic nanoparticles are modified when quantum corrections are introduced in the description of the metal [4]. Subsequently, I will analyse the corresponding situation in the strong-coupling regime, and explore the impact of electron screening and surface-enabled Landau damping on the width and resolvability of the avoided crossings in plasmon—exciton hybridisation [5, 6]. Finally, I will discuss our very recent work on extending such studies to the time domain, and analyse the emergence of interesting non-Markovian dynamics in the relaxation the emitter [7]. Since this topic is closely related to traditional Quantum Optics, throughout this discussion I will be calling for attention whenever transferring quantum-optical concepts to the nanoscopic world leaves room for misinterpretations [8].

References:

[1] S.I. Bozhevolnyi, L. Martin-Moreno and F. Garcia-Vidal (Eds.), Quantum Plasmonics (Springer, 2017).
[2] M. K. Svendsen et al., J. Phys: Condens. Matter 32, 395702 (2021).
[3] P. A. D. Gonçalves et al., Nature Commun. 11, 366 (2020).
[4] C. Tserkezis et al., Nanoscale 8, 17532 (2016).
[5] C. Tserkezis et al., ACS Photonics 5, 133 (2018).
[6] G. P. Zouros et al., Phys. Rev. B 101, 085416 (2020).
[7] V. Karanikolas et al., arXiv: 2101.10832 (2021).
[8] C. Tserkezis et al., Rep. Prog. Phys. 83, 082401 (2021).

IS5

White Light generation from Perylene derivatives: frequency down-conversion and electroluminescence

Canan Varlıklı

Department of Photonics, İzmir Institute of Technology, Urla, 35430 İzmir, Turkey
cananvarlikli@iyte.edu.tr

Perylene derivatives which have great photo and thermal stabilities, high molar absorptivity constants in the visible region, high fluorescence quantum yields (Φ_{PL}) and n-type semiconductor character, represent one of the most widely studied classes of organic semiconductors [1-3]. These features address them as one of the best organic dye alternatives not only for down conversion of energy produced by the blue LED but also to be utilized as emitter and/or electron transport layers in organic light emitting diodes. However, they suffer from low Φ_{PL} values in their films because of the $\pi\pi$ stacking of planar rings. In this talk, the focus will be given to the three approaches we followed; *i)* deterioration of the ring plane by bulky substituents, *ii)* incorporation of the dye in a host matrix and *iii)* utilizing the dye in low concentrations. Where the second one mostly serves frequency down-conversion, last one helps obtaining electroluminescence and the first one serves both of them.

The content will mainly consist of some results obtained and published within the scope of the postgraduate theses of Erkan Aksoy and Volkan Bozkuş [4-9]. Speaker acknowledges the project support fund of the Scientific Research Council of Turkey (Project Number: 119F031).

References:

[1] He, J.; Yang, S.; Zheng, K.; Zhang, Y.; Song, J.; Qu, J. One-Pot Synthesis of Dispersible Thermally Stable Organic Downconversion Materials under DBU Catalyzation for High Performance Hybrid-LED Lamps. Green Chem. 2018, 20 (15), 3557–3565. https://doi.org/10.1039/c8gc01390j.
[2] Zhang, B.; Soleimaninejad, H.; Jones, D. J.; White, J. M.; Ghiggino, K. P.; Smith, T. a.; Wong, W. W. H. Highly Fluorescent Molecularly Insulated Perylene Diimides: Effect of Concentration on Photophysical Properties. Chem. Mater. 2017, 29 (19), 8395–8403. https://doi.org/10.1021/acs.chemmater.7b02968.
[3] Zhang, B.; Lyskov, I.; Wilson, L. J.; Sabatini, R. P.; Manian, A.; Soleimaninejad, H.; White, J. M.; Smith, T. A.; Lakhwani, G.; Jones, D. J.; et al. FRET-Enhanced Photoluminescence of Perylene Diimides by Combining Molecular Aggregation and Insulation. J. Mater. Chem. C 2020, 8 (26), 8953–8961. https://doi.org/10.1039/d0tc02108c.
[4] Aksoy, E. Organik Fotonik Sistemlerde Kullanilabilecek Perilendiimit Türevlerinin Sentezi ve Fotofiziksel Karakterizasyonu, Ege University, 2020.
[5] Bozkus, V. Emission Characteristics of a Solutıon Processed, Single Layer White Organic Light Emitting Diode, İzmir Institute of Technology, 2020.

[6] Guner, T.; Aksoy, E.; Demir, M. M.; Varlikli, C. Perylene-Embedded Electrospun PS Fibers for White Light Generation. Dye. Pigment. 2019, 160 (August 2018), 501–508. https://doi.org/10.1016/j.dyepig.2018.08.040.
[7] Aksoy, E.; Demir, N.; Varlikli, C. White LED Light Production by Using Dibromoperylene Derivatives in down Conversion of Energy. Can. J. Phys. 2018, 96 (7), 734–739. https://doi.org/https://doi.org/10.1139/cjp-2017-0752.
[8] Aksoy, E.; Danos, A.; Varlikli, C.; Monkman, A. P. Navigating CIE Space for Efficient TADF Downconversion WOLEDs. Dye. Pigment. 2020, 183 (May), 108707. https://doi.org/10.1016/j.dyepig.2020.108707.
[9] Bozkus, V.; Aksoy, E.; Varlikli, C. Perylene Based Solution Processed Single Layer Woled with Adjustable CCT and CRI. Electron. 2021, 10 (6), 1–12. https://doi.org/10.3390/electronics10060725.

IS6

Silicon photonics for machine learning and neuromorphic computing

Bhavin J. Shastri

Queen's University, Canada
shastri@ieee.org

Artificial intelligence enabled by neural networks has enabled applications in many fields (e.g., medicine, finance, autonomous vehicles). Software implementations of neural networks on conventional computers are limited in speed and energy efficiency. Neuromorphic engineering aims to build processors in which hardware mimic neurons and synapses in brain for distributed and parallel processing. Neuromorphic engineering enabled by silicon photonics can offer sub nanosecond latencies, and can extend the domain of artificial intelligence and neuromorphic computing applications to machine learning acceleration (vector-matrix multiplications, inference and ultrafast training), nonlinear programming (nonlinear optimization problem and differential equation solving) and intelligent signal processing (wideband RF and fiber-optic communications). We will discuss current progress and challenges of neuromorphic photonics to scale to practical systems.

IS7

Third-harmonic generation in silicon nanowire arrays: Effect of light scattering and nanowire orientation

Golovan, L.A.*[1], Ustinov, A.S.[1], Zabotnov, S.V.[1], Efimova, A.I.[1], Presnov, D.E.[1,2,3], Osminkina, L.A.[1,4], Timoshenko, V.Yu.[1,5]

[1] Physics Department, M.V. Lomonosov Moscow State University, Moscow, 119991, Russia
[2] Skobeltsyn Institute of Nuclear Physics, M.V. Lomonosov Moscow State University, Moscow, 119991, Russia
[3] Quantum Technology Centre, M.V. Lomonosov Moscow State University, Moscow 119991, Russia
[4] Institute for Biological Instrumentation of Russian Academy of Sciences, Pushchino, Moscow Region 142290, Russia
[5] National Research Nuclear University MEPhI, Moscow, 115409, Russia
golovan@physics.msu.ru

Arrays of silicon nanowires (SiNWs) of about 100 nm in diameter formed by metal-assisted chemical etching of crystalline silicon (c-Si) substrates were studied with the help of third-harmonic (TH) generation technique. The SiNW arrays demonstrate strong scattering, which results in enhanced photon lifetime in them as it was supported by measurements of the cross-correlation function for femtosecond pulses scattered by the SiNW arrays. This effect results in an order of magnitude growth of TH generation efficiency compared to the signals for c-Si. Using (110) oriented c-Si substrate we managed to make well-oriented tilted SiNWs demonstrating strongly anisotropy of the TH signal. Numerical simulations of circularly polarized light scattering by a single SiNW and a group of 13 SiNWs used as a geometrical approximation of the real SiNW array indicate maintenance of helical modes in SiNWs for the light incident at an oblique angle to their axis. This result found its experimental confirmation in an experiment on the TH generation pumped by femtosecond laser pulses at 1250 nm demonstrated significant difference in the TH signals for cases of left- and right-handed circularly polarized fundamental radiation. The effect was detected for oblique (60°) light incidence on SiNWs, whereas for the laser radiation propagating along the SiNWs or perpendicularly to them TH signal did not depend on the pump radiation photon helicity sign. This fact is a manifestation of photon spin Hall effect. Thus, geometrical structure of the SiNW arrays, photon lifetime and local field in them strongly effects on efficiency and polarization properties of the third-harmonic generation.

IS8

In pursue of understanding the physical nature of scalar structured beams

Sabino Chávez Cerda

Instituto Nacional De Astrofisica Optica y Electronica, Mexico
sabino@inaoep.mx

More than three decades ago, it was introduced a laser beam that presented “apparent” nondiffracting features that had an intensity profile described by the Bessel function of the first kind; for this reason, with time they were named Bessel beams. Even though there existed several physical and mathematical inconsistencies in their description, they produced a great interest in the optics community and the publications reporting investigation with Bessel beams had an exponential growth. Years passed and they became a hot trending topic of investigation showing that they had more features that were also controversial and sometimes contradictory. In the talk, it will be presented an alternative description based in fundamental waves of the Helmholtz equation and that the reason for those disputed features is due to the fact that Bessel beams are not really beams in the sense that we understand the familiar Gaussian beams. This alternative description solves all of the inconsistencies demonstrating that not a single fundamental law needs to be violated.

IS9

Entanglement generation in semiconductor nanostructures

Ana Predojevic

Department of Physics, Stockholm University, Sweden
ana.predojevic@fysik.su.se

Single self-assembled quantum dots are established emitters of single photons and entangled photon pairs. To be used in quantum information experiments quantum dots need to be excited resonantly and coherently. The use of resonant excitation makes this system well suitable for generation of photon pairs with near-unity efficiency and high purity and also for entangling schemes such as time-bin entanglement. The entanglement of photons generated by quantum dot systems can be employed in free space-and fibre-based quantum communication. In addition to this, the versatility of entanglement can be more optimally used and explored if the photons are entangled simultaneously in more than one degree of freedom – hyperentangled, which was also recently shown to be possible using quantum dots. However, the achievable degree of entanglement and readiness of the source for use in quantum communication protocols, depend on several additional functionalities such as high collection efficiency and coherence of the emitted photon pairs. Here, we will address engineered photonic systems that promise a more efficient and better performing sources of entangled photon pairs.

IS10

Optics touches to our lives

Sezai Elagöz

Vice President, Research and Development Management Vice Presidency, ASELSAN, Ankara, Turkey
selagoz@aselsan.com.tr

ASELSAN Research and Development Management Vice Presidency was founded by the end of 2020 in order to carry the innovative research studies in ASELSAN to a new and higher stage. The current research subjects are ranging from artificial intelligence to advance materials, quantum technologies to biodefence. Imaging nanoparticles at single-particle level is an important subject of our recent research study with intriguing applications, especially in biotechnology. Therefore, a part of our resources is dedicated to the development of custom-made optical microscopes. The aim was to build imaging systems that are sensitive, easy to implement, low-cost and easy-to miniaturize. Next step is to use these imaging systems in creating practical, robust, and cost-effective biosensor solutions for non-laboratory environments. In this presentation, our research studies on detection of individual nanoparticles using our home-built Optical Interference Microscope will be briefly explained. This system enables detection of gold nanoparticles for sizes down to 10 nm and polystyrene nanoparticles for sizes down to 100 nm in diameter. In addition to the optical performance, algorithmic techniques were developed to improve the sensitivity and enhance the resolution of our system. First, using our imaging system, diagnostic studies of Hepatitis B antigen molecules were performed. For this purpose, the substrates including antibodies were prepared using our micro-array spotter and incubated with antigen and labeled-antibody solutions for molecular binding. This system in principle allows diagnostic studies of biological molecules for which the antibodies are available. After the outbreak of COVID-19, the focus changed to the detection of SARS-CoV-2 virus. A prototype sensor for testing SARS-CoV-2 presence was developed, aiming to start clinical trials and testing in near future.

IS11

Phase manipulation with semiconductor optical amplifiers

Deepa Venkitesh* and Aneesh Sobhanan

Department of Electrical Engineering, Indian Institute of Technology Madras, Chennai 600036, India
deepa@ee.iitm.ac.in

Advances in wireless technologies and the increased use of internet has lead to a tremendous increase in the demand for capacity in the back-bone optical fiber networks. These have been met with the increase in spectral efficiency through the use of advanced modulation formats along with wavelength, polarization and space/mode division multiplexing. In coherent optical communication systems that use multi-level amplitude and phase modulations, there are several sources of impairments originating at the transmitter, receiver and the fiber channel. These impairments are compensated using digital signal processing (DSP) algorithms. Complex DSP algorithms can be devised to equalize these impairments, and in this context, the trade-off between the latency and the efficiency of the DSP algorithms need to be considered carefully. In the case of long fiber links, the overhead in digital signal processing (DSP) is the highest for chromatic dispersion compensation. Increase in spectral efficiency also demands larger values of optical signal to noise ratio at the receivers, which is possible with the increase in the transmit power. This may lead to additional nonlinear impairments due to self and cross phase modulations. Even though advanced machine learning algorithms have been used in the recent past for nonlinearity compensation, the corresponding signal processing overheads are typically large. In this context, all-optical techniques - especially optical phase conjugation (OPC) - with mid-span spectral inversion has proved to be effective in compensating for impairments induced by both dispersion and nonlinearity in fibers. Besides, phase conjugation finds several other applications such as time reversing the scattering processes for countering atmospheric turbulence and biological imaging in highly turbid samples. Most of these polarization-sensitive and polarization-insensitive phase conjugate demonstrations have used four-wave mixing (FWM) in highly nonlinear fibers or periodically poled Lithium Niobate as the nonlinear medium - both of which require power levels, typically larger than 100 mW to initiate nonlinear effects. An alternate attractive choice is to use semiconductor optical amplifiers as a nonlinear medium, which have proved to be efficient and compact platform that requires much smaller optical power levels to invoke nonlinearities. Thus exploring SOAs as a promising nonlinear media for a conjugate generation would be advantageous for optical communication systems. In this talk, we will describe the experimental demonstration of all-optical compensation of dispersion and nonlinear impairments though phase conjugation in SOAs. We also demonstrate two and four-level phase quantization with appropriate choice of signal and pump powers, which is useful for phase sensitive amplification.

IS12

Light-matter interaction control with multilayer epsilon-near-zero metamaterials

Hümeyra Çağlayan

Tampere University, Laboratory of Photonics, Tampere, 33880, Finland
humeyra.caglayan@tuni.fi

Optical metamaterials such as hyperbolic metamaterials (HMMs) have a unique property that exhibits high-k modes due to hyperbolic dispersion and the existence of epsilon-near-zero (ENZ) in their electromagnetic spectral range. Besides the existence of ENZ wavelength, HMMs can enhance the radiative recombination rate (spontaneous emission) of quantum emitters. Recently, researchers have investigated deeply the linear properties of ENZ metamaterials. Such investigations lead to achieving a broad range of applications such as novel waveguiding regimes and controlling the radiation pattern of electromagnetic sources. In addition, experimental evidence is presented for the role of ENZ metamaterials to affect optical nonlinearity. Such effect demonstrates the efficient third harmonic generation and nonlinear Kerr index n2 for TCO (transparent conductive oxides) materials and HMMs. We have investigated both the linear and nonlinear effects of a multilayer epsilon-near-zero metamaterial. First of all, we have used the ENZ feature of HMM as a substrate to manipulate the resonance of plasmonic nanoantennas. The localized surface plasmon resonance of metal nanoantenna is significantly influenced by the size, shape, and environment but also its substrate. We demonstrate that the vanishing index of the substrate slows down the resonance shift of the antenna, known as pinning effect. Moreover, we have controlled the pinning effect at different regions by tuning the ENZ wavelength of HMM. Additionally, we have shown the ability to exploit the ENZ regime, for effectively tuning the optical properties of a metamaterial with simple design, operating in the visible range. The applied nonlinear change in the index of refraction leads to an ultrafast light induced metal to dielectric phase change at the ENZ region. The ability to access ultrafast light induced refractive index changes represents a new paradigm for the nonlinear optics. We anticipate that research on the nonlinear optical response of ENZ materials will generate very important results for years to come.

IS13

Efficient inverted Perovskite solar cells by dual interfacial modification

Matteo Degani

University of Pavia, Italy
degani94@gmail.com

The performance of inverted hybrid perovskite solar cells in the so-called pin structure still lags behind that of standard architecture devices. Herein, we report on a dual interfacial modification approach based on the incorporation of large organic cations at both the bottom at top interfaces of the perovskite active layer. Together, this leads to a simultaneous improvement in both the open-circuit voltage and fill factor of the devices. Importantly, this dual interfacial modification is fully compatible with a concomitant bulk optimization of the perovskite active layer by the addition of ionic liquids, leading to both efficient and stable inverted solar cells. The best performing devices reach an efficiency of 23.7%, the highest – to the best of our knowledge – reported for inverted architecture perovskite solar cells to date.

IS14

Collective coupling of an array of atoms near a nanofiber

Beatriz Olmos Sanchez

Institute for Theoretical Physics, University of Tübingen, Germany
ingrid.estiry@uni-tuebingen.de

In this talk, I will summarize some of the latest results we have published in our group on a light-matter system composed of emitters coupled to light modes which propagate in a waveguide. This setup is subject matter of many current experimental studies, as it holds promise of applications in quantum information routing and processing, e.g., as optical isolators and circulators where the light is emitted unidirectionally, or as generators of entangled atomic and photonic states. Among other results, I will show you how due to the collective light-matter interaction with the radiation field, an array of atoms can scatter light from an external laser field almost exclusively into one of the guided modes of the waveguide, allowing for almost lossless and completely unidirectional channeling of photons. Moreover, I will show you that the spectral properties of the scattered light depend strongly on the angle of incidence of the laser field on the array and the dispersive interactions between the light and the atoms, uncovering a modified Bragg condition.

IS15

Geometry of structured and spiral beams: Structural stability and energy flows

Alexander Vladimirovich Volyar

Taurida National V.I. Vernadsky University, Ukraine
volyar@tnu.crimea.ua

The problem of the structural stability of structured vortex beams in both theoretical and experimental optical aspects is considered. We have refined the standard structural stability condition of structured vortex beams by the requirement the fine structure of the intensity pattern to be constant up to scale and rotation when propagating. We have considered three types of the vortex beams: 1) structurally unstable beams consisting of two LG modes with mismatched amplitudes and phases, 2) stable non-rotating beams with matched amplitudes and phases, and 3) spiral vortex beams rotating when propagating. We have revealed that the critical points pattern in the structurally stable non-rotating beams forms three separatrices, which do not allow the external rotating energy flow to involve the beam fine structure into rotation that together with the scale transformations can significantly distort the beam. Analyzing the chaotic speckle structure of a perturbed structured beam, we have shown that measuring their amplitude and phase spectra by the intensity moments technique in LG and HG bases makes it possible to restore the initial mode structure of the beam.

IS16

Broadband image sensors based on 2D materials, integrated with silicon technology

Frank Koppens

Quantum Nano-Optoelectronics group, ICFO, The Institute of Photonics Sciences, Spain
frank.koppens@icfo.eu

Optical sensors and imagers based on 2D materials are inherently of high interest as they can cover a broad wavelength range and can be integrated with low-cost CMOS technology [1,2]. Photodetectors for visible, infrared and terahertz light have been demonstrated and even complete image sensors for wavelength range 300-2000 nm has been realized [3]. Further developments target image sensors for the infrared and terahertz range [4,5], as well as improving the maturity of the wafer scale production process.

Improvements in the maturity of graphene transfer and device integration are key for achieving better performing prototypes and moving the technology closer to product level. We will discuss achievements and challenges in fabrication and integration for image sensors.

References:

[1] Koppens, F. H. L., et al. "Photodetectors based on graphene, other two-dimensional materials and hybrid systems." Nature nanotechnology 9.10 (2014): 780-793.
[2] Akinwande, Deji, et al. "Graphene and two-dimensional materials for silicon technology." Nature 573.7775 (2019): 507-518.
[3] Goossens, Stijn, et al. "Broadband image sensor array based on graphene–CMOS integration." Nature Photonics 11.6 (2017): 366-371.
[4] Castilla, Sebastián, et al. "Fast and sensitive terahertz detection using an antenna-integrated graphene pn junction." Nano letters 19.5 (2019): 2765-2773.
[5] Castilla, Sebastián, et al. "Plasmonic antenna coupling to hyperbolic phonon-polaritons for sensitive and fast mid-infrared photodetection with graphene." Nature Communications (2020).

IS17

Interdisciplinary research by combining small angle X-ray scattering and deep X-ray lithography

Benedetta Marmiroli*[1], Barbara Sartori [1], Alessio Turchet [2] , Amardeep Bharti [2], Heinz Amenitsch[1]

[1] *Institute of Inorganic Chemistry, Graz University of Technology, 8010 Graz, Austria*
[2] *Elettra-Sincrotrone Trieste, 34149 Trieste, Italy*
benedetta.marmiroli@tugraz.at

Micro-nanotechnology has melted the borders between material science, chemistry and biology. The miniaturization of chemical and biological assays, promoted by micro-nanofluidics, requires both a careful selection of the fabrication methods and the development of tailored materials for the specific applications. As a consequence, interdisciplinarity is becoming fundamental also in the combination of microfabrication and characterization techniques both aimed at the construction of new devices and at the development of novel materials. In this communication, we want to underline the advantages obtainable by combining two techniques: Deep X-ray Lithography (DXRL) for microfabrication and Small and Wide Angle X-ray Scattering (SAXS/WAXS) for investigation. First, micro devices fabricated for time resolved experiments of fast reactions, or for the study of the effect of confinement on crystal growth will be discussed. Then, the combination of bottom-up and top-down approaches for the development of new functionalized materials for which characterization with SAXS/WAXS is fundamental will be described: mesoporous materials, Thermally Rearranged polymers and Metal Organic Frameworks.

IS18

Integrating nanostructured electrodes in photovoltaic devices for enhancing efficiency

Fahrettin Yakuphanoğlu

Fırat University, Faculty of Science, Physics Department, Elazig, Turkey
fyhanoglu@firat.edu.tr

Quantum dots have been integrating to nanostructure electrode of quantum dots solar cells to enhance efficiency. Core/shell CdSe/CdS Quantum Dots Sensitized Solar Cells have been fabricated. A number of QDs homogeneously was covered onto the surface of TiO_2. CdSe/CdS Core/Shell quantum dots were treated at various temperature and times to enhance efficiency of solar cells. To enhance efficiency of quantum dots solar cells, excited electrons in the quantum dots are injected into TiO_2 photoanode electrode. The fluorescence spectra of quantum dots and quantum dots-TiO_2 confirm that excited electrons are injected to into TiO_2 photoanode. The efficiency of the quantum dots solar cells were controlled with transition of amorphous structure to crystalline structure of ZnS. The thermal annealing treatment of ZnS enhances the absorption of light and the core/shell is destroyed. But the short circuit current is increased, although the efficiency is decreased. The obtained results suggest that the efficiency of quantum dots solar cells is enhanced with integrating nanostructured electrodes in photovoltaic devices.

IS19

New concept in ultraviolet photodetectors

Hamdaoui. N.*, Ben Amor. F., Ajjel. R.

Department of Physics, University of Sousse, Tunisia
hamdaoui_nejeh@yahoo.fr, hamdaoui_nejeh@protonmail.com

This study introduces a self-powered ultraviolet photodetector that uses Co^{2+}: ZnO diluted magnetic semiconductor nanoparticles (DMS) as a photosensitive layer. Here, for the first time, a high-performance ultraviolet photosensor was developed using Co^{2+}: ZnO nanoparticles based on a low-cost polyol method. In addition to the optical band gap of ZnO, cobalt can also generate another optical absorption band related to the Co + 2 d-d (tetrahedral symmetry) crystal field transition, which can enhance the total optical absorption and produce high responsivity. Many characterization techniques such as XRD, TEM, FTIR, PL and diffuse reflectance (DF) spectroscopy are employed in this research. The performance of our samples was estimated upon exposing to UV light of wavelength 375 nm and at zero bias voltage. The sample shows a sensitivity of 209.7 and a high responsivity about 5.5 10^3 mA/W under intensity of 7.6 mW. The response times (the rise and recovery times) of our sample are 0.62s and about 1.65 s without any external bias, respectively. Our self-powered PD shows higher detectivity about 1.3 10^{13} Jones, compared to the UV PD in other works. Such high responsivity and detectivity lead the Co^{2+}: ZnO PD to have low noise spectral density of 10−24A^2/Hz and low noise equivalent power of 2.6E-11 W $Hz^{-1/2}$. This study proposes an original process for the fabrication of low-cost self-powered PDs with high performance and zero power consumption on a large-scale.

IS20

Optoelectronic properties of low-dimensional materials investigated by TEM-EELS

Raul Arenal[1,2,3]

[1] *Instituto de Nanociencia y Materiales de Aragon (INMA), CSIC-Universidad de Zaragoza, 50009 Zaragoza, Spain*
[2] *Laboratorio de microscopias avanzadas (LMA), U. Zaragoza, C/ Mariano Esquillor s/n, 50018 Zaragoza, Spain*
[3] *ARAID Foundation, 50018 Zaragoza, Spain*
arenal@unizar.es

In the last two decades, transmission electron microscopes (TEM) have undergone a large number of improvements allowing very high energy resolutions (few meV) for a close to one angstrom electron beam. These performances offer new possibilities in different TEM fields, in particular these ones concerning the low-energy-loss measurements: studies of the optical, dielectric and electronic properties of materials with unprecedented spatial information. In this presentation, I will present a selection of recent works taking advantage of these new capabilities for studying the opto-electronic properties of different nanostructures. In particular, I will present the study of the plasmonic response of metallic (gold, silver) nanoparticles and nanowires as well as the optical gap measurements of different kind of 1D and 2D nanomaterials. These works have been carried out via low-loss electron energy loss spectroscopy (EELS) measurements and these studies will be combined with structural, morphological and chemical analyses of all these materials at the local (subnanometer – atomic) scale. In all the cases, the experimental results have been interpreted via different kind of theoretical studies. Some of these theoretical works have been developed in the framework of the discrete dipole approximation (DDA) simulations; others have concerned density functional theory calculations. All these results will be discussed in detail in this contribution.

Acknowledgment
This research has been supported by the Spanish MICINN (PID2019-104739GB 100/AEI/10.13039/501100011033) and European Union H2020 programs “Graphene Flag-ship” (881603) and “ESTEEM3” (823717).

IS21

Ultrafast dynamics in solutions and thin films

Halime Gül Yağlıoğlu

Department of Engineering Physics in Ankara University, Ankara, Turkey
yoglu@eng.ankara.edu.tr

Many natural processes occur in ultrafast time scales, which determine the final performances of devices working based on those natural processes. Therefore, research in ultrafast science has an impact in both fundamental research as well as its applications. Ultrafast dynamics addresses questions such as the role of excess energy in electron injection at photovoltaic interfaces, the dynamics in quantum-confined structures (e.g., multi carrier generation), electron/energy transfer mechanisms in novel compounds and dynamics of ultrafast magnetization processes in magnetic materials. The set of techniques and experiments available is very broad. Ultrafast transient absorption spectroscopy and ultrafast time resolved magneto-optical Kerr effect techniques are two of the examples. In these techniques, a first light pulse (IR, Vis, EUV or X-ray) initiates dynamics, like a chemical reaction, a phase transition, spin, orbital, or charge-density waves in solids and a second pulse, impinging at a variable but well-defined time delay, probes the motion. In this talk, our recent work on ultrafast time resolved magneto-optical Kerr effect technique applied to FeAl thin films will be presented. Besides, ultrafast transient absorption spectroscopy technique applied to various materials or devices at the Engineering Physics Department in Ankara University with the collaboration of other universities will be summarized as well.

Acknowledgment
This work was supported by TUBITAK with grant number 117R017.

IS22

Dipolar Interactions in low-dimensional atom-photonics platforms

Hadiseh Alaeian

ECE and Physics and Astronomy, Purdue University, USA
halaeian@purdue.edu

Light-induced atom-atom interactions at densities higher than 1 atom per cubic wavelength give rise to density shifts and broadenings. When confined in less than a wavelength size, this dipolar interaction leads to collective blockade phenomena, which mostly have been studied using strongly interacting Rydberg states. Here we study this effect for low-lying excited atomic states and confined atoms in two- and one-dimension. The former experiment uses pulsed LIAD (Light-induced atomic desorption) to generate a thin layer of free atoms close to a surface. For a few nanoseconds, the light-induced dipolar interaction on the D1 and D2 line of Rubidium leads to shifts and broadenings according to the so-called Lorentz-Lorenz shifts. In the second approach, we interface the thermal atoms with the highly-confined field of the slot waveguides, where the Purcell-enhanced interaction modifies the interactions and the shifts, further. The latter experiments are done at telecom wavelength where one can observe and integrate the collective quantum effects like the blockade-induced single-photon absorber. Finally, in the outlook, we present the concept of an optical single-atom detector based on a freestanding photonic crystal cavity that leads to the strong atom-light coupling in the transient regime.

IS23

Light management strategies for high efficiency Si solar cells

Raşit Turan

Center for Solar Energy Research and Applications (GÜNAM), Middle East Technical University, 06531, Ankara, Turkey
Department of Physics, Middle East Technical University, 06531, Ankara, Turkey
turanr@metu.edu.tr

Crystalline Si solar cell technology has reached an extremely well maturity level with well-optimized material and process conditions. Further improvements in the cell efficiency and the cost should be based on new and exotic approaches employing new material types and device structures. Among such efforts, light management on the cell surface are attracting special attention due to the potential improvements both in the cell efficiency and material cost. Light trapping techniques aims at increasing the path length and the number of scattering events of the incident photons, thereby increasing the light absorption. Both reflection and transmission through the cell are significantly reduced in this way. Traditionally, surface texturing and anti-reflection coatings have been commonly used for this purpose. Alternatively, Si nanostructures are being extensively studied for light trapping applications in crystalline Si solar cells. Si nanowires can be formed as vertically aligned and integrated arrays on the surface, which was found to bring remarkable light trapping strength. In addition, various photonics structures employing metal and semiconductor nanostructures have been incorporated onto the surface of the device to improve the light conversion properties. Fabrication of Si micro and nanostructures including nanowires and inverted pyramids can be achieved by metal assisted etching technique which employs Ag or Cu nanoparticles. Moreover, the chemical composition of the etching solution can be adjusted to produce the desired surface structures. Optical properties of Si surface can then be tailored to meet the requirement of the optical and electrical performance. These and some other approaches will be discussed and reviewed in this talk.

IS24

Some features of the growth and optical properties of nanomaterials

M.B. Muradov

Nano Research Center, Baku State University, Azerbaijan
mbmuradov@gmail.com

It is known that the optical properties of nanostructures depend on some parameters of nanostructures: size, structure, shape, etc. One of the main parameters that affects the optical, properties is the potential energy of charge carriers in nanostructures. This work examines the influence of the production technology and the interaction of charge carriers in a nanoparticle with the environment on the optical properties of nanoparticles. In this work, the influence of technological parameters of growth on the structures of the formed particles is analyzed. An assumption is made about the influence of technological parameters on the defect structure of nanoparticles. The results of experimental works on the influence of technological conditions on the crystal structure and physical properties of nanostructures are analyzed. The second part of the work is devoted to the analysis of the influence of the interaction of charge carriers with the environment on the optical properties of the nanostructured. The results of experimental work are analyzed. A theoretical model is proposed to explain the results of experimental work.

IS25

Ultra-compact activity Q-switched waveguide lasers based on liquid crystal modulators

Alexander Fuerbach

Department of Physics and Astronomy, Macquarie University, Australia
fuerbach@physics.mq.edu.au

We report on a novel family of miniaturised and all-integrated actively pulsed waveguide lasers. Versatile femtosecond laser-written glass chip lasers based on a depressed-cladding architecture feature the largest fundamental mode-area of any rare-earth doped planar waveguide laser. Combined with novel liquid crystal cells in the deformed helix ferroelectric (DHF) mode, this allows the generation of nanosecond optical pulses with kW peak power level and wavelengths ranging from the visible to the mid-infrared, all in a fully monolithic laser setup with dimensions in the order of only a few cm.

IS26

Absolute quantum advantage in biological imaging

Warwick Bowen

Australian Institute for Bioengineering and Nanotechnology, The University of Queensland, Australia
w.bowen@uq.edu.au

State-of-the-art microscopes use intense lasers that can severely disturb biological processes, function and viability. This introduces hard limits on performance that only quantum photon correlations can overcome. In this talk I will report recent work from my laboratory which demonstrates this absolute quantum advantage. We show, specifically, that quantum correlations enable signal-to-noise beyond the photodamage-free capacity of conventional microscopy. Broadly, this represents the first demonstration that quantum correlations can allow sensing beyond the limits introduced by optical intrusion upon the measurement process. We achieve this in a coherent Raman microscope, which we use to image molecular bonds within a cell with both quantum-enhanced contrast and sub-wavelength resolution. This allows the observation of nanoscale biological structures that would otherwise not be resolved. Coherent Raman microscopes allow highly selective biomolecular finger-printing in unlabeled specimens, but photodamage is a major roadblock for many applications. By showing that this roadblock can be overcome, our work provides a path towards order-of-magnitude improvements in both sensitivity and imaging speed.

IS27

UV-C solar blind photoresistors based on ε-Ga_2O_3 polymorph

Bosi, M.[1,*], Baraldi, A.[2], Bosio, A.[2], Borelli, C.[2], Ferrari, C.[1], Mazzolini, P.[2], Mezzadri, F.[3], Mosca, R.[1], Parisini, A.[2], Pavesi, M.[2], Seravalli, L.[1], and Fornari, R.[1,2]

[1] Institute of Electronic and Magnetic Materials (IMEM-CNR), Viale delle Scienze 37/A, 43124 Parma, Italy
[2] University of Parma, Department of Mathematical, Physical and Computer Sciences, Viale delle Scienze 7/A, 43124 Parma, Italy
[3] Department of Chemistry, Life Sciences and Environmental Sustainability, University of Parma, Parco Area delle Scienze 17/A, 43124 Parma, Italy
matteo.bosi@imem.cnr.it

Ga_2O_3 is an ultra-wide bandgap oxide (E_g>4.5 eV) of great interest for applications in power electronics, opto-electronics, UV-detection, catalysis, etc. Ga_2O_3 can crystallize in several polymorphs, the most common being $\alpha, \beta, \varepsilon,$ with different properties and fields of applications. $\beta - Ga_2O_3$, the thermodynamically stable polymorph, is the most investigated for high-power electronic applications although its anisotropy, due to the monoclinic crystallographic phase, poses some problems in practical realization of devices. The α and ε metastable polymorphs, on the other hand, exhibit higher symmetry lattice (corundum and orthorhombic respectively), permitting easier epitaxial growth conditions and processing. This talk will be focused on the preparation and characterization of $\varepsilon - Ga_2O_3$ epilayers and on the development of solar blind photodetectors for UV-C light. I will discuss the epitaxial growth conditions that permit to tailor the Metal Organic Vapor Phase Epitaxy (MOVPE) growth of $\varepsilon - Ga_2O_3$ with respect to the other polymorphs and present the characterization performed to qualify our material. We developed ohmic contacts and performed the electrical characterization of our samples, aimed at the realization of a test photoresistor showing good responsivity at 250 nm with solar blind characteristics. This detector could find applications in monitoring of the corona effect in high voltage appliances, detecting early failures and defects.

IS28

Photon added cat state: phase space structure and statistics

Prasanta K. Panigrahi

Indian Institute of Science Education and Research Kolkata, India
pprasanta@iiserkol.ac.in

Schrodinger's cat state has played a historically significant role in highlighting the unique nature of the quantum world, as well as the mysterious collapse of the wavefunction. Only recently, these have been produced experimentally and the effect of two photon loss bringing the state back to itself has been shown. This has led to the development of 'Cat Codes' for possible use in quantum processors as correcting errors. Here, we investigate the effect of single photon addition to the Cat state, which leads to subtle but detectable changes in the Wigner function. The change in statistics for the more general 'Cat state' with a relative phase between the 'live' and 'dead' states is found to have significant effect on the intensity-intensity correlation. This may find 'use' in detecting phase shifts due to field quadrature variations as for reporting on 'internal structure'. Effects of single and two photon additions have been explicated for the Kitten states, with possible application in quantum imaging.

IS29

Chalcogenide based two dimensional (2D) structures: New quantum materials

Çakmak, B.*[1,2], Coşkun, A.[2], Güldüren, Z.E.[2] and Turgut, G.[2,3]

[1]*Department of Electrical and Electronic Engineering, Faculty of Engineering and Architecture, Erzurum Technical University, 25050 Erzurum, Turkey*
[2]*Photonics Group, High Technology Research and Application Centre (YUTAM), Erzurum Technical University, 25050 Erzurum, Turkey*
[3]*Department of Basic Sciences, Science Faculty, Erzurum Technical University, 25050 Erzurum, Turkey*
bulent.cakmak@erzurum.edu.tr

Two-dimensional (2D) materials have a great interest after the discovery of graphene in 2004 due to their layer-dependent superior properties. Graphene has superior electrical, thermal and mechanic properties but lack of its bandgap has led to discovering new type of 2D materials such as transition metal dichalcogenides (TMDCs), hexagonal boron nitride (h-BN), layered metal oxides, layered double hydroxides (LDHs), black and blue phosphorus, borophene, germanene (2D). TMDCs, one of 2D materials, are generally shown by the MX_2 formula (M: Transition metal, X: Chalcogen). There is a strong covalent bond between metal and chalcogen, but layers connected by Van der Waals force between layers. It is possible to obtain atomically thin films with undisturbed interfaces by linking this weak interlayer. For 2D TMDCs like MoS_2, band gap changes from indirect to direct with respect to bulk-monolayer. Electron mobility of single-layer MoS_2 and WS_2 is in the range of 1-1000 $cm^2V^{-1}s^{-1}$ and 40-200 $cm^2V^{-1}s^{-1}$, respectively. Many TMDCs are chemically stable and mechanically strength and some of them have superior magnetic properties. Experimental and theoretical studies indicate that these materials are expected to be quantum materials in ten years and more studies should be done to understand their properties. In this study, synthesis of $MoSe_2$ and WSe_2 monolayers via chemical vapor deposition method was investigated. Raman, PL and AFM results for monolayers were obtained in which emission peaks from PL spectra were observed at 1.51 eV and 1.61 eV values. The thickness values of 0.74 nm and 0.82 nm were also measured from AFM images for $MoSe_2$ and WSe_2 flakes. The results obtained are in good agreement with the literature.

IS30

Ultrafast solid-state lasers based on novel materials

Kisel V.E., Rudenkov A.S., Gorbachenya K.N. and Kuleshov N.V.

Center for Optical Materials and Technologies, Belarusian National Technical University, Minsk, Belarus
vekisel@bntu.by

We report on recent results deal with spectroscopic properties and laser performance of novel laser media based on Yb-doped aluminum and lutetium perovskite crystals Unique spectroscopic properties of trivalent ytterbium ions of these host media make these crystals good candidates for active elements of picosecond and femtosecond solid-state laser systems. The features of soliton and non-soliton mode-locking were studied using SESAMs as a saturable absorber. Maximum average output power of 7W with pulse duration of 130fs and 28.1% optical efficiency were obtained in soliton mode-locking regime. 90-fs pulses were generated with reduced to 2.9 W output power. Average output power up to 12W with 2ps pulse duration and 38% optical efficiency was obtained in non-soliton mode-locking regime with extremely low quantum defect between pump (980nm) and laser (999nm) wavelengths under longitudinal diode pumping. Chirped pulse regenerative amplifier based on Yb:LuAP crystal was investigated. Pulse duration as short as 165fs with average output power of 4.5W at 200 kHz pulse repetition frequency was demonstrated.

IS31

Kelvin nanotechnology Ltd: provider of nanofabrication services for over two decades

Alka Swanson

Kelvin Nanotechnology, Glasgow, UK
alka@kntnano.com

Kelvin Nanotechnology (KNT) provides advanced nanofabrication services to customers world-wide. This talk will discuss KNT's capabilities and provide some example of previous processes. The talk will cover large area, multi-level electron beam lithography for technologies including Laser Gratings, Waveguides, Magneto Optical Trap Gratings, Diffractive Optical Elements, Imprint Masters and Transistor Gate Writing. Complimentary Capability in Plasma Processing, Metallisation and Photo/Nanoimprint Lithography enables us to provide services with device geometries as low as 20nm with unparalleled layer-to-layer alignment. Some of the applications include lasers for fibre optics transmission, meta lenses & diffractive optics for augmented reality, and quantum components for various sensor applications. About Kelvin Nanotechnology: An internationally recognised provider of Advanced Photonics and Quantum Components. Taking pride in providing customers with consistent, cost and time effective delivery. Process Innovation, Quality, Customer Service and attention to detail has led us to achieve qualified partner status for multiple international supply chains.

SPEAKERS

S1

Photoeffect in Schottky diodes with an additional electric field

Mamedov R.K.*, Aslanova A.R.

Faculty of Physics, Baku State University, AZ1148, Baku, Z. Khalilov 23, Azerbaijan
rasimaz50@yahoo.com

In real Schottky diodes (SD) with a certain contact surface, an additional electric field (AEF) arises around it due to the potential difference between the interface surface with a potential barrier height of ~ 1 eV and adjacent free metal and semiconductor surfaces with work functions of ~ 4 -5 eV. Relief and potential images of the contact surface of AFM measurements of Au-nGaAs SD with a diameter D of 50 μm, shown in below figures (a and b), show that the AEF covers the free surface of the semiconductor along the periphery of the contact to a width*l*and penetrates into the near-contact region of the semiconductor.

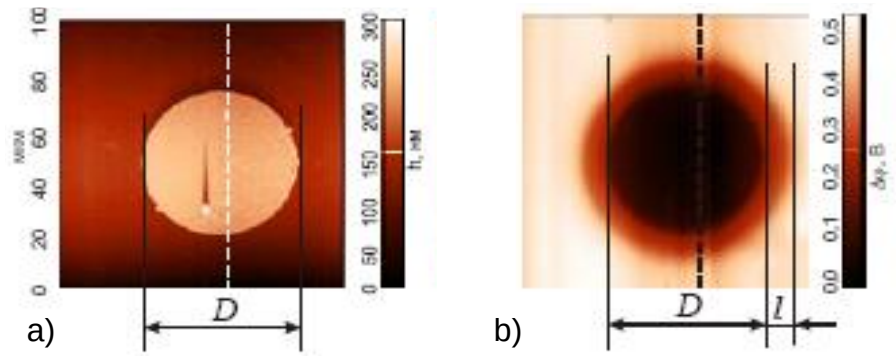

Under the action of the AEF in the near-contact peripheral region SD, a redistribution of free electrons occurs and a voltage drop U_C arises in the opposite direction. The real SD with area S is determined by the energy structure of the two-barrier contact, which consists of a non-equilibrium peripheral part with area S_2 (the potential barrier height Φ_{B2}) and the inner part with area S_1 (the potential barrier height Φ_{B1}), where $S = S_1 + S_2$ and $\Phi_{B1} - \Phi_{B2} = qU_C$. When the Au-nGaAs SD is illuminated, the photovoltage U_{Ph} arises, which is added to the voltage U_C of the AEF, does not affect the forward I-V characteristic of the SD and causes an increase in the saturation current of the reverse I-V characteristic by several orders of magnitude. The potential barrier height for the forward I-V characteristic of the SD becomes numerically equal to the sum of the voltage U_C of the AEF and the potential barrier height for the reverse I–V characteristic. In the photoeffect in a SD with an AEF, the geometric shapes and dimensions of the contact surface have a significant influence, about which interesting results are presented in our next report.

S2

Incoherent spectrophotometry of soda-lime glass (SLG) substrates

Staskov, N.I.[1], Gremenok, V.F.[2], Pyatlitski, A.N.[3], Akçay, N.[4,5]* and Özçelik, S.[4,6]

[1]*A.A. Kuleshov Mogilev State University, 212022, Mogilev, Kosmonavtov str. 1, Republic of Belarus*
[2]*State Scientific and Production Association "Scientific-Practical Materials Research Centre of the National Academy of Sciences of Belarus", 220072, Minsk, P. Brovka str. 19, Republic of Belarus*
[3]*JSC «INTEGRAL» – «INTEGRAL» Holding Managing Company, Minsk, Republic of Belarus*
[4]*Gazi University, Photonics Application & Research Centre, 06500, Ankara, Turkey*
[5]*Department of Mechanical Engineering, Faculty of Engineering, Baskent University, Ankara, Turkey*
[6]*Department of Photonics, Faculty of Applied Sciences, Gazi University, Turkey*
neslihanakcay@baskent.edu.tr, sozcelik@gazi.edu.tr

Millimeter-thick planar soda-lime glasses (SLG) are widely used as substrates for film deposition. In the literature, the optical constants of $n(\lambda)$ and $k(\lambda)$ for technical glass substrates are known calculated from the measured transmittance $T(\lambda)$ and reflectance $R(\lambda)$ at the normal ($\theta = 0^0$) incidence of light in the spectral range from λ=310 nm to λ=3700 nm. This method does not allow us to determine the values of $n(\lambda)$ and $k(\lambda)$ in the spectral region of λ < 310 nm due to the large $k(\lambda)$, because $T(\lambda) \to 0$. To determine the optical characteristics of a homogeneous plane-parallel plate SLG (*d*=1.2 mm), we measured eight spectra of $T_{s,p}(\lambda)$ and $R_{s,p}(\lambda)$ (*s* and *p*: light polarized perpendicular and parallel, respectively) at $\theta_1 = 10^0$ and $\theta_2 = 55^0$ (Photon RT spectrophotometer, Belarus, Minsk). The calculation was performed analytically [1] using the measured spectra of $T_s(\lambda, \theta_j)$ and $R_s(\lambda, \theta_j)$ (j=1, 2) in the spectral range from λ = 250 nm to λ = 800 nm: i) $R_p(\lambda, \theta_j) \times \left[R_s(\lambda, \theta_j)\right]^{-1}$ and $R_s(\lambda, \theta_j)$ in the spectral range from λ=250 nm to λ=310 nm, ii) $R_s(\lambda, \theta_1)$ and $R_s(\lambda, \theta_2)$ in the spectral range from λ=250 nm to λ=310 nm. The correctness of the obtained values is verified by comparing the measured and calculated spectra of ellipsometric angles ($\theta = 56^0$) and $T(\lambda)$, $R(\lambda)$ ($\theta = 0^0$). The spectrum of $n(\lambda)$ is interpolated by the classical dispersion model for the dielectric constant $\varepsilon(\lambda) = (n(\lambda) - ik(\lambda))^2$.

Acknowledgments
This work was supported by the Belarusian State Programme for Research «Physical Material Science, New Materials and Technologies» and TUBITAK with the grant № 118F009.

References:
[1] Sotsky A.B., Mikheev S.S., Stas'kov N.I., Sotskaya L.I. (2020). Spectrophotometry of Layers on Plane Parallel Substrates. Optics and Spectroscopy, 128, (8), 1155–1166.

S3

Dimension dependence of the I-V characteristic of illuminated Au-nGaAs Schottky diodes with an additional electric field

Mamedov, R.K.*[1], Aslanova, A.R.[1], and Babayeva, R.F.

[1]*Faculty of Physics, Baku State University, AZ1148, Baku, Z. Khalilov 23, Azerbaijan*
[2]*Department of Applied Sciences, State University of Economics (UNEC), AZ1010, Baku, Azerbaijan*
rasimaz50@yahoo.com

It is shown that the nature of the effect of illumination on the I-V characteristic of Au-nGaAs Schottky diodes (SD) in the forward and reverse directions noticeably differs due to the additional electric field (AEF) and becomes dependent on the geometric shape and dimensions of the contact surface. The saturation currents of the forward and reverse I-V characteristic of an unilluminated SD with a diameter D of 500 μm almost coincide and become equal to about $2\cdot10^{-11}$ A. With a decrease in the D from 500 to 5 μm, the saturation currents of the forward I-V decrease by four orders of magnitude, and the reverse I-V is only 1.5 order. The currents of the forward I-V of the SD consists of currents flowing through the general contact area ($S=S_1+S_2$), and the reverse I-V consists of currents flowing mainly through the peripheral area (S_2) with a width of about 1 μm. In this case, the potential barrier height of the SD for the forward I-V remains constant, equal to about 0.89 eV, for the reverse I-V, it decreases from 0.90 to 0.75 eV, and the voltage U_C AEF of the SD increases from 20 to 120 mV. The forward and reverse I-V characteristics of the SD with the voltage U_C AEF are well described by the formulas:

$$I_F = I_{F1} + I_{F2} = S_1 A T^2 \exp\left(-\frac{\Phi_{B1}}{\kappa T}\right)\left[\exp\left(\frac{qU}{n_{11}\kappa T}\right) - \exp\left(-\frac{qU}{n_{12}\kappa T}\right)\right] + \\ + S_2 A T^2 \exp\left(-\frac{\Phi_{B2}}{\kappa T}\right)\left[\exp\left(\frac{-n_{21}qU_C+qU}{n_{21}\kappa T}\right) - \exp\left(-\frac{qU}{n_{22}\kappa T}\right)\right] \quad (1)$$

$$I_R = I_{R1} + I_{R2} = S_1 A T^2 \exp\left(-\frac{\Phi_{B1}}{\kappa T}\right)\left[\exp\left(-\frac{qU}{n_{r11}\kappa T}\right) - \exp\left(\frac{qU}{n_{r12}\kappa T}\right)\right] + \\ + S_2 A T^2 \exp\left(-\frac{\Phi_{B2}}{\kappa T}\right)\left[\exp\left(\frac{-n_{r21}qU_C-qU}{n_{r21}\kappa T}\right) - \exp\left(\frac{qU}{n_{r22}\kappa T}\right)\right] \quad (2)$$

Under illumination of Au - nGaAs SD with different D (5 - 500 μm), the photovoltage U_{Ph} appears with a value of ~150 V and it is added to the voltage U_C AEF, which decreases with increasing contact diameter D. Under the influence of light, the saturation current of forward I-V of the SD, consisting of currents flowing over the general contact area, almost do not change. The saturation current of reverse I - V of the SD consist mainly of currents flowing through the periphery of the contacts, increasing by 2-3 orders of magnitude. The equality of $\Phi_{B1}-\Phi_{B2} = q(U_C+U_{Ph})$ for SD with different D is well confirmed experimentally.

S4

Structural and optical characterization of Cu_2SnS_3 thin films prepared by sulfurization of sputtered Cu/Sn/Cu stack layers

Gremenok, V.F.[1,2], Khoroshko, V.V.[2], Pyatlitski, A.N.[3], Akçay, N.[4,5]* and Özçelik, S.[4,6]

[1]*State Scientific and Production Association "Scientific-Practical Materials Research Centre of the National Academy of Sciences of Belarus", 220072, Minsk, P. Brovka Str. 19, Republic of Belarus*
[2]*Belarusian State University of Informatics and Radioelectronics, 220013, Minsk, P. Brovka str., 6, Republic of Belarus*
[3]*JSC «INTEGRAL» – «INTEGRAL» Holding Managing Company, 220108, Minsk, Kazintsa I.P. str., 121A, Republic of Belarus*
[4]*Gazi University, Photonics Application & Research Centre, 06500, Ankara, Turkey*
[5]*Department of Mechanical Engineering, Faculty of Engineering, Baskent University, 06790, Ankara, Turkey*
[6]*Department of Photonics, Faculty of Applied Sciences, Gazi University, 06500, Ankara, Turkey*
neslihanakcay@baskent.edu.tr, sozcelik@gazi.edu.tr

The search of new cheap and non-toxic absorber materials that have suitable optical and electrical properties for use in thin film photovoltaics, is one of the challenges for the researchers. In this context, ternary chalcogenide compound Cu_2SnS_3 has recently attracted a big interest due to its high absorption coefficient over 10^4 cm^{-1} and its direct band gap energy in the range of 0.9-1.0 eV [1]. In this study, the structural and optical properties of Cu_2SnS_3 thin films prepared by using two-stage process, sulfurization of sputtered Cu/Sn/Cu stacked layers in sulfur ambient at 450°C for 30-180 minutes have been investigated. The grazing incident X-ray diffraction and Raman spectroscopy patterns have indicated polycrystalline form and monoclinic structure of Cu_2SnS_3 films. The variation of different structural parameters has been researched and reported as a function of sulfurization time. The scanning electron microscopy revealed the densely packed structures of the films. The optical parameters such as band gap energies, the absorption coefficients of thin films have been determined and analyzed by transmission and reflection spectra. The films have been found to be as direct-gap semiconductors.

Acknowledgments
This work was supported by the Belarusian State Programme for Research «Physical Material Science, New Materials and Technologies» and TUBITAK with the grant № 118F009.

References:
[1] Kanai, A., Toyonaga, K., Chino, K., Katagiri, H., and Araki, H. (2015). Fabrication of Cu2SnS3 thin-film solar cells with power conversion efficiency of over 4%. Japanese Journal of Applied Physics, 54(8S1), 08KC06.

S5

Electrical characteristics and photoconduction behaviour of the Au/Er_2O_3-PVC/n-Si structure

Badali, Y.[1]*, Elamen, H.[2], Güneser, M.T.[3], and Altındal, Ş.[4]

[1]Department *of Electrical and Electronics engineering, Antalya Bilim University, Antalya, Turkey*
[2]*Department of Electrical & Electronics Engineering, Karabük University, Karabük, Turkey*
[3]*Department of Electrical & Electronics Engineering, Karabük University, Karabük, Turkey*
[4]*Department of physics, Gazi University, Ankara, Turkey*
bedeli.yusuf@gmail.com

The electrical and dielectric behaviors of the Au/Er_2O_3-PVC/n-Si structure under varying light intensity were investigated. There is a stunning change in I-V graphs when it shifts from dark to light and also with light intensity change. The values of the ideality factor (n) and the zero-bias barrier height (Φ_{B0}) were extracted using the slope and intercept of the logarithmic I-V curve based on lighting power. Although the Φ_{B0} values decrease with increasing light power, n values increase, and there is a strong linear relationship between them. The values of photo-current (I_{ph}) increase with the increasing lighting power due to the formation of electron-hole pairs. The slopes of the double-logarithmic ln(I_{ph})-ln(P) are 0.78 and 0.80, for 1 V and 3 V respectively, which indicates the ongoing distribution of the surface states (N_{ss}). These slopes also confirmed that the Er_2O_3-PVC nanocomposites exhibit photoconduction behaviour and hence Au/Er_2O_3-PVC/n-Si structure can be used as a photo-device. The observed changes in the current (I) with changing in the light power, capacitance (C) and conductance (G) are the results of trap states located at Er_2O_3-PVC/n-Si interface and so reorder and restructure of them under illumination and bias voltage.

S6

Plasmonic light management in PBDB-T: ITIC-M inverted organic photovoltaics

Kurt, H.

School of Engineering and Natural Sciences, Istanbul Medipol University, Ekinciler Cad. No:19 Kavacik, 34810, Beykoz, Istanbul, Turkey
hasankurt@medipol.edu.tr

The performance of organic photovoltaics (OPV) improved immensely thanks to development of low band gap donor polymers, control of bulk heterojunction (BHJ) morphology and interface engineering reaching power conversion efficiency (PCE) of 13% and 15% for single junction and tandem OPVs, respectively. The increase in performance suggests that OPVs can reach a competitive level of mass production as they reach PCE of 20%. To this end, there are still challenging issues to be addressed in OPV development. In particular, low carrier mobility and small exciton diffusion lengths lead to recombination events in active BHJ layers and severely limit the optimum thickness of an active layer below 200 nm. Limited thickness of active layer results in insufficient absorption of incoming solar radiation hence exhibits low external quantum efficiency and PCE. In this issue, manipulation of incoming light with plasmonic nanostructures as subwavelength antennas arises as a promising remedy for low performance of OPVs. In this junction, the study encompasses a solution based diblock copolymer (DBCP) micelles-based production of 2D quasi-ordered Au plasmonic nanostructures and incorporation of these nanostructures in BHJ – ZnO electron transport layer interface. This provided an important opportunity to study the effects of nanoparticle size and interparticle distance on OPV performance and tailor the plasmonic properties of nanostructure arrays according to the device structure and absorption profile of BHJ blend. In this study, we will outline the methodology for developing plasmon enabled light manipulation within thin film BHJ OPVs using finite-difference time-domain (FDTD) electromagnetic simulations and demonstration of the potential in experimental inverted PBDB-T: ITIC-M BHJ OPV reaching 17% improvement in PCE.

S7

Junction area dependent performance of graphene/n-Si based near-infrared Schottky photodetectors

Fidan, M.*[1], Ünverdi, Ö.[2], and Çelebi, C.[1]

[1]*Quantum Device Laboratory, Department of Physics, İzmir Institute of Technology, 35430 İzmir, Turkey*
[2]*Faculty of Engineering, Department of Electrical and Electronic Engineering, Yaşar University, 35100 İzmir, Turkey*
mehmetfidan.phys@gmail.com

Graphene, as a single-layer of carbon atoms arranged in a hexagonal lattice, has excellent electrical conductivity and optical transmittance with great potential to replace conventional transparent conductive electrodes in optoelectronic device applications such as solar cells and photodetectors. In this work, we experimentally investigated the impact of junction area on the device performance parameters of Graphene/n-type Silicon (Gr/n-Si) based Schottky photodiodes. For the experiments three batches of Gr/n-Si photodiode samples were produced based on various sized CVD grown monolayer graphene layers transferred on individual n-Si substrates. The fabricated devices exhibited strong Schottky diode character and had high spectral sensitivity at 905 nm peak wavelength. The optoelectronic measurements showed that the spectral response of Gr/n-Si Schottky photodiodes has a linear dependence on the active junction area. The sample with 20 mm^2 junction area reached a spectral response of 0.76 AW^{-1}, which is the highest value reported in the literature for self-powered Gr/n-Si Schottky photodiodes without the modification of graphene electrode. In contrast to their spectral responsivities, the response speed of the samples was found to be lowered as a function of the junction area. The experimental results demonstrated that the device performance of Gr/n-Si Schottky photodiodes can be modified simply by changing the size of the graphene electrode on n-Si without need of external doping of graphene layer and/or engineering Gr/n-Si interface. Our study may serve towards the standardization of junction area for the development of high-performance Gr/Si based optoelectronic devices such as solar cells and photodetectors operating in the spectral region between ultraviolet and near-infrared.

S8

Accelerated thermal aging effects on carbon-based Perovskite solar cells: a Joint experimental and theoretical analysis

Pica, G.*[1], Degani, M.[1], Schileo, G.[1], Girella, A.[1], Milanese, Ch.[1], Martineau, D.[2], Andreani, L.C.[3], and Grancini, G.[1]

[1]*Department of Chemistry - University of Pavia, Via T. Taramelli 14, 27100 Pavia, Italy*
[2]*Solaronix S.A Rue de l'Ouriette 129, Aubonne 1170, Switzerland*
[3]*Department of Physics - University of Pavia, Via A. Bassi 6, 27100 Pavia, Italy*
giovanni.pica01@universitadipavia.it

In the search for stable perovskite photovoltaic technology, carbon-based perovskite solar cells (C-PSCs) represent a valid, stable solution for near-future commercialization. However, a complete understanding of the operational device stability calls for assessing the device robustness under thermal stress. Herein, the device response is monitored upon a prolonged thermal cycle aging (heating the device for 1 month up to 80 °C) on state-of-the-art C-PSCs, often neglected, mimicking outdoor conditions. Device characterization is combined with in-house-developed advanced modeling of the current–voltage characteristics of the C-PSCs using an iterative fitting method based on the single-diode equation to extrapolate series (RS) and shunt (RSH) resistances. Two temperature regimes are identified: Below 50 °C C-PSCs are stable, and switching to 80 °C a slow device degradation takes place. This is associated with a net decrease of the device RSH, whereas the RS is unaltered, pointing to interface deterioration. Indeed, structural and optical analyses, by means of X-ray diffraction and photoluminescence studies, reveal no degradation of the perovskite bulk, providing clear evidence that perovskite/contact interfaces are the bottlenecks for thermal-induced degradation in C-PSCs.

S9

Investigation on the negative capacitance of the Au/ZnO/n-GaAs structures at room temperature for 1 MHz

Erbilen Tanrıkulu, E.* and Akın, B.

Department of Physics, Faculty of Science, Gazi University, Ankara, Turkey
eerbilen@gazi.edu.tr

In order to investigate the changes in the capacitance and conductance of the Au/ZnO/n-GaAs (MIS) structures with applied bias voltage, they were measured in the wide range of voltage at 1 MHz and room temperature. Experimental results show that, both the C-V and G/ω-V plots have the inversion, depletion and accumulation regions such as the metal-oxide-semiconductor (MOS) capacitor. Also, the negative capacitance (NC) behavior has been observed in C-V plots at around 1.5 V. The negative capacitance (NC) phenomenon can be explained by the decrease in the charge on the electrodes with increasing voltage and series resistance (R_s) of the structure. Furthermore, the minimum value of C observed at the accumulation region corresponds to the maximum value of G/ω and this change between C and G/ω can be defined as the inductive behavior. Some basic parameters such as the Fermi energy level (E_F), doping concentration of donor atoms (N_D), depletion layer width (W_d), and barrier height (Φ_B) were calculated from the linear part of reverse bias C^{-2} vs V plot. Both the C-V and G/ω-V plots were also corrected to eliminate the effect of R_s. After correction, while the value of C start to increase, G/ω decrease at accumulation region.

S10

Revealing the photo-triggered structural dynamics of photo-responsive MOFs grown on oriented ceramic thin films

Klokic, S. *[1], Naumenko, D.[1], Marmiroli, B.[1], Paolo, F.[2], and Amenitsch, H.[1]

[1] *Institute of Inorganic Chemistry, Graz University of Technology, 8010 Graz, Austria*
[2] *Institute of Physical and Theoretical Chemistry, Graz University of Technology, 8010 Graz, Austria*
sumea.klokic@tugraz.at

At present, most developments based on microelectronics, sensing and optical devices rely on the technology of thin-film fabrication. Recently, numerous functional Metal-Organic Frameworks (MOFs) thin films have been exploited and applied in these fields. This is mainly due to the versatile chemical nature of MOFs that allows to modulate their physical properties as well. These include selective engineering of the MOF porosity, but also to implement susceptibilities to external stimuli such as light to realize a photo-responsive system. One of the most straightforward strategies to modulate the MOF structure by light is to infiltrate MOF pores with photo-responsive chromophores of suitable size (e.g. azobenzene). Herein, we pursue oriented ceramic thin films based on copper hydroxide nanobelts converted to Cu_2bdc_2, [1] which serves as the supporting MOF for the subsequently grown flexible zinc-based DMOF-1 [2]. The infiltration of DMOF-1 by azobenzene was confirmed by ATR and Raman spectroscopy. Our research aims to elucidate the photo-triggered structural dynamics in this class of materials induced by the reversible photo-isomerization of azobenzene between its *trans* (ground state) and *cis* structure (excited state). Hence, the photo-response of the infiltrated azobenzene inside the MOF pores forces the flexible framework structure to adapt to the *trans/cis* isomerization of the chromophore. At the picosecond-pump probe station at the Austrian SAXS beamline at Elettra synchrotron radiation source we successfully pumped the infiltrated thin films by UV light (342 nm) and induced the forward switching of the flexible crystalline thin film, whilst the recovery of the system was achieved by illumination with blue light. The thereby provoked structural transitions of the crystalline film induced by the photo-switchable chromophore were pursued by time-resolved Grazing-Incidence Small Angle X-Ray Scattering (GISAXS) measurements. Thus, we demonstrate the very first photo-switch in oriented MOF thin films accompanied by structural changes of the host system. Further, pursuing our concept proposed herein allows us to reversibly switch the MOF system in centimeter-scale on-demand, which makes the system highly attractive for the development of smart materials in e.g., optoelectronic applications. These results will allow us to gain further knowledge on the underlying structural transitions with the ultimate goal to understand and characterize the photo-induced dynamics in crystalline solids.

References:

[1] Falcaro, P.; Okada, K.; Hara, T.; Ikigaki, K.; Tokudome, Y.; Thornton, A. W.; Hill, A. J.; Williams, T.; Doonan, C.; Takahashi, M.; Falcaro, P. Nature materials 2017, 16, 342.

S11

Illumination effects on the capacitance/conductance-voltage characteristics of Au/(PVC:Er_2O_3)/n-Si (MPS) type structure for 0.5 MHz at room temperature

Ulusoy, M.* and Altındal, Ş.

Department of Physics, Faculty of Sciences, Gazi University, Ankara, Turkey
ulusoymurat@gazi.edu.tr

In this study, Au/(PVC:Er_2O_3)/n-Si (MPS) structure was fabricated and then its capacitance/conductance -voltage (*C/G-V*) measurements were performed both in dark and under 100 mW.cm^{-2} illumination intensity in voltage range of -2/8V by 50 mV step. The basic electrical parameters such as doping-concentration of donor-atoms (N_d), barrier-height (Φ_B), depletion-layer width (W_d), maximum-electric field (E_m) at junction, and series-resistance (R_s) were obtained from the reverse-bias C^{-2}-V plots as 1.44x10^{15} cm^{-3}, 0.72 eV, 4.72x10^{-5} cm, 14.7 kV/cm, 168 Ω in dark and 4.93x10^{15} cm^{-3}, 0.74 eV, 2,69x10^{-5} cm, 28.7 kV/cm, 138 Ω under illumination, respectively. Voltage dependent profile of Illumination induced density of surface states (N_{ss}) was also extracted from the difference between dark and illumination C-V plot at about 1.5x11 eV^{-1}.cm^{-2} mean value. It is clear that there is a shrinking in W_d, increase of N_d, Φ_B, E_m, and decrease of R_s due to restructure and reordering of N_{ss} under illumination effect. In addition, all these results show that (PVC:Er_2O_3) polymer interfacial layer can be successfully instead of an insulator layer in respect of low-cost, flexibility, easy grown method.

S12

Effects of dielectric spacer on absorbance characteristics of a dual-band large-H shaped perfect absorber

Onur, A.* and Turkmen, M.

Department of Electrical and Electronics Engineering, Erciyes University, Kayseri, Turkey
aytac50@gmail.com

In this study, a novel perfect absorber (PA) array based on large H nanoparticles for infrared sensing applications is presented. Proposed PA array has a dual-band spectral response, and the locations of resonances can be adjusted by varying the geometrical dimensions of the structure. Nearly unity absorbance is obtained from the PA array for both resonances. Different dielectric spacers (MgF_2, SiO_2, and Al_2O_3) are used to investigate the effects of dielectric spacer on the absorbance characteristics of proposed PA array. Absorbance characteristics of PA array are analyzed by using finite difference time domain (FDTD) method. In order to control the refractive index sensitivity of proposed PA array, the structures by loading cladding mediums with different refractive indices are analyzed. Due to the high refractive index sensitivity and near-field enhancement, and nearly unity absorbance, the proposed dual-band PA array with adjustable spectral responses can be used for infrared sensing applications.

S13

In operando synchrotron GISAXS studies of nanostructured Pt films show preferential alignment during templated electrodeposition

Wieser, Ph.A.,*[1,2], Moser, D.[3], Gollas, B.[4] and Amenitsch, H.[1,2]

[1] *Institute of Inorganic Chemistry, Graz University of Technology, Graz, Austria*
[2] *Austrian SAXS beamline, Elettra Sincrotrone Trieste, Trieste, Italy*
[3] *Institute of Electron Microscopy and Nanoanalysis, Graz University of Technology, Graz, Austria*
[4] *Institute for Chemistry and Technology of Materials, Graz University of Technology, Graz, Austria*
philipp.wieser@tugraz.at

Well-constructed porous materials have an essential role in a wide range of applications, including energy conversion and storage systems, electrocatalysis, photocatalysis, and sensing. The tailored design of the pores (i.e. pore size, structure, orientation, surface area, etc.) plays an essential role in enabling their full potential. Lyotropic liquid crystal templating represents a versatile and facile way of producing mesoporous materials, by electrodeposition from the desired mesophase containing the liquid crystal template and the metal salt. In the present work, the electrodeposition of mesoporous Pt was studied via Grazing Incidence Small Angle X-Ray Scattering (GISAXS), a non-destructive surface-sensitive technique for structure determination in the nm-regime. The combination of GISAXS with the brilliant synchrotron radiation source at the ELETTRA-Sincrotrone Trieste enabled *in operando* monitoring of the deposited film regarding nanostructure and orientation of the mesopores. The scattering pattern of the porous films showed hexagonal pore structures with centre-to-centre distances of about 6 nm and preferential alignment orthogonal to the sample surface.

S14

Optical system design in LED lighting luminaires

Koç, E.* and Özdür, İ.T.

Electrical and Electronics Engineering, TOBB University of Economics and Technology, Sogutozu Street No: 43, Sogutozu, Ankara, 06560 Turkey
esrakoc@etu.edu.tr

The use of power efficient luminaires not only provides significant energy savings for the environment, but also contributes to the national economy by their longer expected lifespan, lower maintenance and operational cost, and higher productivity due to better lighting. The two main factors affecting led armature efficiency are the electrical and optical losses. The optical power loss can reach to 20% due to both lens and glass breaks. Reducing this value increases the power efficiency of the illumination. One of the most important and critical process in luminaire is the optical system design. The bare lamp may not always give the desired light distribution; therefore, novel optical system designs are needed to engineer the light distribution and direction for higher efficiency. The use of LED (light emitting diode) light sources is increasing in daily lighting mainly due to higher efficiency. However, the illumination properties (divergence, illumination power distribution, etc.) of LEDs are different from traditional lamps hence new optical designs are needed to take full advantage of the LED light sources. In this work, we designed a novel optical system for LED based illumination system. In our talk, first we will introduce our LED light source properties and then explain the optical system design approach. Finally, we will show the results of the LED light source implemented with our optical design. The use of LED light sources is increasing, and we hope that our work will serve to the development of domestic lens design products for LED lighting luminaire.

S15

Development of sensors based on functionalized carbon nanotubes

Musayeva, N.N.[1*], Quluzade, S.A.[1], Elizade, M.T.[1] , Ferrari, C.[2], Frigeri, C.[2], Bosi, M.[2], Trevisi, G.[2], Francesco, S.[3], Francesco, R.[3], and Baldini, L.[3]

[1]Institute of Physics, ANAS, H.Javid ave.131, AZ1073 Baku, Azerbaijan
[2]IMEM-CNR, Area delle Scienze 37A, 43124 Parma, Italy
[3]Dipartimento di Scienze Chimiche, della Vita e della Sostenibilità Ambientale Universita' di Parma, Parco Area delle Scienze 17/a, 43124 Parma
nmusayeva@physics.ab.az

Sensors have been invented for many years and applied in almost every area of our lives (in everyday life, public places, information technology, general production areas, military, etc.) and they are even needed more time to times. So far, sensors have been developed which are based on the various materials and technologies and they have both advantages and disadvantages. Some of them are based on difficult and expensive technology, some take up a large area and become immovable, and some are not selective, or recovering for very long time, and require high temperatures to operate. Carbon nanotubes have been in the spotlight of scientists for many years with their unique properties and due to their good electrical, mechanical, thermal and absorbent properties, they have the potential to be applied to everything from electronics to heavy industry. They are (stable to the effects of the environment), they are simple and light and the surface areas are extremely large and can be manipulated easily, that's why they are object of our research. The formation of functional groups on the outer walls of carbon nanotubes further activates them and increases their application areas. As an example, functionalized carbon nanotubes are well dispersed in different polymers and nanocomposite materials with new properties are obtained. Functionalized carbon nanotubes (CNT) are highly responsive to their physical and chemical environment. CNTs surfaces can be functionalized by different methods. In this work, we will discuss functionalization of carbon nanotubes for sensor application.

S16

Design and fabrication of passive matrix quantum dot red-light emitting diode via spin coating or ink-jet printing technique

Bozkurt, H.*[1], Diker, H.[1], Özgüler, Ş.[1], Ünlütürk, S.S.[2], Özçelik, S.[2], and Varlıklı, C.[1]

[1]*Department of Photonics, Izmir Institute of Technology, 35430 Urla-Izmir, Turkey*
[2]*Department of Chemistry, Izmir Institute of Technology, 35430 Urla-Izmir, Turkey*
hakanbozkurt@iyte.edu.tr

Quantum Dots (QDs) are nanoscale light emitting inorganic crystals which known for their features like narrow emission bandwidth, high material stability and solution processability by using ligands. Although they have a variety of applications in photonics field, they also get attraction in display technologies. Displays available in the market that based on QDs were having benefits of photoluminescent properties of them. For better contrast, electroluminescent QD displays are still developing, and it seems that they will be in the market soon [1].
Possible color gamut of QDs is larger than HDTV standard color triangle. Each corner of this triangle represents subpixel colors in displays; Red, Green and Blue. This study focused on red-light emitting QD (CdSSe/ZnS), which was prepared by hot injection synthetic method. The red-light emitting QD was utilized as emissive layer in passive matrix quantum dot light emitting display (PMQLED). Conventional device structure of "ITO/PEDOT:PSS/PVK/QD/ZnO/LiF/Al" was used in the fabrication of PMQLED. The display consists of 16 x 16 arrays of individual pixels within 1 mm^2 active area. A controller device, which has 7 mm^2 active area also fabricated for performing characterizations. In this study, two different solution processed coating techniques (spin coating or ink-jet printing) used for the emissive layer (QD) of the fabricated device. Text displaying on PMQLED was achieved via driver circuit that was designed by our group.

Keywords: Quantum Dots, red QLED, PMQLEDs, ink-jet printing, spin coating

Acknowledgment
This work is supported by the research project funds of Scientific Research Council of Turkey (TUBITAK) (Project #: 115F616).

References:
[1] https://www.nanosysinc.com/news/2020/12/4/boe-unveils-the-worlds-first-55-inch-uhd-amqled-display

S17

Pulsed infrared laser crystallized silicon and germanium thin-films

Korkut, C.[1], Çınar, K.[2], and Bek, A.[1,3*]

[1]*Department of Physics, Middle East Technical University (METU), 06800 Ankara, Turkey*
[2]*Department of Physics, Gebze Technical University, 41400 Kocaeli, Turkey*
[3]*Center for Solar Energy Research and Applications (GÜNAM), 06800 Ankara, Turkey*
bek@metu.edu.tr

Laser crystallization of amorphous semiconductor layers is an active research field in photonic applications [1]. In literature, typically single laser pulses are used to examine the absorption mediated crystallization of amorphous silicon (Si) and germanium (Ge). The slow quenching regime dynamics for laser crystallization with highly overlapping infrared nanosecond pulses was examined experimentally and theoretically. In contrast to commonly used >10 micrometer thick layers on ~700°C heated substrates, in present study, the thicknesses of deposited amorphous Si layers were decreased down to 1 micrometer range, and the laser crystallization was performed at room temperature [2]. Increasing use of Si in thin-film transistors and photovoltaic applications drive researchers to find cost-effective and efficient ways of manufacturing crystalline Si films on various types of substrates. Similar to Si, high quality crystallization of substrate deposited amorphous Ge films has attracted interests for its uses as IR sensitive material due to its lower band-gap. Understanding the mechanism of the laser crystallization process of semiconductor films by pulsed lasers becomes crucial. We will reveal the laser crystallization mechanism of Si thin films in macroscopic scales by considering heat transfer and accumulation dynamics. The figure shows optical (left panel) and the EBSD (right panel) images of laser crystallized Si with millimeter sized crystalline domains [3]. Our motivation is to describe the dynamics of the laser crystallization of semiconductor films to provide a complimentary guide to produce device-grade crystal Si and Ge films by infrared pulsed laser without employing preheated substrates. This work is supported by TÜBİTAK under grant nr. 115M061.

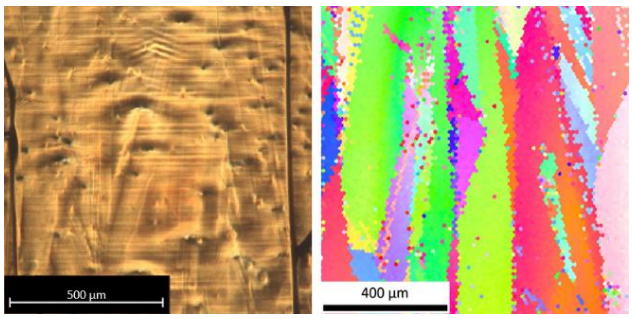

References:

[1] K. Cinar, M. Karaman, and A. Bek, ACS Omega 3 (5), 5846–5852 (2018)
[2] V. Türker, M.E. Yagci, S.H. Salman, K. Cinar, S.K. Eken, and A. Bek, Instruments 3, 31 (2019)
[3] K. Cinar, C. Yesil, and A. Bek, J. Phys. Chem. C 124, 976−985 (2020)

S18

Perylene based efficient TADF down conversion WOLEDs

Aksoy, E.*[1,2,3], Danos, A.[2], Varlikli, C.[3], and Monkman, A.P.[2]

[1]*Solar Energy Institute, Ege University, 35100, Bornova, Izmir, Turkey*
[2]*Department of Physics, Durham University, Durham, DH1 3LE, UK*
[3]*Department of Photonics, Izmir Institute of Technology, 35430, Urla, Izmir, Turkey*
erkanaksoy@iyte.edu.tr

In this presentation, our study published at "Dye. Pigment. 183 (2020) 108707" will be summarized[1]. To produce efficient downconverter (DC) layer and to good white balance, high fluorescent yellow (PTE) and orange emitting perylene (PDI) derivatives dispersed in optic transparent polymer (host) were deposited in multiple low-concentration spin-coating steps on top of blue thermally activated delayed fluorescence (TADF) organic light emitting diode (OLED). Part of the blue EL was filtered by PDI and, emitted its own orange emission. Even though white light was produced with the combination of white and orange, optimal white light CIE coordination could not be approached. This was due to the change in the coordinates of the filtered Blue EL spectrum on the CIE. In order to achieve optimal white light coordinates, PTE was coated on the PDI layer and as a result of their optimization, excellent white color balance (CIE x, y; 0.33, 0.33) with perfect stability, good color rendering (CRI 80), and a high maximum device efficiency (17.2%) produced by navigating the CIE coordinates[1].

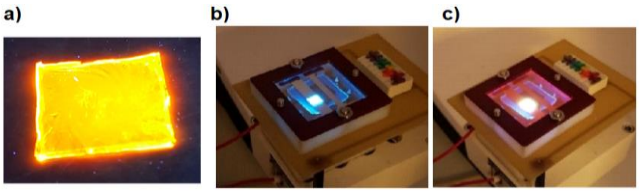

Fig1. a) Image of the optimal DC layer under UV light, b) photo of blue TADF-OLED and c) hybrid DC-TADF-WOLED [1].

Acknowledgment
[EA thanks The Scientific and Technological Research Council of Turkey (TUBITAK) 2214-A Program (Appl. # 1059B141800476) who supported this research financially. EA and CV thank to the project support funds of TUBITAK grant #119F031 for financial support. AD and APM were supported by the Hyper OLED project from the European Unions's Horizon 2020 Research and Innovation Program under grant agreement number 732013.]

References:
[1] E. Aksoy, A. Danos, C. Varlikli, A.P. Monkman, Navigating CIE Space for Efficient TADF Downconversion WOLEDs, Dye. Pigment. 183 (2020) 108707. doi:10.1016/j.dyepig.2020.108707.

S19

Effect of refractive inhomogeneity on the efficiency of SHG in optical fiber

Kasumova, R. J.[1], Tagiev, Z.H.[2], and Amirov, Sh.Sh.*[2]

[1]*Physics Department, Baku State University, acad. Z. Khalilov str. 23, AZ1148, Baku, Azerbaijan*
[2]*Department of Medical and Biological Physics, Azerbaijan Medical University, A. Gasimzade str., 14, AZ 1022, Baku, Azerbaijan*
phys_med@mail.ru

In this paper the effect of inhomogeneity of refractive index on the efficiency of second harmonic generation in an optical fiber is studied in the constant intensity approximation, taking into account the reverse reaction of excited wave on the phase of exciting one. The pulse of Gaussian shape has played the role of pump wave. Effect of regular inhomogeneity of the refractive index on the efficiency of SHG was observed at various levels of pump wave intensity. It was shown that due to inhomogeneity of refractive index one can control the duration of output pulse in optical fibers. Results obtained were compared with the results obtained in the constant field approximation as well as the case of homogeneous medium.

Keywords: regular refractive index inhomogeneity, optical fiber, pulse duration, constant intensity approximation.

References:

[1] F.S. Ghen. Optically induced change of refractive indices in $LiNbO_3$ and $LiNaO_3$. Appl. Phys. 1960, 40(8), 3389-3396.
[2] S.A. Akhmanov, D.P. Krindach, A.P. Sukhorukov, R.V. Khohlov. JETP Letters, 1967. 6(2), 509-513.
[3] G. Agrawal, Nonlinear Fiber Optics. Academic, San-Diego, Calif. (1995).
[4] L. F. Mollenauer, J. P. Gordon. Solitons in Optical Fibers. Fundamentals and Applications. Elsevier, 2006. 296p.
[5] Sh. Shermin A. Khan and Md.S.Islam Pulse broadening induced by second order and third order dispersion in a dispersive fiber. Journal of Information and Communication Technologies, V.3, issue 4, 2013 p.16-21

S20

0D and 2D nanocrystals for efficient electroluminescent devices

Mutlugün, E.

Department of Electrical-Electronics Engineering, Abdullah Gul University, Kayseri
evren.mutlugun@agu.edu.tr

Semiconductor nanocrystals are promising materials for lighting and display technologies for their superior color conversion properties, high absorption coefficient and photo-stabilities. In general, 0D quantum dots based on II-VI and III-V materials and recently emerged 2D nanoplatelets can be excited by optical or electrical pumping and provide high efficiency light generation. Thanks to the quantum confinement, they possess spectrally pure emission and replace the conventional phosphor materials especially for display technologies. They have started to emerge in the display market, providing novel solutions for LCD backlighting to generate superior white light and thus gain commercial importance. Not only for optical pumping, but also for the electrical pumping, nanocrystals can generate the formation of excitons which can be utilized for the display technologies. In this respect, new generation high performance quantum dot LEDs that can provide superior light purity, stability, and brightness will be on focus of technology in the coming years. This talk will emphasize on our recent work on the development of synthesis of colloidal nanocrystals and electroluminescent devices based on them.

S21

Factors affecting the efficiency of the LED

Jabbarov, R.B.[1.2*], Gahramanova, G.K.[1,2], and Orujov, T.Y.[1,2]

[1]Institute of Physics, Azerbaijan National Academy of Sciences, 135 H. Javid ave., AZ1143 Baku, Azerbaijan
[2] High Technology Research Center, Ministry of Transport, Communications and High Technologies of the Republic of Azerbaijan, 4 Inshaatchilar ave., AZ1073 Baku, Azerbaijan
rasim.jabbarov69@gmail.com

Rapid development of high brightness efficient LEDs is affected by many factors, from the selection of the substrate material for growing of the LED chip to the packaging of white LED such as lattice mismatch between GaN LED structure and chosen substrate, green-gap problem, size of phosphorus and applying technology of phosphors on LED chip, packaging etc. In this study, two key factors affecting the efficiency of LEDs, the growing of a high-quality GaN structure and the design of Phosphorus are investigated.

In this work, to improve the quality of white LED, we have mainly analyzed two factors. One of them is the impact of carbon nanotube (CNTs) to improve the crystal quality of the GaN structures by applying CNT as an intermediate layer between sapphire substrate and GaN buffer layers. Second one is the application of multiple pyramid-shaped phosphor structures to negate the reflection and re-absorption of photons in the LED package.

Large differences in fundamental properties such as lattice constants a between GaN layer and sapphire substrate generate structural defects and high density of threading dislocations (TD) that leads to deterioration of optical and structural properties. Therefore, applying hexagonal structured CNTs thin layers with high thermal stability on sapphire as primary layer plays a role to decrease lattice mismatched between sapphire and GaN. Photoluminescent and SEM analyzes showed that the structural quality of the GaN bulk layer increases with the presence of CNT.

Also, such effects in the LED package as total internal reflection and back scattering of photons lead to the absorption of emitted photons by the chips and substrate, which can potentially cause the losses in the LED's light output. Therefore, applying pyramid-shaped phosphor layer to the GaN LEDs, which changes the optical geometry of photon propagation, can improve such negative effects as total internal reflection and back scattering of photons inside the LED package. Photoluminescent analyzes showed increase in luminous flux and efficiency with the use of pyramid-shaped phosphor layer.

S22

Design and analysis of 3x continuous zoom SWIR lens

Selimoğlu Ö.*[1], Tanyeli B.[2], Sağlam S.[2]

[1]*Department of Energy Engineering, Faculty of Engineering, Ankara University, 06380 Gölbaşı, Ankara, Turkey*
[2]*Department of Physics, Faculty of Sciences, Gazi University, 06500 Teknikokullar, Ankara, Turkey*
oselimoglu@ankara.edu.tr

Imaging systems in the Short-Wave Infrared (SWIR) provide important information that are not perceived by the human eye. These systems have become very common in recent years as a result of the progress made in sensor technologies and the need also has been increased for the lens groups specifically designed for SWIR band.
Commercially available lenses are optical systems commonly designed for the visible region. When these systems are used for the SWIR region, their MTF performance decreases due to chromatic aberration. Moreover, the coatings used in these lens systems do not work well in the SWIR region and the light transmittance of the lens decreases dramatically. Some lens manufacturers are trying to adapt existing lens designs by just recoating for the SWIR band but significant reductions in image quality (MTF) arises as the design of the lens is inappropriate for the SWIR band.
In this study, optical design and analysis of 3x zoom SWIR lens has been accomplished to be used with sensors up to 12 mm diagonal for long distance observation applications. The F-number value, which directly affects the amount of light collected by the lens system, has been kept as low as possible. Targeting low F-number is important as it makes SWIR lenses more effective for night time or foggy weather conditions where the illumination is limited. The focal length is adjustable between 30mm and 90mm, while the f-number of the system remains constant at 2.0. As a result of constant f-number through zoom levels, the exposure time of the detector does not need to be changed while zooming. Low f-number increases the signal-to-noise ratio (SNR) by improving the light collection ability of the lens and also makes it possible to obtain higher contrast images by reducing the diffraction effects. Defocusing is prevented by design by using a third moving group (focus group) next to the magnification group and also focal distortion caused by temperature changes is minimized.

S23

The action of losses at three-wave mixing in metamaterials

Kasumova, R.J.[1] and Kerimli, N.V.[2]*

[1]*Physics Department, Baku State University, acad. Z. Khalilov str. 23, AZ1148, Baku, Azerbaijan*
[2]*Corresponding author:(Medical and Biological Physics department, Azerbaijan Medical University Samed Vurgun str.167, AZ1022 Baku, Azerbaijan*
nazaket_kerimli@mail.ru

Frequency conversion process is examined during three wave interactions within metamaterials with negative index of refraction. Conditions which allow to understand the propagation of wave with constant amplitude within medium of negative refraction and its amplification during three wave interactions are examined in presented paper. Analytical expression for amplitude of wave with negative index of refraction is found at phase matched condition. It is obtained that the counterwave loses within metamaterials can be met and adjusted. Impact of straight waves intensities onto generation efficiency also has been examined when the propagation of counterwaves with constant amplitude and amplification of their intensities are possible. It is shown that for each required experiment one can estimate the optimal parametrical amplification of signals by calculation of experimentally required losses and initial value of pump and sum waves within metamaterials of negative index of refraction. Furthermore, it is presented that it is possible to determine parameters which have a strong impact on efficiently parametrical three waves interaction.

S24

Intensity moments technique as a simple and reliable tool for measuring 3D vortex spectra of structured beams

Akimova, Y.* and Bretsko, M.

V. I. Vernadsiy Crimea Federal University, Institute of Physics and Technology (RF)
ak1mova.yana@yandex.ru

Multiple singularities in structured vortex beams form a fine structure of the intensity and phase pattern and insert into it a variety of features associated with orbital and spin angular momentum, informational entropy, topological charge and resistance to weak external perturbations. But all this variety of properties is specified by a special combination of amplitudes and phases of vortex modes in the beam composition. In order to form structured beams and control their properties in real time, a simple and reliable measurement technique and a device based on it are required. We have developed and implemented such a digital technique for measuring the 3D mode spectrum for structured beams employing the intensity moment approach, discussed in detail in our articles *Opt. Lett*., *432(2018)5635– 5638*; *Appl. Opt.*, *58 (2019) 5748–5755*. In our report, we consider the use of the intensity moments technique in speckle patterns and fields caused by an avalanche of optical vortices with a single spherical (or cylindrical) lens and appropriate computer software.

S25

Simulation of a semiconductor laser using AWR design environment

Yergin, H.* and Özdür İ.T.

Department of Electrical and Electronics Engineering, TOBB University of Economics and Technology, Ankara, Turkey
hyergin@etu.edu.tr

The use of fiber optic cables is increasing due to their advantages such as high bandwidth, longer transmission distance and immunity to electromagnetic interference (EMI) in communication systems. Most of the fiber communication is used for digital communication, however, with the implementation of 5G systems direct radio frequency (RF) transmission is also found as an effective way of data transmission. RF over fiber is the transmission of the radio signal between the user and the communication system centers at high speed by modulating the light without subjecting it to another frequency conversion process. The simulation of fiber optic based digital communication is a well-established area and there are very precise commercial simulation environments. However, it was shown that RF transmission over fiber systems does not work well with these environments as the system has both optical and RF components. In our work, we aim to simulate the components and processes in a purely RF simulation environment. AWR Microwave Office program is a free program for academic studies developed for Microwave Circuit Design. Although it has powerful RF libraries, it does not have optoelectronics libraries. Since this study is simulated with radio frequency opto-electronic materials, firstly, the opto-electronic components to be used are modelled. The semiconductor laser is the most important and complicated component of an RF transmission over fiber system. We simulated a semiconductor laser and analyzed its modulation properties using AWR simulation environment. In our talk, we will present the simulation approach for a single frequency semiconductor laser and show the simulation results and the current progress.

S26

Reconstructing polarisation with a digital micro-mirror device

Dudley A.*, Singh K., Nape I. and Forbes A.

School of Physics, University of the Witwatersrand, Private Bag 3, Johannesburg 2050, South Africa
angela.dudley@wits.ac.za

In this work, Stokes's polarimetry is used to extract the polarization structure of optical fields from only four measurements as opposed to the usual six measurements. Here, instead of using static polarization optics, we develop an all-digital technique by implementing a Polarization Grating (PG) which projects a mode into left- and right-circular states which are subsequently directed to a Digital Micromirror Device (DMD) which imparts a phase retardance for full polarization acquisition. We apply our approach in real-time to reconstruct the State of Polarization (SoP) and intra-modal phase of optical modes.

S27

A tunable plasmonic sensor-based metamaterial and graphene with high sensitivity

Lotfi F.*[1], Sang-Nourpour N.[2], and Kheradmand R.[1]

[1]*Physics Faculty, Tabriz University, Tabriz, Iran*
[2]*Department of Mechanical Engineering, University of Alberta, Edmonton, Canada*
f.lotfi@tabrizu.ac.ir

We present a novel and tunable plasmonic refractive index (RI) sensor based on Mach-Zehnder interferometer (MZI). Our nano-scale plasmonic structure is capable to confine surface-plasmon polaritons along the interfaces. Plasmonic waveguides are employed in MZI that made of lossy dispersive media with positive and negative electromagnetic susceptibilities, including metamaterial and graphene, interfaces with dielectrics.

Surface-plasmon polariton is sensitive to the RI of surrounding media. Therefore, we compare the effect of media with different electromagnetic properties in the sensor structure and the sensor sensitivity. The proposed sensor is capable to detect various samples with different RIs. We introduce the sensor structure that is composed of slab metamaterial-dielectric-metamaterial waveguides with a sample domain is located near the up branch of MZI. A monolayer graphene is employed in the boundary between metamaterial and dielectric. This sensor structure shows high sensitivity compared to the previous literature.
Also, we able to tune our sensor structure by applying a gate voltage to a monolayer of graphene in the boundary of metamaterial-dielectric in the waveguide. The proposed tunable sensor structure shows the shift in transmission spectra that affects the sensor sensitivity. Our sensor structure has application to detect liquid/gas chemical samples, medical diagnosis and environmental monitoring.

S28

Accelerated polarization structures with Bessel beams

Buono, W. T.*, Singh, K., Dudley, A., and Forbes, A.

School of Physics, University of the Witwatersrand, Private Bag 3, Johannesburg 2050, South Africa
wagner.tavaresbuono@wits.ac.za

Optical fields can often show unexpected effects when interference effects are used [1]. Examples of these are angularly accelerating beams. In this work we present a novel structure of light that exhibits State-of-Polarization (SoP) structures that rotate with acceleration and deceleration when propagating in free space. We achieve this by creating a superposition of beams with accelerated transport of intensity in different polarization components, as in:

$$\vec{E} = J_l(rk_{r1})\left[\cos\left(\frac{\theta}{2}\right)e^{il\phi} + \sin\left(\frac{\theta}{2}\right)e^{-il\phi}\right]e^{ik_{z1}z}\hat{e_1} \; +$$

$$J_l(rk_{r2})\left[\cos\left(\frac{\theta}{2}\right)e^{-il\phi} + \sin\left(\frac{\theta}{2}\right)e^{il\phi}\right]e^{ik_{z2}z}\hat{e_2} \; .$$

In this way the intensity profile remains constant, but each polarization projection changes differently [2]. The Stokes vector for each point of the transverse profile exhibits a circular trajectory in the Poincaré sphere, showing an accelerated rotation around the axis of the generating polarization basis. We hope that this vector field with non-trivial structures can be used to study the interaction of vector light with matter [3].

References:

[1] C. Schulze, F. S. Roux, A. Dudley, R. Rop, M. Duparré, and A. Forbes, “Accelerated rotation with orbital angular momentum modes,” Phys.Rev. A 91, 043821 (2015).
[2] K. Singh, W.T. Buono, A. Forbes, and A. Dudley, “Accelerating polarization structures in vectorial fields,” Opt. Express 29, 2727 (2021).
[3] J. Wang, F. Castellucci and S. Franke-Arnold,” Vectorial light–matter interaction: Exploring spatially structured complex light fields.” AVS Quantum Sci. 2, 031702 (2020).

S29

Numerical modeling of plasma antennas, application areas, investigation of the effect of nano-phase materials on plasma antenna

Başlar, G.K.[1], Çakır, S.*[2], and Sağlam, N.[1]

[1]*Hacettepe University, Department of Nanotechnology and Nanomedicine, Beytepe, Ankara, Turkey*
[2]*Middle East Technical University, Physics Department, Ankara, Turkey*
cakir@metu.edu.tr

This research investigates analysis of a novel antenna design using plasma antenna technologies. Plasma antenna is a new antenna technology that uses partially or fully ionized gas as a conductive medium instead of metal to form an antenna. Plasma antennas, which are currently under development, are a type of radio frequency antenna that uses plasma as a guide medium for electromagnetic radiation. The rapid growth in both wireless communication and radar systems in recent years has led to a simultaneous growth in the possible applications and requirements of antennas. These new requirements include fast reconfigurability for compactness, suitability, versatility and frequency agility. Recently, researches on the use of ionized gases or plasmas as conductive media that can meet these requirements in antennas have gained momentum. These types of plasma antennas can be presented as an alternative to metal antennas in current applications, considering the general technical requirements.

In this study, it is aimed to perform numerical analysis of plasma column antenna using finite element method (Finite Element Method-FEM) with COMSOL MULTIPHYSICS simulation software. With this simulation program, we will be using Finite Element Method (FEM) to solve coupled Plasma and Maxwell equations. Parameters such as conductivity, plasma frequency, collision frequency, longitudinal and radial permeability of the plasma column used as an antenna to analyze the plasma antenna will be obtained.

The important issue that needs improvement is the durability of the glass tube of the plasma antenna. Efforts will be made to increase the durability of the tube, which is not durable compared to metal antennas. For this purpose, with the advantages offered by nanotechnology, the tube (usually made of glass) material used for the tube of the plasma antenna will be modeled with nano-phase materials, and studies to increase the durability of the plasma antenna and analyze the parameters of the modeled plasma antenna.

An important step has been taken in the application of the plasma antenna with the reinforced frame and it is expected to provide input regarding its use in difficult conditions.

S30

Approaching real-time non-degenerate ghost imaging by deep learning

Moodley, C.S.*, Sephton, B., Rodríguez-Fajardo, V., and Forbes, A.

School of Physics, University of the Witwatersrand, Jan Smuts Avenue, Johannesburg, 2000, South Africa.
chane13.m@gmail.com

Entangled photon pairs are utilized in quantum ghost imaging to facilitate an alternative image acquisition method. Individually, the information contained in each photon does not allow for image reconstruction, however, the image can be reconstructed by considering the correlations that exist between the entangled photon pair. Interestingly, these photon pairs can be either degenerate or non-degenerate in nature. Non-degenerate ghost imaging offers the ability to image with wavelength bandwidths where spatially resolving detectors are impractical or ineffective. Due to the scanning nature of the technique and the inherent low light levels of quantum experiments, imaging speeds are rather unsatisfactory. To overcome this limitation, we propose a two-step deep learning approach to establish an optimal point at which the experiment can be stopped while preserving all necessary object information. Step one enhances the reconstructed image after each measurement, while step two recognizes the image after each measurement. Step one employs a convolutional autoencoder while step two consists of a neural classifier. We achieved a recognition confidence of 75% at 20% of the image reconstruction time, hence reducing the time 5-fold while maintaining the image information. This, therefore, leads to a faster, more efficient image acquisition method. We tested our method on a non-degenerate system however, our procedure can be extended to many such systems that are of quantum nature. We believe that this novel deep learning approach will prove valuable to the community who are focusing on time-efficient ghost imaging.

S31

Ag/AgBr/MIL-53(Al) plasmonic nanocomposite as an enhanced visible light photocatalyst for decomposition of RhB dye

Khodayari, A.* and Sohrabnezhad, Sh.

Department of Chemistry, Faculty of Science, University of Guilan, P.O. Box 1914 Rasht, Iran
alikhodayari@phd.guilan.ac.ir

In the present work, Ag/AgBr/MIL-53(Al) plasmonic nanocomposite was synthesized as a novel plasmonic photocatalyst. The as-prepared nanocomposite was characterized by various characterization techniques such as XRD, HR-TEM, SEM, FT-IR, PL, and UV–vis DRS. The photocatalytic efficiency of Ag/AgBr/MIL-53(Al) was investigated by photo-degradation of rhodamine B (RhB) dye. Results indicated about 94% of dye were removed by prepared photocatalyst under visible-light irradiation in 120 min. The effect of different factors such as illumination time, and initial dye concentration on the photocatalytic performance of Ag/AgBr/MIL-53(Al) were experimentally investigated. The heterojunction between the Ag/AgBr nanoparticles and MIL-53(Al) provided a synergistic effect on fast transferring of the photo-induced electrons and holes for participate in the photocatalytic reactions. The results confirmed that due to some considerable features of MIL-53(Al)/Ag/AgCl such as high surface area, surface plasmon resonance effect, and recyclability, the introduced Ag/AgBr/MIL-53(Al) acts as a high performance photocatalyst for degradation of RhB under visible-light illumination.

S32

Exploiting up-conversion for spatial mode detection

Sephton, B.C.*[1], Vallés, A.[7], Steinlechner, F.[3,4], Konrad, T.[5,6], Torres, J.P.[7,8], Roux, F.S.[9], and Forbes, A.[1]

[1]*Physics, University of the Witwatersrand, Private Bag 3, Wits 2050, South Africa)*
[3]*Fraunhofer Institute for Applied Optics and Precision Engineering, Albert-Einstein-Str. 7, 07745 Jena, Germany*
[4] *Friedrich Schiller University Jena, Abbe Center of Photonics, Albert-Einstein-Str. 6, 07745 Jena, Germany*
[5]*School of Physics, University of KwaZulu-Natal, Durban, South Africa*
[6]*National Institute of Theoretical Physics, UKZN Node, Durban, South Africa*
[7]*Institut de Ciencies Fotoniques (ICFO), Barcelona Institute of Science and Technology, Mediterranean Technology Park,08860 Castelldefels, Barcelona, Spain*
[8]*Department of Signal Theory and Communications, Universitat Politecnica de Catalunya, Campus Nord D3, 08034 Barcelona, Spain*
[9]*National Metrology Institute of South Africa, Meiring Naudé Road, Brummeria, Pretoria 0040, South Africa*
andrew.forbes@wits.ac.za

Light affords a convenient avenue for transmitting, encoding, computing and filtering information where structuring the spatial degree of freedom allows us to perform operations at the speed of light and transfer a large range of information simultaneously in both the classical and quantum realms of physics. For example, exploiting the spatial structure of light provides a notable increase in the rate of transmission in both free-space and optical fiber transmissions. Applying this to photons also extends quantum protocols, entangling experiments into multi-dimensionality.

Accordingly, these schemes rely on the ability to detect and distinguish the structures holding the information encoded. Hermite-Gaussian (HG) or Laguerre-Gaussian (LG) modes are two examples of spatial modes that form an orthogonal basis and thus allows one to identify, extract and thus retrieve the entirety of the states being carried by the beam by projecting onto the individual states.

Traditionally, this is done by unitary transformations whereby the light is passed through linear elements such as a spatial light modulator. Here we demonstrate that this idea is not confined to this, but can also be extended into the non-linear regime by utilizing sum-frequency generation (SFG). By co-linearly directing the beam one would like to analyze into a χ^2crystal with another beam carrying the basis mode one would like to project onto, one can detect the associated information in the resulting color-converted or SFG beam due to the conservation of momentum. Not only is non-linear optics shown to be a viable method for detecting spatial structures, changing the color of the light being detected offers additional flexibility in the detection hardware required as well as encryption schemes, such as high dimensional teleportation.

S33

Investigation of structural properties of Bromineazocalix [4] arene molecule using DFT method

Bayrakdar, A.

Vocational School of Higher Education for Healthcare Services, Igdır University, Igdır 76100, Turkey
alpaslan.bayrakdar@igdir.edu.tr

In this study, Bromineazocalix [4] aren (BrPcalix) compound from Calix[*n*]arene family, which has a cyclic structure and is known for its ability to carry and complex organic molecules, anions and metal cations, was investigated theoretically. First, the theoretical modeling of the BrPcalix compound was made, then its structural parameters properties were investigated with the help of Density Functional Theory (DFT). The molecular structure corresponding to the most stable state of BrPcalix [4] was optimized by using the DFT/B3LYP/ 6-311G (d,p) basis set to theoretically elucidate the structural and electronic properties of the title compound.

Spectroscopic properties of the compound were investigated theoretically using the parameters of the optimized structure. The IR frequency values of BrPcalix [4] were calculated with same method and the values found were multiplied by certain scaling factors. Finally, relationships between experimental and theoretical spectroscopic data were calculated. In this study, it was revealed that experimental and theoretical studies are very compatible with each other.

Keywords: DFT, Calixaren, Spectroscopy, IR

References:

[1] R.P. Haugland, The handbook: a guide to fluorescent probes and labeling technologies, Univerza v Ljubljani, Fakulteta za farmacijo, 2005.
[2] S.K. Kim, J.K. Lee, S.H. Lee, M.S. Lim, S.W. Lee, W. Sim, J.S. Kim, Silver ion shuttling in the Trimer-Mimic thiacalix [4] crown tube, The Journal of organic chemistry 69(8) (2004) 2877-2880.
[3] S.E. Matthews, P.D. Beer, Calixarene-based anion receptors, Supramolecular Chemistry 17(6) (2005) 411-435.
[4] C.D. Gutsche, Calixarenes: an introduction, Royal Society of Chemistry2008.
[5] V. Furer, L. Potapova, D. Chachkov, I. Vatsouro, V. Kovalev, E. Shokova, V. Kovalenko, Study of p-(3-carboxy-1-adamantyl)-calix [4] arene with hydrogen bonds along the upper and lower rim by IR spectroscopy and DFT, Journal of molecular modeling 26(7) (2020) 1-7.

S34

Investigation of the effects of vortex beam propagation through a medium including nanostructurs

Nourani, F.*[1], Saber, A. [1], and Azizian-Kalandaragh, Y. [2]

[1]Department of physics, University of Mohaghegh Ardabili, Ardabil, Iran
[2]Faculty of Applied Sciences, Department of Photonics, Gazi University, Ankara, Turkey
fnourani95@gmail.com

An optical vortex beam, which has spiral wavefronts, carries an orbital angular momentum (OAM) of $l\hbar$ per photon because of an azimuthal phase term $\exp(il\theta)$, where l is the topological charges (TCs). The OAM of vortex beams has important potential applications, such as quantum information coding, particle trapping, and optical communications, etc.

To produce a vortex Laguerre–Gaussian (LG) beam, a computer hologram is designed using MATLAB program and then transmitted to a Spatial Light Modulator (SLM). Bypassing a plane wave through the modulator, a vortex beam with the desired topological charge is created.

The Mach-Zener interferometer was used to measure the TCs of LG vortex beams. To measure the topological charge, the vortex beam and a reference beam are placed in two Mach-Zener interferometer arms and their interference pattern is recorded by a camera. The topological charge is determined by analyzing the interference pattern of the Mach-Zener interferometer. The analysis of topological charge determination was as follows by counting the bright upper and lower branches and their difference from each other.

Also, the measurement of the topological charge for the two nanostructured environments of titanium oxide and magnesium ferrite was investigated. It was shown that the topological charge of vortex beams remains constant in passing through such solutions.

S35

The VCSEL solid state laser, its photonic MEMS and their several applications in 3D ToF lidar

Ceylan, C.

GÖKTÜRK Bilgi Teknolojiler Ltd. 5G RF Laboratory and ASIC R&D Center Statup project, Istanbul-Turkey
cenkceylan@turkishforensic.com

LiDAR perception is a powerful link that integrates the physical world and the information world and guarantees the realization of a safe and reliable sense, measuring autonomous traffic and mission critical tasks digital transformation system. For sample during the rapid driving of rail trains, small obstacles or millimeter-level deviations are major sources of hidden danger. Therefore, rail traffic has more stringent requirements on the performance and reliability of the LiDAR sensors.

A VCSEL laser with Lidar sensors is embedded with artificial intelligence, and the excellent angular resolution can achieve effective detection of the small-sized targets in the long range. 3D Lidar can reliably provide a real-time model of the vehicle's surroundings for precise localization and object tracking in autonomous driving to ensure the drivers and vehicles safety.

The VCSEL Lidar sensors boost the building, human flying, car driving and development of smart cities, to make city management easier, and to bring people easy, safe and high-efficiency outing experience. Lidar have been applied to the intelligent light pole for biological life balance in some cities.

S36

Numerical investigation of self-healing characteristic of generalized parabolic beams

Rashid-Farrokhian, N.*[1], Mashayekhi, H.R.[1], Azizian-kalandargah, Y.[2], and Amiri, P.[3,4]

[1]*Department of photonics, Faculty of physics, Shahid Bahonar University of Kerman, Kerman, Iran*
[2]*Department of photonics, Faculty of Applied Sciences, Gazi University, 06500, Ankara, Turkey*
[3]*Department of Advanced Technologies, University of Mohaghegh Ardabil, Namin, Iran*
[4]*Department of Engineering Sciences, Sabalan University of Advanced Technologies (SUAT), Namin, Iran*
neda6980@gmail.com

In this work, the self-healing characteristic of generalized parabolic beams is investigated numerically. Since two important parameters 'a' and 'm', respectively related to the size of the dark parabolic region and the number of rotated repetitions of the beam structure in the frequency space, are effective parameters in changing the intensity distribution of generalized parabolic beams, then the self-healing property of beams has been studied for various amounts of 'a' and 'm'. For this purpose, circular and squared obstacles of different sizes have been applied on the central part of beams, and then the masked optical fields of the beams propagated in the z-axis direction via the Angular Spectrum Method (ASM). To quantitatively compare the value of beams self-healing, a similarity function has been used in the simulation process.

The obtained results of simulation depict that by increasing the parameter 'm', despite the similarity percent of the disturbed beams and non-disturbed ones increases at the optimum distance (the shortest distance from the initial plane where the beams have more self-healing amount), the beam self-healing amount decreases. The reason for this event can be that by placing the obstacle on the central part of the beams, the applied disturbance to the beams is less for larger values of 'm', and therefore the ratio of the similarity percent of the beams in the optimal plane to similarity percent in the initial plane is also less. This also happens for larger values of parameter 'a', and when the value of 'a' increases, the self-healing amount of the beams reduces for each 'm'. It should be noted that in all cases, the central part of the beams has a better self-healing behavior than other parts and restores its initial intensity distribution to a desirable level.

S37

Optical sense of anticancer drug doxorubicin (DOX) on PANI nanostructures

Sherwani, A. R.* and Can, M. M.

Renewable Energy and Oxide Hybrid Systems Laboratory, Department of Physics, Faculty of Science, Istanbul University, Istanbul, Turkey
attaurrehmansherwani@ogr.iu.edu.tr

The flexible biomaterials can be a cutting edge for the healthcare market. Promising candidate materials for flexible biomaterials in close future can be assumed as flexible conductive polymers which may lead to the development of artificial skin, electro-mechanical actuators, neural implants, biosensors, and drug delivery systems. The functional group on the surface of polymer may tune the electrochemical performance and sensitivity to the free radicals which allow to carry or sense ionic radicals for drug delivery or biosensor. Polyaniline (PANI) is the one of well-known conductive polymers, especially for potential usage in biotechnology applications, due to its high electrical conductivity, hydrophilic nature, low-toxicity, chemical stability, low solubility, and biocompatibility. In this study we focused on improving surface functionalized PANI as a biomaterial suitable to load Doxorubicin (DOX) and loading abilities of PANI were investigated by absorption peak of DOX.

S38

The investigation of self-healing feature of vortex Hermite-Gaussian beams

Emadoleslami, A.*[1], Mashayekhi, H.R.[1], Azizian-kalandargah, Y.[2], and Amiri, P.[3,4]

[1]*Department of photonics, Faculty of physics, Shahid Bahonar University of Kerman, Kerman, Iran*
[2]*Department of photonics, Faculty of Applied Sciences, Gazi University, 06500, Ankara, Turkey*
[3]*Department of Advanced Technologies, University of Mohaghegh Ardabil, Namin, Iran*
[4]*Department of Engineering Sciences, Sabalan University of Advanced Technologies (SUAT), Namin, Iran*
atefe.emad.666@gmail.com

In this work, using numerical simulation, a comparative study has been accomplished on vortex Hermit-Gaussian (vHG) beams' self-healing behavior and has been measured their self-healing amount in the propagation direction. For this purpose, the obstacles with different sizes and shapes of circle, oval, and ring have been simulated and located on different parts of the beam. Then, employing the Angular Spectrum Method (ASM), the beams have been propagated along the z-axis and the beams' self-healing property was inspected during the propagation direction. To get numerical values of self-healing and so quantitative comparison of this feature of beams, a similarity function has been used to compare between the intensity distribution of perturbed and non-perturbed beams during propagation.

The results show that vHG beams similar to the non-diffracting beams, such as Bessel, Airy, Parabolic, and Mathieu beams, have the self-healing property although have less self-healing amount in comparison with them. Clearly, by changing the size and shape of the obstacle and its position on the beam, the self-healing behavior of the beam also varies. If the obstacle is closer to the central part of the beam, the beam self-healing behavior is more desirable so that it reconstructs the initial intensity distribution to a desirable amount and so the similarity percent of the propagated two perturbed and non-perturbed beams in the optimum distance becomes higher. On the other hand, the self-healing behavior of vHG beams depends on two effective parameters, the Hermite polynomial order (n) and 'a' which the argument of Hermite function is dependent on it. Increasing the value of the parameters 'n' and 'a', the beams' self-healing behavior improves in many cases.

S39

FDTD simulation of propagation of Hermite-Cosh Gaussian high intensity laser beam in inhomogeneous plasma and modeling of ponderomotive force and magnetic field

Alilou, S.* and Shahrassai, L.

Department of Physics and Technology of Plasma, Faculty of Physics, University of Tabriz, Iran
a.alilu@tabrizu.ac.ir

The interaction of laser beams with plasma is very important in many wave-particle phenomena. In this paper, we investigate the interaction of intense Hermite-Cosh Gaussian laser beams with Inhomogeneous plasma. We study the distribution of magnetic and electric fields of plasma and drew the related diagrams and then we compare them together. Because high-power lasers cause nonlinear effects on the plasma that lead to the nonlinear Ponderomotive force, the behavior of the ponderomotive force resulting from this radiation was investigated.

Keywords: Hermite-Cosh Gaussian beam, Inhomogeneous plasma, Simulation FDTD.

Reference:

[1] Walia, Keshav, R. K. Verma, and Arvinder Singh. "Second harmonic generation of laser beam in quantum plasma under collective influence of relativistic-ponderomotive nonlinearities." Optik 225 (2021): 165745.
[2] Kant, Niti, Manzoor Ahmad Wani, and Asheel Kumar. "Self-focusing of Hermite–Gaussian laser beams in plasma under plasma density ramp." Optics Communications 285.21-22 (2012): 4483-4487.
[3] Walia, Keshav. "Nonlinear interaction of high-power beam in weakly relativistic and ponderomotive cold quantum plasma." Optik 219 (2020): 165040.
[4] Shahrassai, L., S. Sobhanian, and H. Khosravi. "The Effect of Ponderomotive Force of a Laser Pulse on the Frequency Shift of its X-mode Propagation." AIP Conference Proceedings. Vol. 1400. No. 1. American Institute of Physics, 2011.
[5] Singh, Mamta, Krishna Gopal, and Devki Nandan Gupta. "Temporally asymmetric laser pulse for magnetic-field generation in plasmas." Physics Letters A 380.16 (2016): 1437-1441.

S40

A comparative study on self-healing property of elliptical and circular Airy beam

Hashemi, Z.*[1], Mashayekhi, H.R.[1], Azizian-kalandargah, Y.[2], and Amiri, P.[3,4]

[1]*Department of photonics, Faculty of physics, Shahid Bahonar University of Kerman, Kerman, Iran*
[2]*Department of photonics, Faculty of Applied Sciences, Gazi University, 06500, Ankara, Turkey*
[3]*Department of Advanced Technologies, University of Mohaghegh Ardabil, Namin, Iran*
[4]*Department of Engineering Sciences, Sabalan University of Advanced Technologies (SUAT), Namin, Iran*
zohre.hashemiiii1376@gmail.com

In this research, the self-healing behavior of circular and elliptical Airy beams has been studied numerically. Since the size, shape, and position of the applied disturbance on the beam optical field affect the beam reconstructing and self-healing behavior, then the different obstacles with various sizes and shapes (square, circle, or circular sector) are simulated and applied in different positions of optical field of the beams. Then by using two different propagation methods, Angular Spectrum Method (ASM) and Huygens Convolution Method (HCM), the beams have propagated in the z-axis direction. In addition to investigating the self-healing behavior of the beams, the amount of self-healing at different propagation distances has been calculated utilizing the employed similarity function in the simulation and compared for both circular and elliptical Airy beams.

The simulation results show that both types of beams can optimally reconstruct their disrupted intensity distribution during propagation and the self-healing property of the beams is more desirable when the obstacles are placed on the main lobe of the beams entirely. If the obstacle only covers the main lobe of the beams, the intensity distribution of the central ring of the beams repairs to the extent desirable in short distances. Further, if the obstacle is displaced in the radial direction and moved away from the beam center, the self-healing occurs in shorter distances for elliptical beams in comparison with circular ones. On the other hand, there exist several incomplete rings at further distances from the center despite the central rings reconstructed in a complete ring form.

From the obtained results, it can be seen that the self-healing amount of both types of beams disturbed with square and circular masks is more and reached the maximum self-healing at a shorter distance from the initial plane when the beams propagated via ASM. Elliptical beams have better self-healing behavior in most cases in comparison with the circular ones, especially in the use of the angular spectrum method.

S41

Determination of the presence and molecular orientation of the liquid crystal in the core-sheath structure of the electrospun fiber by optical method

Mamuk, A.E.*[1], Koçak, Ç.[2], and Demirci Dönmez, Ç.E.[3]

[1]*Liquid Crystals Laboratory, Department of Physics, Muğla Sitki Koçman University, TR48000, Muğla, Turkey*
[2]*Molecular Nano-Materials Laboratory, Department of Physics, Muğla Sitki Koçman University, TR48000, Muğla, Turkey*
[3]*The Center of Research Laboratories, Muğla Sitki Koçman University, TR48000, Muğla, Turkey*
aemamuk@mu.edu.tr

The electrospinning method is basically the process of spinning of a pure polymer or polymer solution containing various additives under high electric field. This method is simple but highly effective for gaining woven or non-woven fibers in nano- and micro-size. Electrospun fibers can show high mechanical strength and also have a large surface area when grown on different substrates. Liquid crystals are specific materials that exhibit anisotropy and have a weak crystalline order within a significant temperature range. In recent years, several studies have been carried out on fabricating and characterizing the electrospun fibers in core-sheath structure by mixing liquid crystals, which are affected by electric field due to their distinct anisotropy, with various polymers.

The polarization direction of the incident light can be changed depending on the angle between the analyzer and the uniaxial liquid crystal molecules, which is placed between the crossed-polarizers. It is also known that liquid crystals do not exhibit any texture between crossed-polarizers due to their isotropic behavior at temperatures above the phase range. With taking advantage of these features of liquid crystals, the determination of the presence and molecular orientation of liquid crystals within the electrospun liquid crystal-polymer core-sheath fibers, which were produced by single-needle electrospinning, by using Polarized Optical Microscopy method is given in this study.

Acknowledgement
The authors would like to thank The Center of Research Laboratories, Muğla Sıtkı Koçman University for technical support.

S42

Structural and morphological characterization of nitrogen doped ZnO thin films

Aydınoğlu, H.S.*[1], Hopoğlu, H.[2], and Şenadım Tüzemen, E.[3,4]

[1]*Department of Medical Services and Techniques, Program of Opticianry, Vocational School of Healthcare, Sivas Cumhuriyet University, 58140, Sivas, Turkey*
[2]*Faculty of Technology, Department of Optical Engineering,Sivas Cumhuriyet University, 58140, Sivas, Turkey*
[3]*Nanophotonics Research and Application Center, Sivas Cumhuriyet University, 58140, Sivas, Turkey*
[4]*Department of Physics, Faculty of Science, Sivas Cumhuriyet University, 58140, Sivas, Turkey*
hsaydinoglu@cumhuriyet.edu.tr

Morphological and structural properties of ZnO thin films with 2.5%, 5%, 7.5% and 12.5% nitrogen were investigated. The films were deposited at room temperature on n-Si by RF magnetron sputtering method. The films have been characterized by X-Ray Diffraction, SEM and FTIR. It was observed from XRD measurements that the films had a type of peak with hexagonal structure and preferential orientation along (002) crystal plane. And particle size changed as the nitrogen contribution changed. As a result of FTIR analysis, although all the materials produced seem to have a similar spectrum, with nitrogen entering the film observed a peak at approximately 1380 cm^{-1}. As the percentage of nitrogen increased, the peak intensity increased. This peak was predicted as the Zn-N bond. SEM analysis was done on surfaces at 10 kV with a working distance of 9mm. Secondary electron (SE) imaging was not used since the surfaces doesn't have any phases other than ZnO. In all samples, the spherical grain size morphology was followed. This could be attributed to the formation of a good sputter regime and energy within the substrate and ZnO accompanied by N doping.

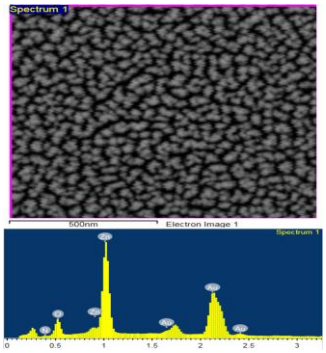

SEM-EDX analysis of 5% N doping on ZnO and its spectrum.

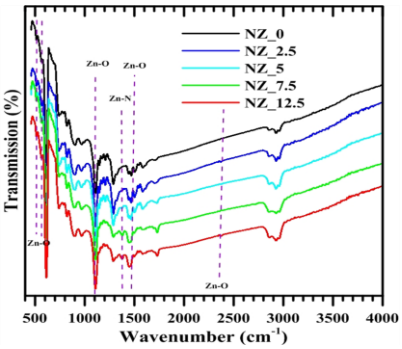

Plot of transmittance by wave number.

S43

Influence of various technological factors on the optical properties of $Cd_xZn_{1-x}S$ nanoparticles

Gahramanli, L.*, Muradov, M.B., and Eyvazova, G.M.

Baku State University, Nano Research Center, Azerbaijan, Baku
qahramanli.lala@mail.ru

Recently, $Cd_xZn_{1-x}S$ semiconductor nanomaterials have great attentions due to unique properties and wide potential application fields. In nanoscale, the optical properties of these materials are closely related to the dimensions and other parameters. $Cd_xZn_{1-x}S$ nanomaterials can form compounds of different composition depending on the x value. There is different method for synthesis of nanomaterials. $Cd_xZn_{1-x}S$ nananomaterials have been synthesis with different methods such as ionic diffusion, solvothermal synthesis, vapor liquid solid (VLS) growth, vapour-solid (VS) reaction, hard template, gamma irradiation, sonochemical and SILAR synthesis method. Dependence of different technological conditions, the optical properties can be varied. In this paper, the optical properties of nanomaterials obtained by SILAR and sonochemical synthesis were analyzed comparatively depending on the technological conditions.

In SILAR technique, thin films are formed in several cycles. As increasing of cycles, the particle sizes and thickness of thin film are increase. As a result of these, the band gap values of $Cd_xZn_{1-x}S$ are decreases. At the same time, for investigation of influence of temperature, the formed samples are thermal annealed at different temperatures. The results show that, as an increasing of temperature, the band gap values are decreasing.

In addition to the low yield loss in nanomaterials synthesized by sonochemical methods, it is considered a cost-effective method for the synthesis of nanoparticles. At the same time, it is possible to select and easily supply any voltage, reaction time, temperature and any reaction medium. Here, the particles are obtained in smaller sizes. The formed materials have a better crystalline size and the diffraction angles shifted toward larger angles. At the same time, as the amount of Zn ions increases, the value of the band gap increases in the ternary compounds. In the samples formed by, the structure transfer from the cubic phase to the hexagonal phase. The crystallinity degree of samples obtained by sonochemical methods is higher than the crystallinity degree of samples obtained by SILAR method.

The optical properties of prepared sample ($Cd_{0.2}Zn_{0.8}S$) by two different method is varied. The band gap value of $Cd_{0.2}Zn_{0.8}S$ nanomaterials by SILAR method is 3.05 eV and by sonochemical method is 2.8 eV. This difference is due to the peculiarities of the particles of the growth mechanism. At the same time, the band gap values of the sample which thermal annealed are change. Increasing of the thermal annealing temperature and synthesis temperature, the band gap values are decreasing.

S44

Structural and electrical properties of p-type NiO thin films produced by thermal evaporation on different substrates

Aydınoğlu, H.S.*[1], Kaya, D.[2], Şenadım Tüzemen, E.[3,4], and Ekicibil, A.[5]

[1]*Department of Medical Services and Techniques, Program of Opticianry, Vocational School of Healthcare, Sivas Cumhuriyet University, 58140, Sivas, Turkey*
[2] *Department of Electronics and Automation, Vocational School of Adana, Cukurova University, 01160, Adana, Turkey*
[3]*Nanophotonics Research and Application Center, Sivas Cumhuriyet University, 58140, Sivas, Turkey*
[4]*Department of Physics, Faculty of Science, Sivas Cumhuriyet University, 58140, Sivas, Turkey*
[5]*Department of Physics, Faculty of Art and Sciences, Cukurova University, 01330, Adana, Turkey*
hsaydinoglu@cumhuriyet.edu.tr

In this study, high-quality p-type NiO semiconductor thin film was investigated by thermal evaporation method by annealing 50 nm of Ni layer at 450 °C for 2.5 h. NiO thin film forms simultaneously on different nature of substrates; glass, sapphire, Si (100), InP, and GaAs. The films have been characterized by X-Ray Diffraction, SEM and Hall-effect measurements. The structural properties of NiO film were determined as cubic phase with space group of $Fm\bar{3}m$ by x-ray diffraction analysis that revealed two possible formations; with (sapphire, InP, and GaAs) and without (glass and Si (100)) Ni-surface interactions. Due to annealing process, Ni ions diffuse into the sapphire, InP, and GaAs substrates and secondary phases of NiAl, Ni_xP/Ni_2InP, and NiAs/Ni_2GaAs were formed. Scanning electron microscopy images managed to determine the average film thickness that is also effect of Ni-surface interactions. The optical transparency was obtained at approximately 94% and 89% transmittance in the range of 300-800 nm for the NiO film on sapphire and glass samples, respectively. The direct optical band gap of NiO film on glass and sapphire substrates were calculated by Tauc's equation and found to be 3.63 eV and 3.67 eV, respectively. NiO film on glass and sapphire surfaces exhibited a p-type characteristic that was confirmed by Hall-effect measurements.

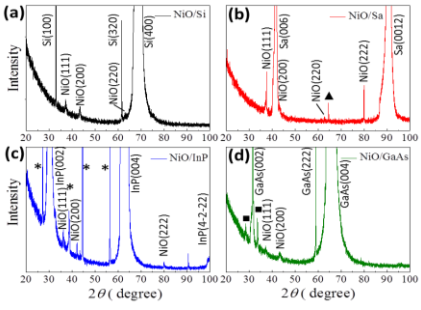

The XRD patterns of oxidized Ni layer at 450 °C for 2.5 h in the air on (a) Si (100) (black line), (b) Sapphire (red line), (c) InP and (d) GaAs substrates.

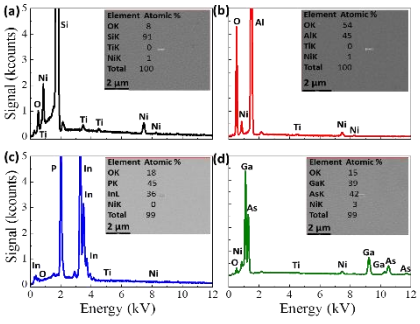

EDS analysis of oxidized Ni layer on (a) Si (100), (b) Sapphire, (c) InP and (d) GaAs substrates. Inset images show data points with elemental analysis results of compositions.

S45

The effect of magnetic field on structural and optical properties of Ni/NiO nanochains

Mammadyarova, S.J.*[1], Muradov, M.B.[1], Eyvazova, G.M.[1], Aghamaliyev, Z.A.[1], and Balayeva, O.O.[2]

[1]*Department of Physics, Baku State University, Baku, Azerbaijan*
[2]*Department of Chemistry, Baku State University, Baku, Azerbaijan*
sevinc.memmedyarova@inbox.ru

In this study, Ni/NiO nanochains were successfully synthesized by a facile chemical reduction method under different magnetic fields (25 mT and 81 mT), followed by thermal oxidation at high temperatures (400ºC, 500ºC, 600ºC). For the synthesis of Ni nanoparticles, hydrazine hydrate and sodium borohydride were used as reducing agents. In order to determine the size, structure, optical properties and morphology, the obtained products were characterized by X-ray diffraction (XRD), ultraviolet-visible Spectroscopy (UV–Vis), and scanning electron microscopy (SEM). The average crystallite size of Ni nanochains synthesized under 25 mT and 81 mT external magnetic fields are 5.82 nm and 2.19 nm, respectively. The average size of as-prepared Ni nanoparticles in nanochain decreases with increasing magnetic force. After oxidation of samples at 600ºC, the size of NiO formed on the surface of Ni nanochains increases with increasing magnetic force. This is related to the faster oxidation of small particles due to their high surface energy. For samples oxidized at different temperatures, the crystallite size was estimated separately for Ni and NiO based on the most intense peak in the diffractogram. The optical band gaps of Ni/NiO nanochains (synthesized under 25 mT) annealed 400ºC, 500ºC and 600ºC temperature are 3.81 eV, 3.99 eV and 3.67 eV, respectively. The optical band gaps of Ni/NiO nanochains (synthesized under 81 mT) annealed 400ºC, 500ºC and 600ºC temperature are 3.86 eV, 4.0 eV and 3.87 eV, respectively. The size of NiO (in Ni/NiO nanochains synthesized at 25 mT magnetic field) decreases (from 16.84 nm to 15.38 nm) when the temperature rises from 400ºC to 500ºC and the band gap increases from 3.81 eV to 3.99 eV due to quantum size confinement. However, there are some exceptions. For example, when the temperature rises from 500ºC to 600ºC, the size of NiO (in Ni/NiO nanochains synthesized at 25 mT and 81 mT) decreases and the band gap decreases too. We can't explain it with quantum theory, because according to quantum theory, the band gap must increase with decreasing size. However, the reason of this can be explained by the fact that all metals including Ni have a very low band gap. When the size of NiO increases, the absorption of UV rays increases too. Therefore, Ni cannot prevent the lowering of the band gap of the oxide. At relatively high temperature, the size of NiO decreases and Ni hinders the increase of the band gap of oxide. The optical properties are highly dependent on nanoparticle size. As can be seen from the results, it is possible to control the particle size by changing the reaction parameters. Optical band gap is an important issue for semiconductors, which make possibly their application in optoelectronics and photocatalysis. From SEM measurements chain-like morphology was observed.

S46

Sol-gel spin coated Nb_2O_5 thin films with different thicknesses

Akkaya Kömürcü, H.[1,2,*], Ataşer, T.[1], Akın Sönmez, N.[1,3], Asar, T.[1,2], and Özçelik, S.[1,3]

[1]*Photonics Application and Research Center, Gazi University,06500 Ankara, Turkey*
[2]*Department of Physics, Faculty of Science, Gazi University, Ankara 06500, Turkey*
[3]*Department of Photonics, Faculty of Applied Science, Gazi University, Ankara 06500, Turkey*
akkayahuda@gmail.com, sozcelik@gazi.edu.tr

Metal oxide thin films such as Niobium pentoxide (Nb_2O_5) are promising candidates for a wide variety of optical and micro-electronic applications [1]. Nb_2O_5 is one of the useful optical thin film materials with its stability in air and water, resistance to acids and bases, wide forbidden energy range (3-4 eV) and high refractive index (2.2-2.6). Multilayer Nb_2O_5 thin films were deposited on Si and glass substrates using sol-gel spin coating technique which is an economical and fast deposition technique. The solution was made by mixing 1.6 g $NbCl_5$ with 33.2 ml ethanol and 0.68 ml distilled water at room temperature. It was stirred for 24 h using magnetic-stirrer and so it was homogeneous, transparent and stable. 0.4 ml of this solution was dropped onto the substrates, and coated by using a spin coating system having a speed of 3500 rotation/s for 30 s. After deposition, obtained films were sintered to dry on heater at 120 °C for 30 min. The procedure was repeated 2 and 3 times to make thin films as a multilayer. X-ray Diffractometer, Secondary Ion Mass Spectroscopy, Atomic Force Microscope and UV-Vis Spectrometer were used to investigate the effect of the number of Nb_2O_5 spinning cycles on the structural, morphological, and optical properties of the obtained films. The all Nb_2O_5 films had an amorphous structure, and they have fluctuations in the visible range of the transmittance spectra due to the interference of light on the film/air and film/substrate interfaces. The optical band gap of the films became narrower from 3.77 to 3.72 eV, with increasing the number of layers. The thicknesses determined as 68, 116 and 178 nm for 1, 2 and 3 layered films, respectively. It is worth remarking that the material properties of the Nb_2O_5 films control with film thickness which in turn will affect the optoelectronic device properties because the transition metal oxide Nb_2O_5 films are an optical layer determining the amount of light entering the device.

Acknowledgment
This work was supported SBB (TR) and BAP (Gazi University) with the project numbers 2016K121220 and 70/2020-01 respectively.

References:
[1] Ataşer T. (2020). Characterization of Nb_2O_5 Thin Films Coated by Sol-gel Method. Çanakkale Onsekiz Mart Üniversitesi Fen Bilimleri Enstitüsü Dergisi 6(1), 49-56. https://doi.org/10.28979/comufbed.595184.

S47

Influence of Electron Incidence Angle on Position Resolution in Crystal Calorimeters

Yahya, M.F.O.* and Koçak, F.

Department of Physics, Bursa Uludag University, 16059, Bursa, Turkey
muddather211@gmail.com, fkocak@uludag.edu.tr

Inorganic scintillation crystals are frequently used in calorimeter units of detectors in high-energy physics experiments. The most commonly used inorganic crystals are crystals such as PWO, CsI, CsI(Tl). In recent years, the LYSO crystal has also attracted attention due to its high light yield and radiation hardness. This crystal emits scintillation photons between 360-600 nm. Due to these properties, LYSO crystals have been proposed for the electromagnetic calorimeter parts in various high-energy physics experiments such as the COMET experiment at J-PARC, the proposed SuperB forward parts of the endcap calorimeter, the KLOE experiment, and the Muon-to Electron (Mu2e) experiment.

When a particle such as an electron or photon hits the crystal calorimeter, its energy is deposited in the central crystal and nearby crystals. The impact position of the incident particle can be obtained from the weighted mean of the position of energy deposits in the crystals. This method is known as the center of gravity technique. In this study, the dependence of position resolution on the angle of the incident electron was calculated for the LYSO crystal using the Geant4 Monte Carlo simulation program. It was found that as the incidence angle of the electron increases, the position resolution deteriorates and the best position resolution is obtained when the incident electron hits the LYSO matrix at zero degree.

S48

Investigation of quantum confinement effect in ultrathin TiO_2 films

Gözlekçi, G.*[1,2], Akın Sönmez, N.[1,3], Azizian-Kalandaragh, Y.[1,3], and Özçelik, S.[1,3]

[1]Gazi University, Photonics Application and Research Center, Ankara, Turkey
[2]Gazi University, Department of Advanced Technologies, Ankara, Turkey
[3]Gazi University, Faculty of Applied Science, Department of Photonics, Ankara, Turkey
gokhan.gozlekci@gmail.com, sozcelik@gazi.edu.tr

Titanium dioxide (TiO_2) is one of the most popular metal oxides due to its unique optoelectronic properties such as high refractive index, wide bandgap, and chemical stability in harsh environments [1]. These properties make it an extensively studied material in optical applications such as either to increase the reflectance or transmittance, photocatalyst, and sensors. Crystal structure, surface morphology, and grain size have also a great impact on the performance of TiO_2 films. Grain size and surface morphology are influenced by the film thickness which is associated growth of larger particles. In ultrathin TiO_2 films, the bandgap of thinner than 15 nm films are shifted by the quantum confinement effect compared to bulk state.

In this study, TiO_2 thin films having thicknesses of 5 nm to 35 nm were deposited on Si and glass substrates at room temperature using magnetron sputtering system. Their surface morphologies were examined in 3 μm * 3 μm area with Atomic Force Microscope. The transmittance of the TiO_2 films in 300-1100 nm obtained with a UV-Visible Spectrometer. By using the transmittance data, absorbance and optical band gap of films were calculated with Tauc Plot. It was observed that the optical band gap of the films decreased with increasing the film thickness. This shifts to the blue region in thin films with low thicknesses is due to the quantum confinement effect in a two-dimensional quantum system. In these thin films, charge carriers move freely in two dimensions, but in the third dimension, which are nanometers thick, they have very limited movement and confined. In this study, it has also been observed that with increasing the thickness of the semiconductor thin films, the amount of shift towards the blue region is reduced, which indicates that the movement of charge carriers is freer and thus the quantum effects are reduced. Controlling the thickness of semiconductor layers in nanometer dimensions can be very efficient for engineering energy gap to make optoelectronic devices.

Acknowledgement
This work was supported by Development Minister in Turkey with the project numbers 2016K121220.

References:
[1] Möls, K., Aarik, L., Mändar, H., Kasikov, A., Niilisk, A., Rammula, R., Aarik, J. (2019). Influence of phase composition on optical properties of TiO2: Dependence of refractive index and band gap on formation of TiO2-II phase in thin films. Optical Materials, 96, 109335.

S49

A new approach to enhance the bandwidth value of UTC-PD

Gencal, H.* and Öztürk, T.

Electrical-Electronics Engineering, Bursa Technical University, Bursa, Turkey
huriyegencal@gmail.com

In this paper, the bandwidth (BW) value of uni-traveling-carrier photodiode (UTC-PD) is analyzed by changing inside structure in between absorber and collector. Previously published and designed UTC-PD structure is repeated to utilizing TCAD (Lumerical) simulator program. Two aspect illumination from x and z-axis is applied with inserted different types of materials to show the bandwidth performance of UTC-PD. By the proposed approach, which is quasi embedded waveguide, the BW value is enhanced. The aim is here to change the electric field and accelerate the electron velocity.

S50

Optical properties of nitrogen doped ZnO thin films grown on n-Si and glass substrate

Hopoğlu, H.*[1], Aydınoğlu, H.S.[2], and Şenadım Tüzemen, E.[3,4]

[1]*Faculty of Technology, Department of Optical Engineering,Sivas Cumhuriyet University, 58140, Sivas, Turkey*
[2]*Department of Medical Services and Techniques, Program of Opticianry, Vocational School of Healthcare, Sivas Cumhuriyet University, 58140, Sivas, Turkey*
[3]*Nanophotonics Research and Application Center, Sivas Cumhuriyet University, 58140, Sivas, Turkey*
[4]*Department of Physics, Faculty of Science, Sivas Cumhuriyet University, 58140, Sivas*, Turkey
20199251008@cumhuriyet.edu.tr

Undoped and nitrogen doped ZnO thin films were grown by using RF magnetron sputtering method changing the nitrogen ratio between 0% -12.5% on n-Si and glass substrate. Optical properties of the grown samples were examined by optical spectrophotometer and spectroscopic ellipsometer. Transmittance spectra were obtained by spectrophotometer measurements and the effect of nitrogen ratio was investigated. It has been observed that as the nitrogen ratio increases, the transmittance decreases up to ~ 500 nm and then increases. By using the transmittance curve, the absorption coefficient and then the energy band gap were calculated. It has been observed that the energy band gap varies between 3.281 eV and 3.274 eV.

Further detailed optical analysis was made by the spectroscopic ellipsometry technique. It provides information about the optical system that changes the polarization state of the polarized light coming onto the material. This technique is an important thin film measurement technology for its nondestructive and sensitive advantages. In this study, Cauchy model was selected as the model for thin films. Fitting was performed to ensure the agreement between the experimentally obtained Ψ values and theoretically determined Ψ values using the Cauchy model. As a result, the refractive index was found for each film and it was observed that the refractive index decreased as the nitrogen ratio increased.

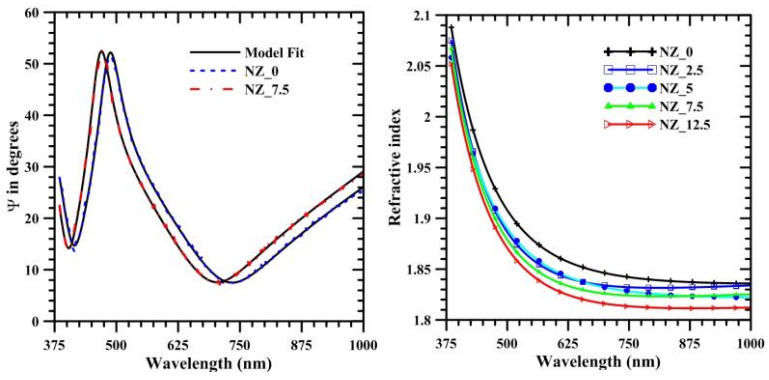

S51

Distributed current sensing via optical reflectometry

Şirin, Ş.* and Yüksel Aldoğan, K.

Department of Electrical and Electronics Engineering, Izmir Institute of Technology, Izmir, Turkey
samilsirin@iyte.edu.tr

The popularity of fiber optic solutions in current sensing has increased due to their advantages such as their small size, light weight, and passive nature as compared to bulky transformers. The vast majority of the fiber optic current sensing techniques are based on the measurement of the magnetic field created around the current of interest. The measurement principle relies on the Faraday effect i.e. on the generation of a circular birefringence along an optical fiber subject to an axial magnetic field. Since the circular birefringence rotates the polarization axes of propagating light, the total amount of rotation is detected in most of the sensing configurations to obtain the average magnetic field. Optical Time Domain Reflectometry (OTDR) techniques allow tracking the magnetic field distribution throughout the fiber. Hence, non-uniform magnetic field distribution due to imperfect coil shape, temperature variations, or cross-talks may be monitored, providing an improved reliability. In this study, the feasibility of employing popular OTDR-based interrogators, for current sensing is discussed through simulation works.

S52

Thickness dependence of structural and optical properties of nitrogen doped ZnO thin films on glass

Hopoğlu, H. *[1], Aydınoğlu, H.S.[2], Özer, A.[3,4], and Şenadım Tüzemen, E.[5,6]

[1]*Faculty of Technology, Department of Optical Engineering,Sivas Cumhuriyet University, 58140, Sivas, Turkey*
[2]*Department of Medical Services and Techniques, Program of Opticianry, Vocational School of Healthcare, Sivas Cumhuriyet University, 58140, Sivas, Turkey*
[3]*Department of Metallurgical and Materials Engineering, Sivas Cumhuriyet University, 58140, Sivas, Turkey*
[4]*Advanced Technology R&D Center, Sivas Cumhuriyet University, 58140, Sivas, Turkey*
[5]*Nanophotonics Research and Application Center, Sivas Cumhuriyet University, 58140, Sivas, Turkey*
[6]Department of Physics, Faculty of Science, Sivas Cumhuriyet University, 58140, Sivas, Turkey
20199251008@cumhuriyet.edu.tr

In this study, 5% nitrogen doped ZnO thin films were grown on glass substrates by RF magnetron sputtering method. Nitrogen ratio was adjusted to be 5% N2 -95% Ar in the coating device and 4 samples were sputtered at thicknesses of 250 nm-350 nm-450 nm-550 nm. The optical properties and SEM analyzes of these grown samples were employed. In addition, it was seen that as a result of SEM-EDX analysis, the amount of nitrogen in the samples increased as the thickness increased. By the studies, it is concluded that the layer thickness is caused by the increase of dopant effect of N by interfacing with ZnO and the effective sputter possibility of N and O elements with Zn. Transmittance spectra was obtained by spectrophotometer measurements and the effect of thickness on spectra was investigated. By using the transmittance curve, the absorption coefficient and then the energy band gap were calculated. It has been observed that as the thickness increases, the energy band gap decreases from 3.252 eV to 3.199 eV. The structural and crystallographic properties of the films were determined by x-ray diffraction. It was observed that as the thickness increased, the peak intensities of the ZnO increased.

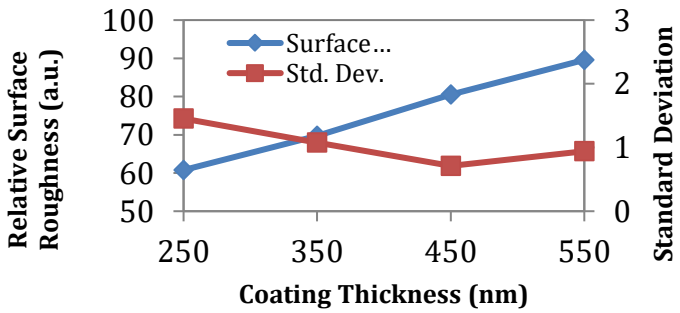

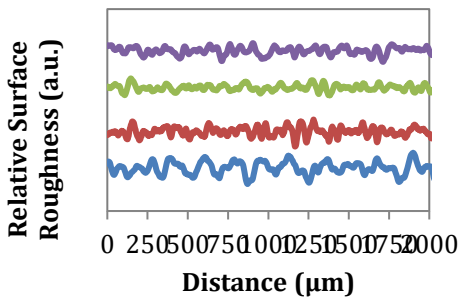

S53

Simulation tool development for FBG-aided Φ-OTDR vibration sensors

Koçal, E.B.* and Yüksel Aldoğan, K.

Department of Electrical and Electronics Engineering, Izmir Institute of Technology, Izmir, Turkey
ertungakocal@iyte.edu.tr

Phase-sensitive optical time-domain reflectometry (Φ-OTDR) has attracted a great deal of attention since its emergence in the early 90s. By virtue of the advantages of optical fiber technology such as having small-size, lightweight, immunity to electromagnetic interference and, their durability in harsh environments, it has found application in multiple sectors and has been commonly used in distributed vibration sensing applications. The integration of fiber Bragg gratings in distributed optical sensing systems has gained popularity in the last decade due to their capability to detect temperature, strain, pressure, chemical substances, etc. Although various system configurations based on Φ-OTDR have been proposed to improve the sensing performance, design and test processes are costly and time-consuming. With a perspective of reducing product development costs, we have developed a simulation tool for FBG-aided Φ-OTDR vibration sensors. We will present basic modeling principles of the simulation tool and obtained design parameter values for particular system configurations.

S54

Synthesis and optical characterization of $Gd_3Ga_{5-x}Al_xO_{12}$:Nd,Cr persistent phosphors

Balci, E.*[1,2,3], Du, J.[4], and Poelman, D.[4]

[1]*Department of Physics, Ankara Hacı Bayram Veli University, Polatlı 06900, Turkey*
[2]*Photonics Application and Research Center, Gazi University, Teknikokullar, Ankara, Turkey*
[3]*Department of Physics, Faculty of Science, Gazi University, Teknikokullar, Ankara, Turkey*
[4]*LumiLab, Department of Solid State Sciences, Ghent University, Krijgslaan 281-S1, B-9000 Ghent, Belgium*
esrabalci3@gmail.com

Persistent luminescent materials or glow-in-the-dark compounds have been studied and developed since a long time and are finding more and more applications in everyday life such as toys, road signs, clothing. [1] Phosphors, consisting of an inorganic host doped with impurity ions, are luminescent materials that emit light after absorption of energy, not due to the heating of the materials. This energy can be provided by electromagnetic radiation, electric fields, charged particles or a chemical reaction [2] Near-infrared emitting phosphors could be useful in night vision or security applications and bio-imaging.

In this study, $Gd_3Ga_{5-x}Al_xO_{12}$: Nd,Cr was synthesized using two dopants (Nd, Cr) together and separately by microwave-assisted solid state reaction method. Nd^{+3} and Cr^{+3} dopants were used because of their unique optical properties. Nd^{+3} has numerous excitation wavelengths between UV spectrum and NIR range, while Cr^{+3} has several excitation bands in the UV and in the visible region of the electromagnetic spectrum. [2,3] The synthesis steps and optical characteristics of $Gd_3Ga_{5-x}Al_xO_{12}$:Nd & Cr will be explained in detail for x=0,1 and 2 in the presentation.

References:

[1] Poelman, D., Van der Heggen D., Du J., Cosaert E., Smet P.F., Persistent phosphors for the future: fit for the right application, J. Appl. Phys. 128 (2020) 240903.
[2] Cosaert, E. (2018). Near-infrared emitting phosphors for time-gated in vivo imaging (thesis Ghent University).
[3] Nimmegeers, B., Cosaert E., Carbonati T., Meroni D., Poelman D., Synthesis and characterization of GdVO4:Nd near-infrared phosphors for optical time-gated in vivo imaging, Materials 13 (2020) 3564.

S55

Development of IR optical chopper disc by thermal evaporated ZnS thin films

Gümüşay, Y. M.*[1,2,3], Efkere, H. İ.[1], Gözlekçi, G.[1], Başköse, Ü. C.[1], Cömert Sertel, B.[1], Dönmez Kaya, M.[1], Akman, L. B.[1] and Özçelik, S.[1,4]

[1]Photonics Application and Research Center, Gazi University, Ankara, Turkey
[2]Department of Advanced Technologies, Graduate School of Natural and Applied Sciences, Gazi University, Ankara, Turkey
[3]Defense and Energy Technologies Inc. (ASENTEK), Ostim Technopark, Ankara, Turkey
[4]Department of Photonics, Faculty of Applied Science, Gazi University, Ankara,Turkey
yusufmert.gumusay@gmail.com, sozcelik@gazi.edu.tr

In pyroelectric thermal cameras, the light falling on the detector takes the form of a sinusoidal wave with the help of a light chopper, and thus, the image is obtained by converting the temperature differences in the sensor into electric current. The chopper consists of two parts on the surface of the Silicon (Si) substrate, one is Archimedean spiral and the other is a non-patterned surface. It is aimed to achieve a permeability of approximately 30% in the patterned area and 90% or more in the non-patterned surface. The Archimedes spiral, which converts the light into a sinusoidal wave, is patterned on the surface by lithography method. In this work, Zinc Sulfide (ZnS) thin films were deposited on undoped Si substrate with 69 mm diameter and 650 um thickness at 500 and 1000 nm thickness at room temperature by thermal evaporation method to increase transmittance in IR wavelength. Coatings were carried out using a ZnS pellet and Sulfide of 99,9% purity at 10^5 mbar. ZnS pellet and Sulfide powder in different evaporation boats were evaporated at the same time to prevent deficiency of Sulfide on thin film surface.

Thickness of deposited thin films are measured by a tylus type (Dektak150) profilometer. structural properties of the films were evaluated by X-Ray Diffractometer (Bruker D8 Advance with CuKα1 X-ray source, λ= 1.54178 Å) and X-Ray Photoelectron Spectroscopy (XPS) (Omicron XPS using MgKα excitation source (*hv* = 1253.6 eV)) systems Optical properties are evaluated by Fourier-Transform Infrared Spectroscopy (FTIR). As a result of optical analysis, it is observed that IR transmittance of samples with 1000 nm thickness is 90% at unpatterned and about 30% at patterned surface. Optical and structural analysis show that sulfide deficiency occurs on the surface of thin film by evaporating only ZnS pellet. In this work proper one-layer ZnS pattern without sulfide deficiency is obtained by evaporating ZnS pellet and sulfide powder at the same time by using thermal evaporation technique.

Acknowledgement
This work was supported SBB (TR) with the project number 2016K121220 and KOSGEB with the project number 2019-701-429 (in ASENTEK).

S56

Structural and optical properties of SnS thin films deposited with sputtering method

Erenler, B.*[1,2], Ateş, H.[1,2], and Özçelik, S.[1,3]

[1]*Photonics Application and Research Center, Gazi University, 06500 Ankara, Turkey,*
[2]*Department of Metallurgy and Materials Engineering, Gazi University 06500, Ankara, Turkey,*
[3]*Department of Photonics, Gazi University 06500, Ankara,*
berkcan.erenler@gazi.edu.tr, sozcelik@gazi.edu.tr

The Tin Sulfide (SnS), one of the IV-VI compounds' semiconductors, which is well-known to have a high theoretical power conversion efficiency (%30 for solar cell) [1]. Due to its excellent structural, optical and electrical properties such as high absorption coefficient (>10^4 cm^{-1}), earth abundant, less toxic, low cost, suitable energy band gap range of 1.1-1.4 eV, high free carrier concentration (10^{15} - 10^{18} cm^{-3}), tin sulfide is as a potential absorber material for the commercial solar cells [2,3]. The sputtering method has excellent advantages mass manufacture capability, fabrication by one step directly, homogeneous and high growth than the other methods such as chemical vapor deposition (CVD), thermal evaporation, chemical bath deposition (CBD), atomic layer deposition (ALD) [4]. In this study, SnS thin films were grown by radio frequency (RF) sputtering method at room temperature. The RF power was 60W and the working pressure and argon flow rate during the growth was 30 mTorr and 20 sccm, respectively. The growth thin films were characterized by X-ray diffraction (XRD) and UV-visible spectroscopy in order to investigate the structural and optical properties of that thin films. It is clearly understood from XRD analysis that all peaks in the SnS thin films were matched to orthorhombic crystal structure. The energy band gap of the SnS thin films are calculated as 1.3 eV from Tauc plot.

Acknowledgement
This work was supported by Presidency of Turkey, Presidency of Strategy and Budget with 2016K121220 project number.

References:
[1] Son, S.I., Shin, D., Son, Y.G., Son, C.S., Kim, D.R., Park, J.H., Song, P. (2020). Effect of working pressure on the properties of RF sputtered SnS thin films and photovoltaic performance of SnS-based solar cells. Journal of Alloys and Compounds, 831, 154626.
[2] N. Koteeswara Reddy, M. Devika, E.S.R. Gopal, Review on tin (II) sulfide (SnS) material: synthesis, properties, and applications, Crit. Rev. Solid State Mater.
[3] A.R.H.F. Ettema, R.A. de Groot, C. Haas, T.S. Turner, Electronic structure of SnS deduced from photoelectron spectra and band-structure calculations, Phys. Rev. B 46 (1992) 7363–7373
[4] Arepalli, V. K., Shin, Y., Kim, J. (2019). Photovoltaic behavior of the room temperature grown RF-Sputtered SnS thin films. Optical Materials, 88, 594-600.

S57

Controllable synthesis of $Ni_xZn_{1-x}S$ nanoparticles on the base of NiZnAl Layered Double Hydroxide/PVA composite matrix

Balayeva, O.O.*, Azizov, A.A., Muradov, M.B., Mammadova, S.F., Alosmanov, R.M., Gahramanli, L.R., and Allahyarova, S.Y.

Baku State University, Z. Khalilov str., 23, AZ-1148, Azerbaijan
ofeliyabalayeva@bsu.edu.az

In the presented work, NiZnAl-based layered double hydroxides (LDH) / polyvinyl alcohol (PVA) nanocomposite was synthesized by co-formation method [1]. The synthesis of the nanocomposite was carried out in an aqueous medium at 90°C. $Ni_xZn_{1-x}S$ nanoparticles were synthesized on the basis of obtained NiZnAl-LDH/PVA and their optical and structural properties were studied. Ultraviolet-visible spectroscopy (UV-Vis) results show that the synthesized samples can be used in various industries for optical, photocatalytic and photoelectric applications.

In the experiment work, $NiSO_4 \cdot 7H_2O$, $ZnSO_4 \cdot 7H_2O$ and $Al_2(SO_4) \cdot 18H_2O$ salts were used as the metal sources. The ratio of divalent (Ni^{2+} and Zn^{2+}) and trivalent (Al^{3+}) metal ions in the solution was 3/1. $Ni_xZn_{1-x}S$ (x=0.2; 05 and 08) nanoparticles were synthesized by the successive ionic layer adsorption and reaction (SILAR) method in 5 cycles on the basis of the obtained NiZnAl-LDH/PVA. The properties of the samples were studied by UV-Vis and powder X-ray diffractometry (XRD).

According to the results of UV spectroscopy, the bandgap of NiZnAl-LIH / PVS nanocomposite was estimated to be 3.05 eV. After the formation of ternary $Ni_xZn_{1-x}S$ nanoparticles the band gaps were determined as 2.98; 3.00 and 3.10 eV when the x value changed as x=0.2; 05 and 08, respectively. Based on the results of XRD, high-crystalline NiZnAl-LDH layered structures were synthesized. Diffraction peaks of 2θ = 27.76; 28.10 and 28.18 degrees indicate $Ni_xZn_{1-x}S$ nanocrystals where x=0.2, 05, 08, respectively. The XRD pattern of pure hexagonal ZnS exhibits the 2θ=28.65° diffraction peak at (0016) planes (JCPDS 89–2424) [2, 3]. With the formation of ternary NiZnS nanoparticles, the spectra remained the same hexagonal phase of ZnS, which reveals that Ni atoms have participated in the hexagonal structure of ZnS, and therefore the peaks were observed at a low angle between transmitted and reflected beam (2theta) [3].

References:

[1] Balayeva O.O. Journal of Dispersion Science and Technology 2021, DOI: 10.1080/01932691.2020.1848580.
[2] Muradov M.B., Gahramanli L.R., Balayeva O.O., et al. Results in Physics, 18 (2020) 103280.
[3] Kaliaraj G.S., Ramadoss A. Materials Science in Semiconductor Processing 105 (2020) 104709.

S58

Tm^{3+}:KY $(WO_4)_2$ single crystals prepared by the modified Czochralski method: growth and optical properties

Lubochko, N.A.[1*], Guretskii, S.A.[1], Gorbachenya, K.N.[2], Kisel, V.E.[2], Karpinsky, D.V.[1], Özen, Y.[3], Özçelik, S.[3,4] and Kuleshov, N.V.[2]

[1]*Scientific and Practical Materials Research Center NAS Belarus, Minsk, Belarus*
[2]*Center for Optical Materials and Technologies, Belarusian National Technical University, Nezavisimosty Ave., 65, Minsk 220013, Belarus*
[3]*Photonics Application & Research Center, Gazi University, Ankara, Turkey*
[4]*Photonics Department of Applied Science Faculty, Gazi University, Ankara, Turkey*
nadzeya.lubochko@gmail.com

Laser sources emitting in the 1.9–2 μm spectral range are of high interest for a variety of practical applications in medicine, remote sensing, optical and other materials. The present study is focused on the growth and optical characterization of Tm doped KYW crystals used for lasers working in near IR range.

Growth of the KYW crystals has been carried out at temperatures below the point of the phase transition (900÷985 ℃) using the oriented crystal seed which gradually pull up upon slow cooling of the solution-melt. Stoichiometric composition of crystal forming components was fused with a total mass of solution-melt of about 1600-1800 g. Growth temperature was in the range 900-985°C. During the growth process an overcooling parameter was about 1.5-2.2°C; crystal pulling speed was about 3.3-3.5mm/d; the weight of the grown crystals was about 600g.

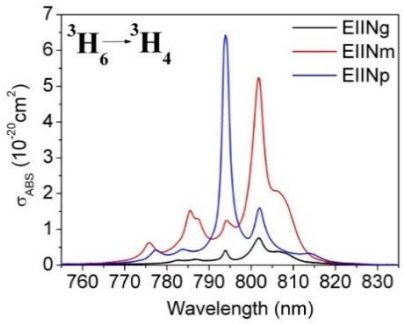

Figure 1. Polarized absorption cross-section spectra of Tm:KYW crystal at near 800 nm.

The room-temperature polarized absorption cross-section spectra of the Tm:KYW crystal in the spectral range of 750–850 nm ($^3H_6 \rightarrow ^3H_4$ transition) are shown in Fig. 1. The crystal belongs to monoclinic crystallographic system and consequently, it is bi-axial optical system. The clearly visible maxima can be seen on the polarized absorption spectra. Anisotropy of analyzed Tm^{3+} absorption in KYW crystal is substantial and it can be perceived that the $^3H_6 \rightarrow ^3H_4$ absorption spectrum recorded for $E//N_g$ is not intense and structureless. On the other hand, the prominent components can be found for polarized absorption spectra measured for $E//N_m$ and $E//N_p$. The A maximum absorption cross-section of 6.4×10^{-20} cm^2 was determined at 794 nm with a bandwidth (FWHM) of 2.2 nm for light polarization $E//N_p$ axis. Based on the aforementioned results, it can be concluded that geometry of Tm:KYW crystal and the adequate configuration of optical pumping source are crucial for effective near-infrared Tm^{3+} laser operation.

Acknowledgements
This research is performed in the framework of the bilateral project supported by NAS of Belarus and Tubitak (project number 120N014).

FULL TEXTS

FT1

Topological charge of a superposition of optical vortices

Kotlyar V.V.*[1,2], Kovalev A.A.[1,2]

Image Processing Systems Institute of RAS – Branch of the FSRC "Crystallography and Photonics" RAS, 151 Molodogvardeyskaya St., Samara 443001, Russia
kotlyar@ipsiras.ru

Here, we expand a remarkable finding reported by M.S. Soskin et al. in Phys. Rev. A 56, 4064 (1997). We show that for an on-axis superposition of two different-waist Laguerre-Gaussian (LG) beams with numbers (0,*n*) and (0,*m*), the topological charge (TC) changes from *m* to *n* (if the LG beam (0,*m*) has a larger waist) in the plane where the beams widths are the same. We explain this effect by extra off-axis optical vortices (OVs) with TC=+1 (or -1), which move to (or from) infinity with a higher-than-light speed.

Keywords: optical vortex, hidden phase, screw dislocation, topological charge

Introduction

While the orbital angular momentum of paraxial optical vortex (OV) beams conserves on space propagation [1], it is not so evident for the topological charge (TC). All symmetric OVs, e.g. Laguerre-Gaussian (LG) beams and some asymmetric OVs conserve their TC [2]. No general proof of TC conservation has so far been offered, although some works discussed examples of OVs with nonconserving TC. M.S. Soskin et al. were the first to demonstrate this effect [3] for a superposition of a Gaussian beam and a LG mode of different waist radii. These beams diverge differently, causing TC to change. Upon propagation, a fractional Gaussian beam was theoretically [4] and experimentally [5,6] shown to have in the near-field an integer TC nearest to the initial fractional TC. In the Fresnel zone [7], however, TC becomes equal to the closest larger integer. Similar study was conducted in [8], but in the Fourier-plane, and the results are different from [7].

Following the pioneering research by M. Soskin et al. [3], we show here that in the superposition of two different-waist LG beams, TC does not conserve on propagation because phase singularities partly either 'go to' or 'come from' infinity. Interestingly, the phase singularities 'go to and come from' infinity with a higher-than-light speed.

Theory

The topological charge can be calculated using a formula proposed by M.V. Berry [4]:

$$TC = (2\pi)^{-1} \lim_{r\to\infty} \mathrm{Im} \int_0^{2\pi} E^{-1}(r,\varphi)\left[\partial E(r,\varphi)/\partial\varphi\right] d\varphi \,. \quad (1)$$

In [3], using a superposition of two LG beams as an example, its TC was shown not to conserve on propagation. However, no direct TC calculation by (1) was done [3]. Below, we generalize the results from [3] and calculate TC directly by (1) for a field composed of two different-waist LG modes (0,*n*) and (0,*m*) with the initial waist radii w_{10} and w_{20} (the case $w_{10} = w_{20}$ was studied in [9] and TC = max(*m*,*n*)):

$$E(r,\varphi,z)=a(z)\left[r/w_1(z)\right]^{|n|}e^{-r^2/w_1^2(z)+ikr^2/2R_1(z)+in\varphi}+b(z)\left[r/w_2(z)\right]^{|m|}e^{-r^2/w_2^2(z)+ikr^2/2R_2(z)+im\varphi}, \quad (2)$$

where $w_i(z) = w_{i0}[1+(z/z_i)^2]^{1/2}$ (i=1,2) are waist radii of two Gaussian beams at the distance z, $z_i = kw_{i0}^2/2$ are the Rayleigh distances, $R_i(z)=z[1+(z_i/z)^2]$ are the wavefront curvature radii, $a(z)=2^{|n|/2}[w_{10}/w_1(z)]\exp[-i(n+1)\arctan(z/z_1)]$ ($b(z)$ is defined similarly), n and m are TCs of the OVs. Substituting (2) into (1) yields:

$$TC=\begin{cases} m, & w_1(z)\le w_2(z), \\ n, & w_1(z)>w_2(z). \end{cases} \quad (3)$$

The TC (3) was obtained as follows. Substituting (2) into (1) yields the integral of the ratio of sums of two exponentials. Putting $w_{10} > w_{20}$, we obtain that $w_1(z) > w_2(z)$ at $z < z_0 = kw_{10}w_{20}/2$ and the condition $z < z_0$ (or $z < z_0$) defines which exponential dominates, thus switching the TC from n to m at $z = z_0$. On the contrary, if $w_{10} < w_{20}$, then at $z = z_0$, TC changes from m to n. Thus, we can infer that on free-space propagation of beam (2), $|n-m|$ OVs with TC = -1 are born (or annihilated) at some distance.

Movement of phase singularities in the propagating beam

Equating amplitudes of the two constituent LG beams in (2) yields: $a(z)\left[r/w_1(z)\right]^{|n|}e^{-r^2/w_2^2(z)} = b(z)\left[r/w_2(z)\right]^{|m|}e^{-r^2/w_2^2(z)}$. This equation can be rewritten as (putting $n>m>0$)

$$\left[a(z)/b(z)\right]\left[w_2^m(z)/w_1^n(z)\right]r^{n-m}=\exp\left\{-\left[1/w_2^2(z)-1/w_1^2(z)\right]r^2\right\}. \quad (4)$$

The left-hand side of (4) is a power function of r, which grows from zero to infinity. The right-hand side is an exponential, which either grows from unity to infinity or drops to zero. At some distance z, the waist radii get equal to each other [$w_1(z) = w_2(z)$]:

$$z_0 = kw_{10}w_{20}/2. \quad (5)$$

Equations (5) and (4) suggest the following evolution of OVs in field (2) on propagation. According to [5], the near-axis ($r << 1$) TC of the beam (2) equals TC of the larger-amplitude constituent OV. If $n > m$, then $a(z)[r/w_1(z)]^n < b(z)[r/w_2(z)]^m$. Hence, at any distance z there is an on-axis OV with TC = m. Other OVs are on the circles with radii given by (4). If $w_{20} > w_{10}$, the exponential function in (4) intersects the curve r^{n-m} twice. The first (second) intersection means n-m OVs with TC +1 (-1) on a circle of radius R_1 (R_2). Thus, in the initial plane and the near field, these off-axis OVs cancel each other. On further propagation from z=0 to z=z_0, the smaller waist $w_1(z)$ grows faster than the larger waist $w_2(z)$. The exponential function in (4) grows slower and the radius R_2 increases. Thus, n-m OVs with TC -1 (on the circle of radius R_2) move from the center to periphery. In the plane z_0 with $w_1(z) = w_2(z)$, according to (4), $R_2 \to \infty$, i.e. (n-m) OVs with TC = -1 'going to' infinity. Thus, at $z > z_0$, the beam (2) has TC = m+(n-m)=n. The OVs may be thought of as moving with a larger-than-light speed, which does not contradict to the relativity theory as the movement of OVs is due to interference of two waves. Similar effects are known in optics (e.g., for the diffraction-free Bessel beam).
If $w_{20} < w_{10}$, according to (4), the evolution of the off-axis OVs in the beam (2) is opposite. At $z < z_0$, beam (2) has TC = n, but at $z > z_0$, n-m OVs with TC=-1 'come from' infinity with a larger-than-light velocity, and the TC becomes equal to TC = n-(n-m)=m.

Summing up, we can infer that at $w_{20} \neq w_{10}$, beam (2) is a proving example of the non-conservation of TC of the propagating OVs. However, it is worth noting that although the OVs partly 'go to' infinity this does not mean that they fully disappear. If the OVs at infinity are taken into account, the total TC of the superposition is conserved.

Numerical simulation

The initial field is given by (2). We analyzed a situation when $n>m$ and $w_{10}<w_{20}$. The simulation was conducted for n=5, w_{10}=3 μm, m=2, w_{20}=4 μm, λ=532 nm, the entire 20 × 20 μm field was confined by a 10-μm pupil. According to Fig.1a,b, TC = 2 in the initial field, since at the opposite ends of three segments, opposite-sign OVs are cancelled. From (5) and for given simulation parameters, the waists of the LG beams become equal at the distance z_0 = 70.86 μm. TC was found to change from the value of 2 to 5 on the radius R_1=1.85 μm, and from 5 to 2 on the radius R_2 = 10.5 μm.

With increasing distance z, the radii R_1 and R_2 at which TC changes its value also grow. Fig. 1c,d shows the amplitude and phase of the beam (2) at z=20 μm. Similar to Fig.1a,b, three OVs are located on the circle of radius R_1, each having TC = +1 (with the OVs centered at the closer ends of three segments in Fig.1d), with three other OVs, with TC = -1, found on a circle of radius R_2 (at the remote ends of the three segments) in Fig.1d. The OVs with TC = -1 are seen to be shifted further from the optical axis.

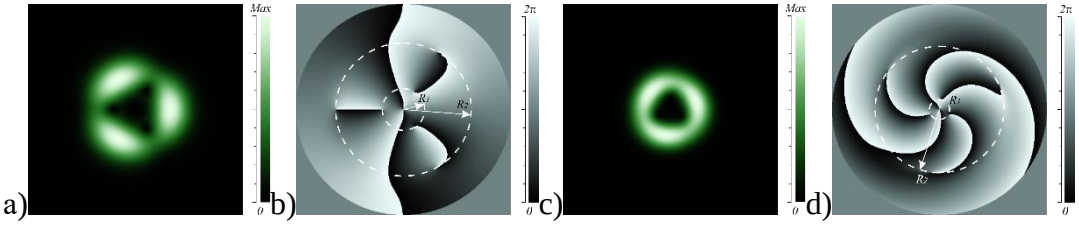

Fig. 1. Amplitude (a,c) and phase (b,d) of the field (2) in the planes z = 0 (a,b) and z=20 μm (c,d). The images are of size 20 × 20 μm (a,b) and 40 × 40 μm (c,d).

It was numerically obtained that the radius R_2 of a circle with three OVs with TC = -1 grows increasingly faster with distance z, tending to infinity at $z \approx 71$ μm. The radius R_2 depends on z approximately as follows (c_1=0.152, c_2=-0.0021, b=3.95):

$$R_2 = b + \left(c_1 + c_2 z\right)^{-1} \tag{6}$$

Next, we analyze the reverse case ($w_{10}>w_{20}$). The simulation parameters are the same as in Fig. 1, but w_{10}=4 μm and w_{20}=3 μm. The amplitude and the phase of field (2) in the initial plane (at z=0) are shown in Fig. 2a,b. From Fig. 2b, field (2) has TC = 5, with a near-vertical wavy line of phase jump passing through the origin (adds +2 to the TC) and three rays outgoing from a circle of radius R_1 with three OVs, each with TC = +1. As field (2) propagates, its total TC remains equal to 5, but the radius R_1 of the circle with three OVs grows. After the beam travels the distance of equal waists (5), z_0 = 70.86 μm, TC gets equal to TC = 2. Fig. 2c depicts the field phase at the distance z=90 μm.

From Fig. 2c, three OVs appear on a circle $R_2 \approx$45 μm, each with TC = -1, which compensate for three OVs with TC = +1. So that an on-axis OV with TC = +2 is the only one that remains noncompensated for. As before, the radius R_2 of a circle with three

OVs with TC = -1 depends on z approximately as given by (6), but with c_1=-0.258, c_2=0.00366, b=30. Thus, the radius R_2 is seen to tend to infinity at $z \approx 69.8$ μm.

Conclusion

Summing up, we have shown that in an on-axis superposition of two different-waist LG beams with the numbers (0,n) and (0,m), TC remains equal to m until the beam reaches a plane of the equal waists, given that the LG mode (0,m) has a larger waist, after which the TC becomes equal to n. This because in the initial plane, the superposition contains an on-axis OV with TC = m, with (n-m) OVs with TC = +1 and (n-m) OVs with TC = -1 centered at different-radius circles. On approaching an equal-waists plane, the OVs with TC = -1 'go to' infinity with a larger-than-light speed, with the superposition acquiring TC = n. In the opposite case, i.e. when the LG beam (0,m) has a smaller waist, TC in the equal-waists plane changes its value from n to m. In this case, on the contrary, n-m OVs with TC = -1 'come from' infinity with a larger-than-light speed.

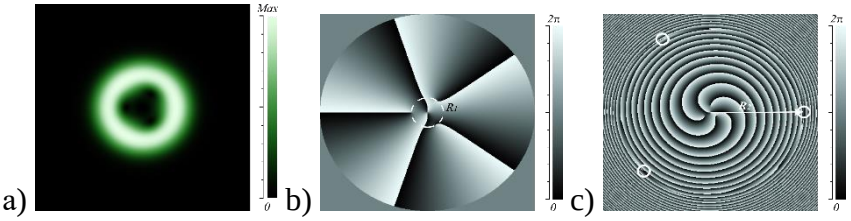

Fig. 2. Amplitude (a) and phase (b,c) of the initial field (a,b) and at the distance z=90 μm (c). The images are of size 20 × 20 μm (a,b) and 100 × 100 μm (c).

Acknowledgment

The work was partly funded by the Russian Foundation for Basic Research under RFBR grant # 18-29-20003 (theory) and the RF Ministry of Science and Higher Education under a government project of FSRC "Crystallography and Photonics" RAS (simulation).

References

[1] L. Allen, M. Beijersbergen, R. Spreeuw, J. Woerdman, "Orbital angular momentum of light and the transformation of Laguerre-Gaussian laser modes," Phys. Rev. A, vol. 45, pp. 8185, June 1992.
[2] V.V. Kotlyar and A.A. Kovalev, "Topological charge of asymmetric optical vortices," Optics Express vol. 28, pp. 20449-20460, July 2020.
[3] M.S. Soskin, V.N. Gorshkov, M.V. Vastnetsov, J.T. Malos, N.R. Heckenberg, "Topological charge and angular momentum of light beams carrying optical vortex," Phys. Rev. A, vol. 56, pp. 4064-4075, November 1997.
[4] M.V. Berry, "Optical vortices evolving from helicoidal integer and fractional phase steps," J. Opt. A: Pure Appl. Opt. vol. 6, pp. 259–268, January 2004.
[5] J.B. Gotte, S. Franke-Arnold, R. Zambrini, S.M. Barnett, "Quantum formulation of fractional orbital angular momentum," J. Mod. Opt., vol. 54, pp. 1723–1738, September 2007.
[6] A.J. Jesus-Silva, E.J.S. Fonseca, J.M. Hickmann, "Study of the birth of a vortex at Fraunhofer zone," Opt. Lett. vol. 37, pp. 4552-4554, November 2012.

[7] J. Wen, L. Wang, X. Yang, J. Zhang, S. Zhu, "Vortex strength and beam propagation factor of fractional vortex beams," Opt. Express, vol. 27, pp. 5893-5904, February 2019.
[8] V.V. Kotlyar, A.A. Kovalev, A.G. Nalimov, A.P. Porfirev, "Evolution of an optical vortex with an initial fractional topological charge," Phys. Rev. A, vol. 102, pp. 023516, August 2020.
[9] V.V. Kotlyar, A.A. Kovalev, A.V. Volyar, "Topological charge of a linear combination of optical vortices: topological competition," Opt. Express, vol. 28, pp. 8266-8281, March 2020.

FT2

Effect of refractive inhomogeneity on the efficiency of SHG in optical fiber

Kasumova R. J.[1], Tagiev Z.H.[2], Amirov Sh.Sh.*[2]

[1]Physics Department, Baku State University, acad. Z. Khalilov str. 23, AZ1148, Baku, Azerbaijan
[2]Department of Medical and Biological Physics, Azerbaijan Medical University, A. Gasimzade str., 14, AZ 1022, Baku, Azerbaijan
phys_med@mail.ru

In this paper the effect of inhomogeneity of refractive index on the efficiency of second harmonic generation in an optical fiber is studied in the constant intensity approximation, taking into account the reverse reaction of excited wave on the phase of exciting one. The pulse of Gaussian shape has played the role of pump wave. Effect of regular inhomogeneity of the refractive index on the efficiency of SHG was observed at various levels of pump wave intensity. It was shown that due to inhomogeneity of refractive index one can control the duration of output pulse in optical fibers. Results obtained were compared with the results obtained in the constant field approximation as well as the case of homogeneous medium.

Keywords: regular refractive index inhomogeneity, optical fiber, pulse duration, constant intensity approximation

Introduction

Optical inhomogeneity occurs due to inhomogeneous composition, the presence of impurities, defects, etc. This results in an inconsistent refractive index along the entire length of the material. In the case of optical fiber, the sample is fabricated with a refractive index gradient where the core size and refractive index profile must be kept strictly constant. Note that dispersion in an optical fiber plays the main role in the propagation of short laser pulses. A distinction is made between static inhomogeneity, when either the direction of the optical axis changes randomly, and regular inhomogeneity, when the change in the refractive index can be described analytically [1-2]. Both types of inhomogeneity can be inherent in the nonlinear medium itself or arise as a result of parametric interaction under the action of laser radiation on a parameter of the medium. The degree of inhomogeneity directly affects the efficiency of the transducers as well as the parametric gain threshold.

Scientific research of the world's leading laboratories over the past decades has confirmed the promising nature of using optical fiber for information transmission. In particular, optical solitons are used for this purpose, i.e. laser pulses propagating practically without changing the pulse shape due to compensation arising from two opposite effects: dispersive broadening and narrowing of the spectrum of laser radiation during propagation in a nonlinear medium. In addition, using solitons, it is possible to control the parameters of ultrashort optical pulses [3-4].

Effects of second and third order dispersions on the pulse broadening in linear dispersive standard single mode fiber are studied in [5] In general two types of inhomogeneity can be distinguished in optical fibers. One of those is related to the irregular character of the change in the orientation of optical axis of the medium. Up to now the optical fibers have mainly be studied by employment of constant field approximation in which the complex amplitudes of interacting waves were considered to be fixed [3,4]. In this case information related to alteration in the phase of waves are lost. Thus, considering the regular inhomogeneity we have discussed generation of second harmonic in the constant intensity approximation (CIA) [6-11] which has allowed to take into account reverse reaction of the generated wave to the incident (pump) wave. In this approximation, we have already analyzed nonlinear processes at SHG and CARS in an optical fiber, the effects of the self–phase and cross–phase modulations [12-13].

Theory

In this paper we analyze generation of second harmonic in optical fiber with an optical inhomogeneity. Discussion will be carried out in the first order dispersion theory. The set of reduced equations describing the second harmonic generation in the dissipative medium is given in [3, 12]:

$$\frac{\partial A_1}{\partial z}+\frac{1}{u_1}\frac{\partial A_1}{\partial t}+\delta_1 A_1=-i\gamma(|A_1|^2+2|A_2|^2)A_1-i\beta_1 A_1^* A_2\, exp[\,i\Delta_0 z+i\psi(z)],$$
$$\frac{\partial A_2}{\partial z}+\frac{1}{u_2}\frac{\partial A_2}{\partial t}+\delta_2 A_2=-i\gamma(|A_2|^2+2|A_1|^2)A_2-i\beta_2 A_1^2\, exp[\,-i\Delta_0 z-i\psi(z)]. \quad (1)$$

where $A_{1,2}$ are the complex amplitudes of the pump wave (ω_1) and second harmonic ($\omega_2=2\omega_1$),$u_{1,2}$ are the group velocities of the corresponding waves, $\delta_{1,2}$ are the linear losses of the interacting waves, γ is an average value of nonlinear coupling coefficient of the interacting waves where the contribution is imported by the self – phase and cross – phase modulation processes, $\beta_1=\gamma_{SH}^*/2,\quad \beta_2=\gamma_{SH},\quad \gamma_{SH}=3\omega_1\varepsilon_o^2\alpha_{SH}f_{112}\chi^{(3)}|E_p|^2|E_{SH}|,\quad \varepsilon_0$ is a dielectric constant of vacuum, α_{SH} is a constant, depending on the microscopic process, f_{112} is an integral of the overlapping, defining through mode distribution for optical fields and average on transverse coordinates x and y [14], E_p is a field of pumping at frequency ω_p, E_{SH} is a field of a weak seed second harmonic at frequency $2\omega_p$. $\Delta_0=k_2-2k_1-\Delta(z)$, where Δ_0 and $\Delta(z)$ denote the constant and variable parts of the wave parts of the phase detuning between the interacting waves, respectively, and$\psi(z)=\int_0^z\Delta(z')dz'$. For further simplification the above overlap integrals $f_{ijk}\cong f_{112}\cong 1/A_{eff}\quad (i,j,k=1,\ 2,\ 3)$ (A_{eff} is the effective area of a fiber core) are taken identical, that is valid for single-mode waveguides [3]. Here we study generation of second harmonic with employment of following boundary conditions:

$$A_1(z=0)=A_{10}(t),\qquad A_2(z=0)=0 \quad (2)$$

To investigate the process considered we use quasi-static approximation for which we take equality of group velocities and then substitute new variables for coordinate z→ z and time t→ $\eta=t-z/u$.

$$\frac{\partial A_1}{\partial z}+\delta_1' A_1=-i\beta_1 A_1^* A_2\, exp[\,i\Delta_0 z+i\psi(z)],$$
$$\frac{\partial A_2}{\partial z}+\delta_2' A_2=-i\beta_2 A_1^2\, exp[\,-i\Delta_0 z-i\psi(z)], \quad (3)$$

Where
$\delta_1^{'} = \delta_1 + i\gamma(|A_1|^2 + 2|A_2|^2)$, $\delta_2^{'} = \delta_2 + i\gamma(|A_2|^2 + 2|A_1|^2)$
Solving equation (3) with boundary conditions (2) for output amplitude $A_2(z)$ and further finding efficiency yields ($I_2(z) = A_2(z) \cdot A_2^*$)

$$I_2(z)/I_{10} = (|\beta_2|z)^2 I_{10}(\eta)\left\{[1 - \frac{1}{3}|\alpha|z^2 + \frac{1}{30}(2|\alpha|^2 z^4 - \Gamma^4 z^4)]^2 + \left[\frac{1}{3} - \frac{1}{10}|\alpha|z^2\right]^2 \Gamma^4 z^4\right\} exp(-4\delta_1 z) \quad (4)$$

From equation (4) in case of $\Delta(z) = 0$ ($\alpha = 0$), for a homogeneous medium we obtain $I_2^{CIA}(z) = |\beta_2|^2 I_{10}^2(\eta) z^2 \cdot exp(-4\delta_1 z)\{1 + \frac{(\Gamma z)^4}{45}[2 + \frac{(\Gamma z)^4}{20}]\}$. Here the case of $\beta_1 = 0$ ($\Gamma = 0$) corresponds to the result of constant field approximation. In the absence of linear losses δ_1=0, from (4) we obtain $I_2^{CFA}(z) = |\beta_2|^2 I_{10}^2(\eta) z^2$, and in the stationary case $I_2^{CFA}(z) = |\beta_2|^2 I_{10}^2 z^2$ [16].

Assuming that the pump wave is of Gaussian shape $A_{10}(\eta) = A_{10}\, exp(-\eta^2/2\tau_1^2)$ we can analyze the equation (4) for both weak ($|\alpha|z^2 < 1$) and strong ($|\alpha|z^2 > 1$) inhomogeneity of the medium in the case of short interaction length $\Gamma z < 1$. For both cases the equation (4) is simplified and we obtain expressions for the output pulse durations $\tau_2 1_{inhom}\sqrt{1 - \frac{4}{45}\Gamma(0)^4 z^4}$ for a weak inhomogeneity and $\tau_2 1_{inhom}\sqrt{1 - \frac{2}{15}|\alpha|\Gamma(0)^4 z^4}$ for strong inhomogeneity respectively in the constant intensity approximation (CIA). As can be seen since ($\Gamma = 0$) in the CFA both formulas result in $\tau_2 1_{inhom}$ which means that change in pulse duration cannot be taken into account in CFA.
Analysis formula (4) in the CIA yields the results different from CFA. In the CIA we have obtained that an increase in the degree in inhomogeneity of the nonlinear medium efficiency of conversion of pump wave energy into harmonic wave decreases. It is obtained that the pulse duration increases with increase in the degree in inhomogeneity. Unlike the results of CFA a broadening of the second harmonic pulse in a regular inhomogeneous medium as compared to the case of a homogeneous medium as well as the saturation of the second harmonic intensity in the process of frequency conversion are observed.

References:

[1] F.S. Ghen. Optically induced change of refractive indices in LiNbO3 and LiNaO3. Appl. Phys. 1960, 40(8), 3389-3396.
[2] S.A. Akhmanov, D.P. Krindach, A.P. Sukhorukov, R.V. Khohlov. JETP Letters, 1967. 6(2), 509-513.
[3] G. Agrawal, Nonlinear Fiber Optics. Academic, San-Diego, Calif. (1995).
[4] L. F. Mollenauer, J. P. Gordon. Solitons in Optical Fibers. Fundamentals and Applications. Elsevier, 2006. 296p.

[5] Sh. Shermin A. Khan and Md.S.Islam Pulse broadening induced by second order and third order dispersion in a dispersive fiber. Journal of Information and Communication Technologies, V.3, issue 4, 2013 p.16-21
[6] A. Bukhamsin, R. Horne (2014) Paper SPE 170679-MS Presented at the 2014 SPE Annual Technical Conference and Exhibition held in Amsterdam, the Netherlands, 27-29 October 2014 p. 1-19.
[7] N. Blombergen. Nonlinear Optics. W.A. Benjamin, Inc. New York-Amsterdam, (1965)
[8] Y.R. Shen. Principles of Nonlinear Optics, Wiley, New York, 1984
[9] M.D. Reid, P.D. Drummond, Phys. Rev. Lett., 60, 2731 (1988).
[10] R.W. Boyd, Nonlinear optics. San Diego, Academic Press, 2008, -613p.
[11] Z.H. Tagiev, and A.S. Chirkin, Fixed intensity approximation in the theory of nonlinear waves, Zh. Eksp. Teor. Fiz. 73 (1977) 1271-1282;
[12] Z.H. Tagiev, R.J. Kasumova, R.A. Salmanova, N.V. Kerimova J. Opt. B: Quantum Semiclas. Opt. 3, 84 (2001).
[13] Z.H. Tagiev, R.J. Kasumova. Theoretical studies on frequency doubling in glass optical fibers in constant-intensity approximation. Optics & Communications, 2006, v.261, p.258-265.
[14] R.J. Kasumova, N.V. Kerimli, G.A. Safarova. Phase effects on coherent anti-Stokes Raman scattering. J. of Applied Spectroscopy.
[15] J.G. Gabriagues, L. Fersing, in Digest of Conference on Lasers and ElectroOptics, OSA, Washington, D.C., 1984, p.176. J.G. Gabriagues, H. Fevrier, Opt. Lett., 12, 720 (1987).
[16] V.G. Dmitriev, L.V. Tarasov. Applied Nonlinear Optics. Fizmatlit, Moscow, 2004, 360.

FT3

FDTD simulation of propagation of Hermite-Cosh Gaussian high intensity laser beam in inhomogeneous plasma and modeling of ponderomotive force and magnetic field

Alilou, S.* and Shahrassai, L.

Department of Physics and Technology of Plasma, Faculty of Physics, University of Tabriz, Iran
s.alilu@tabrizu.ac.ir

The interaction of laser beams with plasma is very important in many wave-particle phenomena. In this paper, we investigate the interaction of intense Hermite-Cosh Gaussian laser beams with Inhomogeneous plasma. We study the distribution of magnetic and electric fields of plasma and drew the related diagrams and then we compare them together. Because high-power lasers cause nonlinear effects on the plasma that lead to the nonlinear Ponderomotive force, the behavior of the ponderomotive force resulting from this radiation was investigated.

Keywords: Hermite-Cosh Gaussian beam, Inhomogeneous plasma, Simulation FDTD

Introduction

The field of nonlinear optics is one of the most prominent developments, which have come from the expansion of the laser almost 70 years ago. Laser-plasma coupling is an immense research topic amongst various research groups worldwide because of its significance in various applications including inertial confinement fusion (ICF), super-continuum generation, X-ray lasers, and acceleration of charged particles [1–3]. When an electromagnetic wave such as a high-power laser propagates in plasma, it acts on it via a nonlinear force known as ponderomotive force. This force causes some changes in the refractive index of the medium and hence alters its propagation Characteristics [4]. A variety of mechanisms capable of produce large and small-scale magnetic fields in plasmas, have been proposed by including temperature gradients in plasma, the ponderomotive force of the laser pulse, inverse Faraday Effect non-collinear density, Biermann-battery effect and etc. [5,6]. FDTD is the gold standard for modelling in Nano-photonic devices, processes, and materials. In this paper, both theory and simulation based on FDTD are used which are complementary to each other. Particle simulation allows one to test the theory and develop some nonlinear effects. The propagation of a high-intensity laser beam in plasmas, had been investigated by various workers in both theoretical and numerical analysis. The following describes the propagation of the Hermit-Cosh Gaussian beam electric field in Inhomogeneous plasma and discusses about the magnetic field, the nonlinear ponderomotive force.

Simulations and calculations

In the simulation of this paper, the FDTD program is used, which is two-dimensional plasma with dimensions of 3 × 3 micrometres. Plasma has a density profile of $1/x$, in which case the refractive index of non-collision plasma is defined as follows [7]:

$$\varepsilon = 1 - \frac{\omega_p^2}{\omega^2} \rightarrow \omega_p^2 = \frac{4\pi n_0 e^2}{m}, \omega^2 = \frac{4\pi n e^2}{m} \quad (1)$$

In this relation ω is the laser frequency, e is the electric charge, m is the electron mass, n is the electron density,n_0 Initial electron density, and ω_p is the plasma frequency. Related to placement:

$$\varepsilon = 1 - \frac{\frac{4\pi n_0 e^2}{m}}{\frac{4\pi n e^2}{m}} = 1 - \frac{n_0}{n} \rightarrow if \leftrightarrow n = 1/x$$

$$\varepsilon = 1 - n_0 x \quad (2)$$

The defined source of the Hermit-Cosh Gaussian electric field propagates vertically in the plasma, which is related as follows [8]:

$$E_{mn} = E_0 H_n(\frac{\sqrt{2}z}{\omega_0}) H_m(\frac{\sqrt{2}y}{\omega_0})\, Cosh(\Omega_0 z)\, Cosh(\Omega_0 y) e^{(-\frac{y^2}{\omega_0^2} - \frac{z^2}{\omega_0^2})}$$

$$E_{11}(0, y, z) = 4E_0 zy\, Cosh(\Omega_0 z)\, Cosh(\Omega_0 y) e^{(-\frac{y^2}{\omega_0^2} - \frac{z^2}{\omega_0^2})} \quad (3)$$

In the above relation, H_{mn} are hermetic polynomials and,$\Omega_0 = \frac{b}{\omega_0}$, which is b = 1. Using Faraday induction law, we can calculate the magnetic field from the electric field mentioned above as follows [8]:

$$B = -\frac{ic}{\omega}\frac{\partial E}{\partial z} = -\frac{ic}{\omega} 4e^{\frac{-y^2 - z^2}{\omega_0^2}} (y\, cosh(\Omega_0 y)\, cosh(\Omega_0 z) - 2yz^2\, cosh(\Omega_0 y)\, cosh(\Omega_0 z)$$

$$+ yz\, cosh(\Omega_0 y)\, sinh(\Omega_0 z)) \quad (4)$$

and, the ponderomotive force is obtained as follows:

$$F_P = -\frac{e^2}{4m\omega^2} \nabla(\langle E^2 \rangle)$$

$$F_P = -\frac{e^2}{4m\omega^2}(-32E_0 e^{-2(y^2+z^2)/\omega_0^2} y(-1 + 2y^2)z^2) \quad (5)$$

Analytical and simulation results

In Fig. 1, we can see the intensity of the electric field, which is in the form of a hermit-Cosh Gaussian beam in two dimensions. The resulting electric field intensity actually has four peaks. In the following, we see an electric field inside a inhomogeneous plasma with a two-dimensional inverse line density profile in Fig. 2, which in comparison with Figure 1, areas with high electric field intensity, the penetration of Hermit-Cosh Gaussian cosine beam in these areas of plasma is high. The center of these points is at z≈ ±0.75 where the intensity of the electric field is equal to 0.735(V / micron).

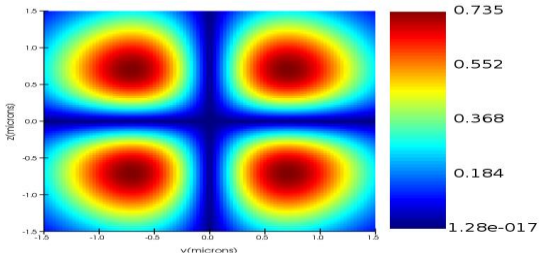

Figure 1: The Intensity Hermite-cosh Gaussian electric field in the direction of the axis ZY

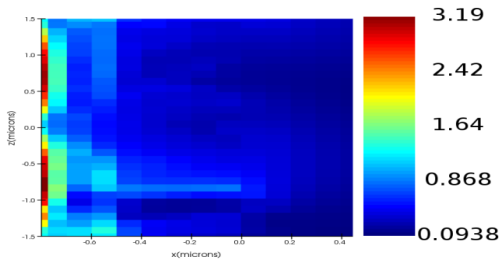

Figure 2: Intensity of electric field penetration inside inhomogeneous plasma in axial

The behavior of the resulting magnetic field inside the plasma is shown in Figure 3. That the given magnetic field is perpendicular to the electric field, we observe the $\frac{\pi}{2}$ phase difference between the magnetic and electric fields. The maximum value of the magnetic field at the point z≈0 is 9.08×10^{-3}(G). In addition, in places where the intensity of the electric field is maximum, the intensity of the magnetic field is minimum. The phase difference between the normalized electric and magnetic fields in one dimension and the Z axis is shown in Figure 4.

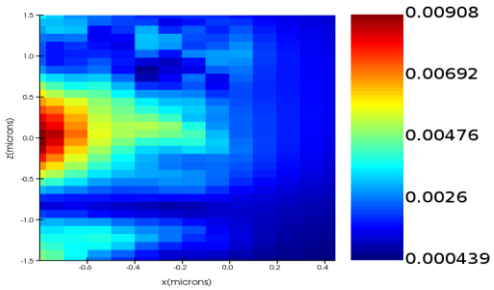

Figure 3: Intensity of magnetic field penetration inside inhomogeneous plasma in axial direction XZ.

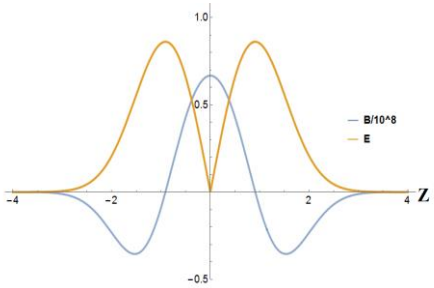

Figure 4: Diagram of 1D magnetic and electric fields in the direction of z.

As mentioned above, the considered plasma has a density index of the form 1 / x, so with the penetration of the Hermit-Cosh Gaussian beam into the inhomogeneous plasma; we will have phenomena such as reflection, transmission, absorption, and so on. Using equation 5, we see the behavior of the ponderomotive force in Figure 5, which changes periodically. The effect of the ponderomotive force is very small due to the weight of the ions, but high for the electrons, which have a lower mass.

Conclusion

The interaction of laser beams with plasma is important in many wave-particle phenomena. In this paper, we investigated the interaction of hermit-Cosh Gaussian beam with inhomogeneous plasma with variable density profile. We observed and compared the behavior of magnetic and electric fields. Because high power lasers in plasma cause nonlinear effects thus leads to ponderomotive force, the behavior of the resulting force was also examined. Of course, noticeable changes in plasma density can be expected due to the ponderomotive force, although we have overlooked these changes. Applications of ponderomotive force include the study of the motion of charged particles in self-focusing, trapping particles, etc. Simulations for this topic have been performed by using a FDTD method. In conclusion, for high intensity Gaussian laser-plasma interaction, we have

observed that the results from simulation are in good agreement with an analytic calculation employing.

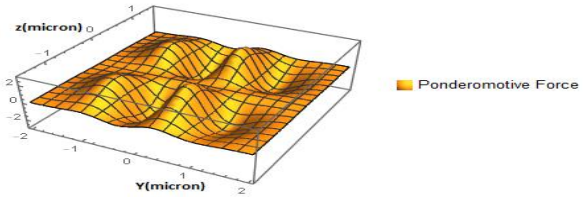

Figure 5: The ponderomotive Force in the direction of YZ.

References:

[1] Walia, Keshav, R. K. Verma, and Arvinder Singh. "Second harmonic generation of laser beam in quantum plasma under collective influence of relativistic-ponderomotive nonlinearities." Optik 225 (2021): 165745.
[2] Kant, Niti, Manzoor Ahmad Wani, and Asheel Kumar. "Self-focusing of Hermite–Gaussian laser beams in plasma under plasma density ramp." Optics Communications 285.21-22 (2012): 4483-4487.
[3] Walia, Keshav. "Nonlinear interaction of high power beam in weakly relativistic and ponderomotive cold quantum plasma." Optik 219 (2020): 165040.
[4] Shahrassai, L., S. Sobhanian, and H. Khosravi. "The Effect of Ponderomotive Force of a Laser Pulse on the Frequency Shift of its X-mode Propagation." AIP Conference Proceedings. Vol. 1400. No. 1. American Institute of Physics, 2011.
[5] Singh, Mamta, Krishna Gopal, and Devki Nandan Gupta. "Temporally asymmetric laser pulse for magnetic-field generation in plasmas." Physics Letters A 380.16 (2016): 1437-1441.
[6] García-Rubio, F., et al. "Magnetic-field generation and its effect on ablative Rayleigh–Taylor instability in diffusive ablation fronts." Physics of Plasmas 28.1 (2021): 012103.
[7] Alilou S., Shahrassai L. "NL Effects of Interaction Gaussian laser Beam with inhomogeneous and Nonrelativistic plasma and Calculation of the Waves Magnetic Field "26th Optics and Photonics Society of Iran - ICOP & ICPET (2020).
[8] Karimi, Ebrahim, et al. "Hypergeometric-gaussian modes." Optics letters 32.21 (2007).

FT4

A new approach to enhance the bandwidth value of UTC-PD

Gencal, H.* and Öztürk, T.

Electrical-Electronics Engineering, Bursa Technical University, Bursa, Turkey
huriyegencal@gmail.com

In this paper, the bandwidth (BW) value of uni-traveling-carrier photodiode (UTC-PD) is analyzed by changing inside structure in between absorber and collector. Previously published and designed UTC-PD structure is repeated to utilizing TCAD (Lumerical) simulator program. Two aspect illumination from x and z-axis is applied with inserted different types of materials to show the bandwidth performance of UTC-PD. By the proposed approach, which is quasi embedded waveguide, the BW value is enhanced. The aim is here to change the electric field and accelerate the electron velocity.

Keywords: optoelectronics, photonics, photodiode, terahertz, UTC-PD

Introduction

Terahertz (THz) waves are in the electromagnetic spectrum between 0.1-10 THz. With the development of applications such as radar, remote sensing, imaging, spectroscopy and wireless communication, the importance of THz waves has become more remarkable recently. To meet the demands of applications developed in the THz range, it is necessary to develop photodiodes, which are the important components of the system. Although the success performance of the photodiode varies according to the purpose of use and the application frequency range, its high power and speed are the two most basic parameters. The aim is to increase the output power and achieve the opportunity to work up to higher frequencies [1–5].

Extending the BW value of UTC-PD is interested by researchers since photodiodes are required for photonic integrated circuits (PICs) to use many applications such as communications, measurement spectroscopy, and remote sensing. There are two prime factors limiting the BW which are RC time constant and transit time. In conventional PIN-PD, the frequency response is dominated by transit time. To improve the response and reduce the transit time, the high field carrier velocity is required. In addition, to increase the photocurrent density space charge effect (SCE) is supressed. These solving suggestions was applied by a new PD structure which was invented in 1997 firstly. In this structure, only electrons are employed as traveling carriers through the collection layer. Since the electron's velocity is higher than the holes, high output and high speed can be achieved by new and novel structure [2–4,6–8].

In this study, a new design has been developed by changing the structure of UTC-PD, which can be operated at very high speeds. By adding an embedded material in the device between absorber and collector, the transit of the electrons is changed, and BW value is increased when compared to the repeated UTC-PD structure. To clarify the

understanding of embedded structure in UTC-PD, four different materials are used with different radius of circle. In addition, the illumination is applied from two different side to demonstrate the changing of BW value according to illumination aspect. It has been determined that it contributes to obtaining the BW value according to the size and shape of the embedded material as well as the material types.

Fundamentals of UTC-PD

Active region of UTC-PDs consists of two layers; one is the p-type InGaAs absorption layer and the other is the n-type doped InP collection layer. After the light is injected from bottom N-contact to device and passed on through the collector, it is absorbed by absorber as shown in Fig. 1. The collection layer is composed of InP which is wide energy gap material. The absorption layer is composed of InGaAs which is narrow energy gap material. The light is not really absorbed until it reaches the absorption layer. The hole and electron pairs are generated in absorber and carrier electrons are diffused and drifted through to collector. [2–4].

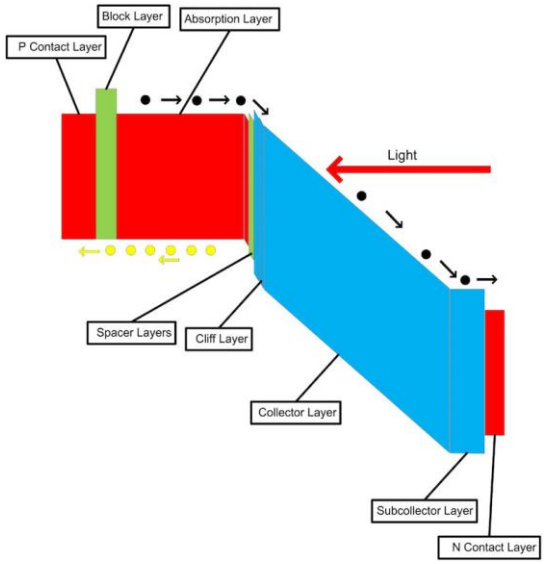

Figure 1. Energy band diagram of UTC-PD [3]

High speed and high output power photodiodes are needed as they are the main component for photonic integrated circuits (PICs). To reduce the space charge effect, achieve higher speed and power performance, UTC-PDs have been proposed as an alternative to traditional pin structure. UTC-PD has three important advantages different from PIN-PD. The first of these advantages is that it should have a high operating speed since the electrons behave as active carriers. The second important advantage is that UTC-PD has high saturation output due to less space charge effect in the depletion layer. Finally, low voltage operating capacity is another important advantage of UTC-PD. The high velocity of electrons can be maintained under a low electric field or by the electric field existing in the p-n junction itself. [2,9–12].

Design of UTC-PD by using Lumerical

The UTC-PD was designed by using Lumerical (Ansys) with its two modules which are FDTD and DEVICE. The Lumerical can be used for photonic integrated circuits (PICs) design, optical solvers, and device-level carrier transport. The FDTD module of Lumerical can give best solution for accurate simulation of photonic and optical structures. The DEVICE module of Lumerical is a multi-physics simulator for charge carrier transport and optical problems in semiconductor-based devices. Here, the FDTD module is required to obtain the optical generation ratio and it is used in DEVICE module to perform electrical analysis of device. Firstly, the UTC-PD with 1x1 μm2 device area existing in the literature is designed and bandwidth under 0V and -5V has been investigated to verify the outputs with reference device. The information given in the reference study was used to make the results comparable. The epitaxial layer structure of reference UTC-PD is given in Table I.

Table I. Epitaxial layer structure of the reference UTC-PD [3]

Layer	Material	Ban Gap (eV)	Thickness (nm)	Doping Level (cm^{-3})	Dopant Type
P Contact	InGaAs	0.73	50	3×10^{19}	p
Block	InGaAsP	0.85	20	2×10^{19}	p
Absorption	InGaAs	0.73	220	1×10^{18}	p
Spacer	InGaAs	0.73	8	1×10^{15}	undoped
Spacer	InGaAsP	1.00	16	1×10^{15}	undoped
Spacer	InP	1.35	6	1×10^{15}	undoped
Cliff	InP	1.35	7	1×10^{18}	n
Collector	InP	1.35	263	1×10^{16}	n
Sub-collector	InP	1.35	50	5×10^{18}	n
N Contact	InGaAs	0.73	10	1×10^{19}	n

The purpose here is to show the change in BW value by placing the circle material horizontally or vertically between the absorber (InGaAs material) and collector (InP material) and in the centre of device. The 3D structures of the UTC-PD designed by using DEVICE module of Lumerical are shown as seen in Fig. 2. To show the inserted circle material, the graphical rendering of absorber and collector was decreased.

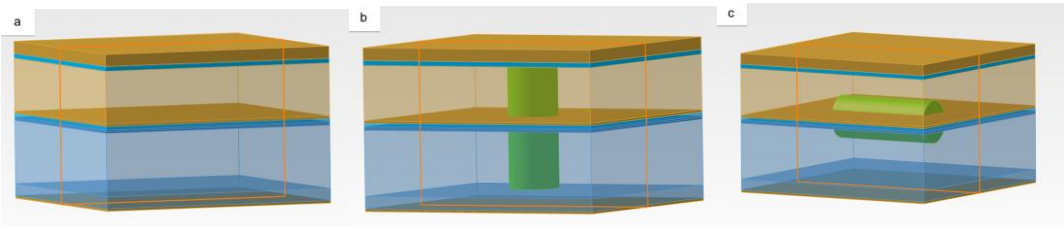

Figure 2. Designed UTC-PDs a) reference b) vertical c) horizontal

Results and Discussion

The main factors limiting the performance of a UTC-PD can be sorted as self-heating, RC charging time, carrier transit time, space charge effect. Increasing reverse bias will boost the effect of self-heating since the main Joule heat is equal to the product of the reverse biasing and the output photocurrent. Thus, a reduced active field size is typically required to achieve 3-dB bandwidth from DC to THz/sub-THz. However, this

may cause self-heating convenience in the optical coupling and thermal failure during high power operation. Therefore, a study has been carried out under zero-bias operation.

In reference UTC-PD, the EF in absorber is nearly zero and the block layer was used to prevent the electrons to pass towards p-contact layer. A cliff layer was used to boost the EF and simplify the transport of electrons between absorber and collector. To understand clearly structure of UTC-PD, the change of EF values for each design are viewed. The BW value has been obtained as 20 GHz for reference UTC-PD as shown in Fig. 3. This value is very small under zero-bias operation. In addition, the BW under 5V reverse bias is 32 GHz as demonstrated in the reference study.

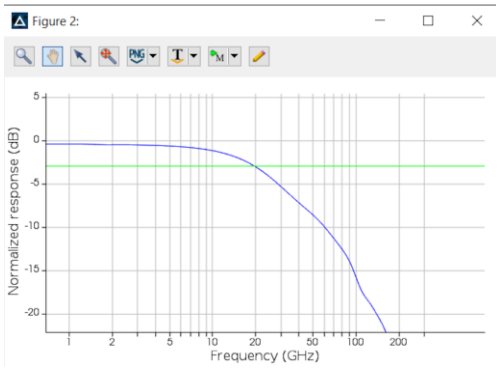

Figure 3. BW value for reference UTC-PD

To verify the BW value obtained by Lumerical Charger module, impulse and step responses are required as shown in Fig. 4.

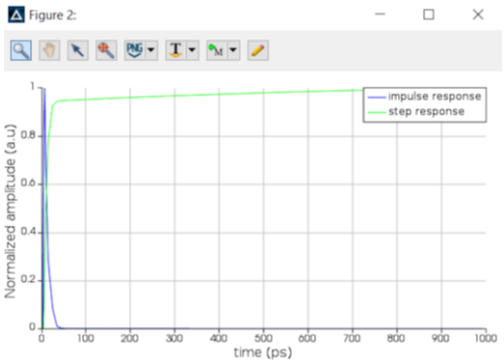

Figure 4. Impulse and step responses for reference UTC-PD

When an embedded structure is inserted between absorber and collector as quasi-waveguide, the BW value is increased as shown in Fig.5. The obtained value of BW is acceptable to use the designed device in THz frequency range.

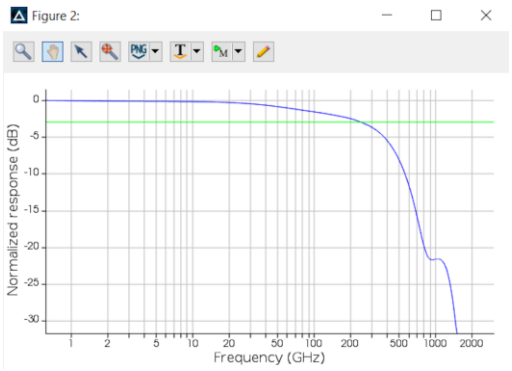

Figure 5. BW value for modified UTC-PD

The Au, Ag, Cu and Si materials were selected for embedded structure. And two illumination types were used to see the electron changes and acceleration in the structure of device. For two illumination directions and four different embedded materials, the results are summarized in Table II to show the contribution of embedded structure. The radius was selected between 50 and 250 nm as minimum and maximum value, respectively. As seen in table, the high value of BW was achieved when the radius value is 250 nm with z-direction (bottom side) illumination. In addition, when the material of embedded structure is selected as Au, this situation will be more convenient for BW and performance of UTC-PD compared to other materials.

Table II. Comparison of BW value for different materials and illumination directions

	BW value for x-direction illuminated (Horizontal structure) [GHz]				**BW value for z-direction illuminated (Vertical structure) [GHz]**			
Radius (nm)	Au	Ag	Cu	Si	Au	Ag	Cu	Si
50	33	28	31	22	38	31	27	28
100	50	45	50	30	37	28	28	27
150	81	48	48	39	32	34	28	29
200	53	63	58	50	58	42	39	36
240	94	78	59	54	102	51	43	35
250	83	67	55	55	239	46	48	41

When the obtained results are examined, it has been shown that the electron movement between the layers of UTC-PD modified can be changed with an embedded material and thus, BW value can be obtained at a high value to use the device in THz frequency range. The change can also be applied to other UTC-PD variants. According to results, at least a few times more of the BW value obtained with the published and produced designs can be obtained by proposed approach.

Conclusion

To increase the BW value, generally high reverse bias is applied, the device field surface is reduced, or the device is integrated with components such as waveguide/antenna. With this study, a new approach is proposed to increase the BW value of UTC-PD, and no changes are made in the 3-dimensional size of the device or in the device area. In addition, the UTC-PD is operated under zero bias that means no power consumption due to bias circuit and removing the self-heating effect. To obtain the best results, two different illumination direction and four different materials as embedded waveguide are tried to achieve the high-level BW value. According to results Au material should be selected to produce the UTC-PD and the light should be applied from z-direction (bottom side).

References:

[1] Duan N, Liow T-Y, Lim AE-J, Ding L, Lo GQ. 310 GHz gain-bandwidth product Ge/Si avalanche photodetector for 1550 nm light detection. Opt Express 2012;20:11031. https://doi.org/10.1364/oe.20.011031.
[2] Ishibashi T, Ito H. Uni-traveling-carrier photodiodes. J Appl Phys 2020;127. https://doi.org/10.1063/1.5128444.
[3] Xu J, Zhang X, Kishk A. Design of high speed InGaAs/InP one-sided junction photodiodes with low junction capacitance. Opt Commun 2019;437:321–9. https://doi.org/10.1016/j.optcom.2018.12.085.
[4] Xu J, Zhang X, Kishk A. Design of modified InGaAs/InP one-sided junction photodiodes with improved response at high light intensity. Appl Opt 2018;57:9365. https://doi.org/10.1364/ao.57.009365.
[5] Xu J, Zhang X, Kishk A. Numerical Study of the Evanescently Coupled One-Sided Junction Waveguide Photodiode. Proc Int Conf Numer Simul Optoelectron Devices, NUSOD 2019;2019-July:103–4. https://doi.org/10.1109/NUSOD.2019.8806990.
[6] Ishibashi T, Kodama S, Shimizu N, Furuta T. High-Speed Response of Uni-Traveling-Carrier Photodiodes. Jpn J Appl Phys 1997;36:6263–8. https://doi.org/10.1143/JJAP.36.6263.
[7] Xie S, Liu LS, Kang WP, Song RL, Mao LH, Zhang SL. Theoretical analysis and simulation of InP-based uni-traveling-carrier photodetector. Chinese Sci Bull 2009;54:3691–6. https://doi.org/10.1007/s11434-009-0394-x.
[8] Photodiodes U, Ishibashi T, Shimizu N, Kodama S, Ito H, Nagatsuma T, et al. Uni-Traveling-Carrier Photodiodes 1997;13. https://doi.org/10.1364/UEO.1997.UC3.
[9] Natrella M, Liu C-P, Graham C, van Dijk F, Liu H, Renaud CC, et al. Modelling and measurement of the absolute level of power radiated by antenna integrated THz UTC photodiodes. Opt Express 2016;24:11793. https://doi.org/10.1364/oe.24.011793.
[10] Xu J, Zhang X, Kishk A. InGaAs/InP evanescently coupled one-sided junction waveguide photodiode design. Opt Quantum Electron 2020;52. https://doi.org/10.1007/s11082-020-02392-8.
[11] Ito H, Furuta T, Kodama S, Ishibashi T. InP/InGaAs uni-travelling-carrier photodiode with 310 GHz bandwidth. Electron Lett 2000;36:1809. https://doi.org/10.1049/el:20001274.
[12] Ito H, Furuta T, Kodama S, Watanabe S, Ishibashi T. InP/InGaAs uni-travelling-carrier photodiode with 220GHz bandwidth. Electron Lett 1999;35:1556–7. https://doi.org/10.1049/el.

FT5

Investigation of structural properties of Bromineazocalix [4] arene molecule using DFT method

Bayrakdar, A.

Vocational School of Higher Education for Healthcare Services, Igdır University, Igdır 76100, Turkey
alpaslan.bayrakdar@igdir.edu.tr

In this study, Bromineazocalix[4]aren (BrPcalix) compound from Calix[*n*]arene family, which has a cyclic structure and is known for its ability to carry and complex organic molecules, anions and metal cations, was investigated theoretically. First, the theoretical modeling of the BrPcalix compound was made, then its structural parameters properties were investigated with the help of Density Functional Theory (DFT). The molecular structure corresponding to the most stable state of BrPcalix [4] was optimized by using the DFT/B3LYP/ 6-311G (d,p) basis set to theoretically elucidate the structural and electronic properties of the title compound.

Spectroscopic properties of the compound were investigated theoretically using the parameters of the optimized structure. The IR frequency values of BrPcalix [4] were calculated with same method and the values found were multiplied by certain scaling factors. Finally, relationships between experimental and theoretical spectroscopic data were calculated. In this study, it was revealed that experimental and theoretical studies are very compatible with each other.

Keywords: DFT, Calixaren, Spectroscopy, IR

Introduction

Development of options that can be used at the receptor position that will provide highly effective molecular recognition and selection functions are very important steps, especially for biological and chemical-based studies [1-3]. Calixaren families are popular and prominent receptors in this field due to their fascinating chemical and physical properties [4]. The Calixarenes are compounds belonging to the cavitands class, which are well known in host–guest chemistry and have the ability to hold ions and smaller molecules with the help of their hydrophobic spaces. The Calixarenes, under the influence of groups on the upper edge, the hydroxyl groups on the lower edge approach each other and strengthen the hydrogen bonds formed by the lower edge OH groups [5].

On the other hand, as a result of the recent developments in the field of computational chemistry, Density Functional Theory (DFT) has started to be used very actively for new biological and chemical based designs [6]. In this study, BrPcalix compound, one of the azocalixarenes containing brominated structure on the upper edges, was investigated theoretically using the DFT/B3LYP/6-311 G(d,p) basis set.

Vibration spectroscopy is one of the most effective methods used to examine the molecular structure of a compound and the functional groups it contains [7]. Also, Vibration spectroscopy is widely used in the investigation of hydrogen bonds in the structure of compounds [8, 9].
In this study, the properties of hydrogen bonds formed at the lower edge of the structure by bromine atoms added to the upper edge of the Azocalix*[4]* are with the help of IR spectroscopy were investigated. On the other hand, with the HNMR study, the molecular structure of the title compound was determined theoretically using DFT/B3LYP and 6-311 G(d,p) basis set.
In the theoretical investigation with Dft, it was determined that four hydrogen bonds were formed between O33—H34...O38, O38—H75...O36, O36—H37...O35 and O35—H76...O33 atoms. The presence of these hydrogen bonds has been observed even in the experimental IR spectrum.

Experimental Part
In this study, vibrational frequencies of the title compounds were measured using FT-IR spectroscopy. The FT-IR spectrum is recorded with a Perkin-Elmer 2000 FT-IR spectrophotometer in the 4000-400 cm^{-1} range.

Computational procedure
The BrPcalix compound was optimized with DFT/B3LYP level and 6-311 G (d, p) basis set to determine the most stable geometry of the molecule, which will form the basis of theoretical studies on the molecule. An open source licensed Avogadro molecular visualition program was used to visually examine the hydrogen bonds formed in the optimized structure [10].

The vibration frequency analysis of the BrPcalix molecule was theoretically performed in gas phase with the help of Gaussian09W software. Since the compound contains 104 atoms in its structure, the 6–311G(d,p) basis set was chosen in the theoretical study because it is one of the most optimum basis sets as calculation cost. In this theoretical study, all calculations were made in gas phase by means of Gaussian G09W program.

Results and discussion
The optimization process and vibration frequency analysis of the BrPcalix molecule were carried out theoretically. It was determined that four hydrogen bonds were formed between the atoms O33—H34···O38, O38—H75···O36, O36—H37···O35 and O35—H76···O33 in the structure of BrPcalix. The optimized structure of the molecule mentioned in the title and the hydrogen bonds formed are shown in Figure 1. The bond length and bond angles of these hydrogen bonds are given in Table 1. The IR data calculated in the next step was compared with the experimental IR data.

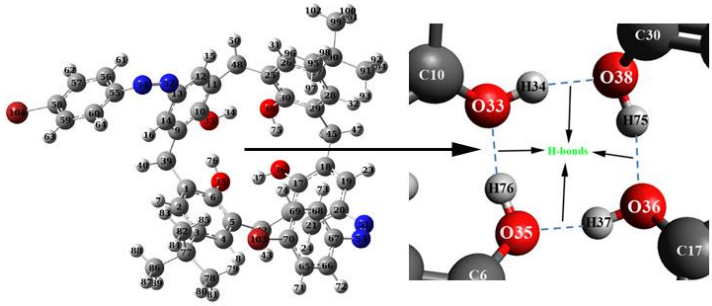

Figure 1. Calculated optimized structure and Hydrogen bonds of the BrPcalix molecule.

Table 1. Hydrogen-bond geometry (Å,º) of the title compounds in the ground state.

	BrPCalix			
D—H···A	**D-H·**	**H···A**	**D···A**	**D-H···A˚**
O33—H34···O38	0.99	1.70	2.658	162
O38—H75···O36	0.98	1.71	2.663	162
O36—H37···O35	0.99	1.66	2.623	163
O35—H76···O33	0.98	1.73	2.679	162

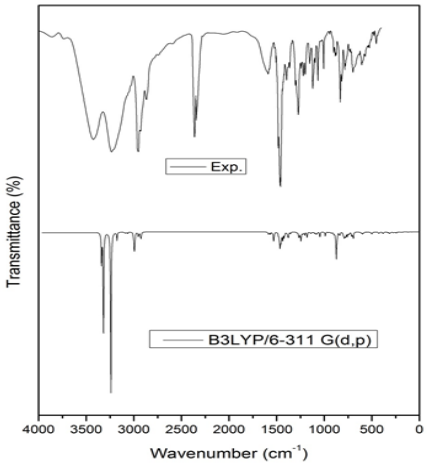

Figure 2. Experimental and theoretical wavenumber of the title compound by using DFT/B3LYP with the 6–311G(d,p) basis set.

Theoretically, the studies are carried out in the gas phase, so a discrepancy occurs with experimental studies with solid phases. To compensate for this mismatch, the calculated frequencies are scaled with a coefficient called the scaling factor. This scaling factor is different for each set of bases. All calculated wavenumbers are scaled with 0.9617 for the 6-311G(d,p) basis set. Correlation R^2 value between calculated and experimental wavenumbers values for the title molecule was found to be 0.9996 for the B3LYP/6-311G(d,p) basis set. The results are quite compatible with each other. The broad OH peak in the experimental IR spectrum indicates that there is hydrogen bond in the molecular structure.

Conclusion

In this article, it was determined in the theoretical study that four hydrogen bonds were formed between OH groups at the lower edge of the BrPcalix molecule. The presence of these hydrogen bonds has also been observed in the experimental IR spectrum with a broad OH peak. The correlation study revealed that the DFT/B3LYP level amd 6-311 G(d,p) basis set is compatible with the experimental study. According to this result, it is quite clear that the DFT method can make a prediction for the experimental studies to be carried out for the calixaren molecule containing a large number of atoms.

References:

[1] R.P. Haugland, The handbook: a guide to fluorescent probes and labeling technologies, Univerza v Ljubljani, Fakulteta za farmacijo, 2005.
[2] S.K. Kim, J.K. Lee, S.H. Lee, M.S. Lim, S.W. Lee, W. Sim, J.S. Kim, Silver ion shuttling in the Trimer-Mimic thiacalix [4] crown tube, The Journal of organic chemistry 69(8) (2004) 2877-2880.
[3] S.E. Matthews, P.D. Beer, Calixarene-based anion receptors, Supramolecular Chemistry 17(6) (2005) 411-435.
[4] C.D. Gutsche, Calixarenes: an introduction, Royal Society of Chemistry2008.
[5] V. Furer, L. Potapova, D. Chachkov, I. Vatsouro, V. Kovalev, E. Shokova, V. Kovalenko, Study of p-(3-carboxy-1-adamantyl)-calix [4] arene with hydrogen bonds along the upper and lower rim by IR spectroscopy and DFT, Journal of molecular modeling 26(7) (2020) 1-7.
[6] D. Sholl, J.A. Steckel, Density functional theory: a practical introduction, John Wiley & Sons2011.
[7] P. Larkin, Infrared and Raman spectroscopy: principles and spectral interpretation Elsevier, San Diego (2011).
[8] V. Furer, L. Potapova, I. Vatsouro, V. Kovalev, E. Shokova, V. Kovalenko, Study of conformation and hydrogen bonds in the p-1-adamantylcalix [8] arene by IR spectroscopy and DFT, Journal of Inclusion Phenomena and Macrocyclic Chemistry 95(1) (2019) 63-71.
[9] V. Furer, A. Vandyukov, A. Khamatgalimov, S. Kleshnina, S. Solovieva, I. Antipin, V. Kovalenko, Investigation of hydrogen bonding in p-sulfonatocalix [4] arene and its thermal stability by vibrational spectroscopy, Journal of Molecular Structure 1195 (2019) 403-410.
[10] M.D. Hanwell, D.E. Curtis, D.C. Lonie, T. Vandermeersch, E. Zurek, G.R. Hutchison, Avogadro: an advanced semantic chemical editor, visualization, and analysis platform, Journal of cheminformatics 4(1) (2012) 1-17.

AUTHOR INDEX

Author's Name	Abstract No
Aghamaliyev, Z.A.	S45
Akçay, N.	S2, S4
Akimova, Y.	S24
Akın, B.	S9
Akın Sönmez, N.	S46, S48
Akkaya Kömürcü H.	S46
Akman Latif, B.	S55
Aksoy, E.	S18
Ajjel, R.	IS19
Alaeian, H.	IS22
Alilou, S.	S39, FT3
Allahyarova, S.Y.	S57
Alosmanov, R.M.	S57
Alonso, M.	PS6
Altındal, Ş.	S5, S11
Amenitsch, H.	S10, S13
Amiri, P.	S36, S38, S40
Amirov, M.	S19, FT2
Amor, F.B.	IS19
Andreani, L.C.	S8
Arenal, R.	IS20
Asar, T.	S47
Aslanova, A.R.	S1, S3
Ataşer, T.	S47
Ateş, H.	S56
Aydınoğlu, H.S.	S42, S44, S50, S52
Azizov, A.A.	S57
Azizian-Kalandaragh, Y.	S34, S36, S38, S40, S48
Babayeva, R.F.	S3
Balas, C.	IS1
Badali, Y.	S5
Balayeva, O.O.	S45, S57
Balci, E.	S54
Baldini, L.	S15
Baraldi, A.	IS27
Başköse Ü., C.	S55
Bayrakdar, A.	S33, FT5
Bek, A.	S17
Bharti, A.	IS17
Booth, M.J.	IS3
Borelli, C.	IS27
Bosi, M.	IS27, S15
Bosio, A.	IS27
Bowen, W.	IS26
Bozkurt, H.	S16
Bretsko, M.	S24
Buono, W.T.	S28
Can, M. M.	S37
Ceylan, C.	S35
Chao, Yu-Faye	IS2
Chávez-Cerda, S.	IS8
Chormaic, S.N.	PS9

Author's Name	Abstract No
Coşkun, A.	IS29
Cömert Sertel, B.	S55
Çakır, S.	S29
Çakmak, B.	IS29
Çağlayan, H.	IS12
Çelebi, C.	S7
Çınar, K.	S17
Danos, A.	S18
Degani, M.	IS13, S8
Demirci Dönmez, Ç.E.	S41
Diker, H.	S16
Dönmez Kaya, M.	S55
Du, J.	S54
Dudley, A.	S26, S28
Efkere, H.İ.	S55
Efimova, A.I.	IS7
Ekicibil, A.	S44
Elagöz, S.	IS10
Elamen, H.	S5
Eliceiri, K.	PS10
Elizade, M.T.	S15
Emadoleslami, A.	S38
Erbilen Tanrıkulu, E.	S9
Erenler, B.	S56
Eyvazova, G.M.	S43, S45
Ferrari, C.	IS27, S15
Fidan, M.	S7
Forbes, A.	PS1, S26, S28, S30, S32
Fornari, R.	IS27
Francesco, R.	S15
Francesco, S.	S15
Frigeri, C.	S15
Fuerbach, A.	IS25
Gahramanli, L.	S43, S57
Gahramanova, G.K.	S21
Gencal, H.	S49
Girella, A.	S8
Gollas, B.	S13
Golovan, L.A.	IS7
Gorbachenya, K.N.	IS30, S58
Gözlekçi, G.	S48, S55
Grancini, G.	S8
Gremenok, V.F.	S2, S4
Güneşer, M.T.	S5
Guretskii, S.A.	S58
Güldüren, Z.E.	IS29
Gümüşay, Y.M.	S55
Hamdaoui, N.	IS19
Hashemi, Z.	S40
Hopoğlu, H.	S42, S50, S52
Jabbarov, R.B.	S21
Karpinsky, D.V.	S58

Author's Name	Abstract No
Kasumova, R.J.	S19, S23, FT2
Kaya, D.	S44
Kerimli, N.V.	S23
Kheradmand, R.	S27
Khodayari, A.	S31
Khoroshko, V.V.	S4
Kisel, V.E.	IS30, S58
Kılıçerkan Başlar, G.	S30
Klokic, S.	S10
Konrad, T.	S32
Koppens, F.	IS16
Korkut, C.	S17
Kotlyar, V.V.	PS4, FT1
Kovalev, A.A.	PS4, FT1
Koç, E.	S14
Koçak, Ç.	S41
Koçak, F.	S47
Koçal, E.B.	S53
Kuleshov, N.V.	IS30, S58
Kurt, H.	S6
Lotfi, F.	S27
Lubochko, N.A.	S58
Mamedov, R.K.	S1, S3
Mammadova, S.F.	S57
Mammadyarova, S.J.	S45
Mamuk, A.E.	S41
Marmiroli, B.	IS17, S10
Martineau, D.	S8
Mashayekhi, H.R.	S36, S38, S40
Mazzolini, P.	IS27
Mezzadri, F.	IS27
Milanese, C.	S8
Missous, M.	PS5
Monkman, A.P.	S18
Moodley, Ch.S.	S30
Mosca, R.	IS27
Moser, D.	S13
Muradov, M.B.	IS24, S43, S45, S57
Musayeva, N.N.	S15
Mutlugün, E.	S20
Nape, I.	S26
Naumenko, D.	S10
Nourani, F.	S34
Olivier, J.F.M.	PS7
Onur, A.	S12
Orujov, T.Y.	S21
Osminkina, L.A.	IS7
Özbay, E.	PS2
Özçelik, S.	S16
Özçelik, S.	S2, S4, S46, S48, S55, S56, S58
Özdür, İ.T.	S14, S25
Özen, Y.	S58

Author's Name	Abstract No
Özer, A.	S52
Özgüler, Ş.	S16
Öztürk, T.	S49, FT4
Panigrahi, P.K.	IS28
Paolo, F.	S10
Parisini, A.	IS27
Pavesi, M.	IS27
Pica, G.	S8
Poelman, D.	S54
Predojevic, A.	IS9
Presnov, D.E.	IS7
Pyatlitski, A.N.	S2, S4
Quluzade, S.A.	S15
Rashid-Farrokhian, N.	S36
Razeghi, M.	PS3
Rodríguez-Fajardo, V.	S30
Roux, F.S.	S32
Rudenkov, A.S.	IS30
Saber, A.	S34
Sağlam, N.	S29
Sağlam, S.	S22
Sanchez, B.O.	IS14
Sang-Nourpour, N.	S27
Sartori, B.	IS17
Schileo, G.	S8
Selimoğlu, Ö.	S22
Sephton, B.C.	S30, S32
Seravalli, L.	IS27
Shahrassai, L.	S39, FT3
Shastri, B.J.	IS6
Sherwani, A.R.	S37
Singh, K.	S26, S28
Sobhanan, A.	IS11
Sohrabnezhad, Sh.	S31
Staskov, N.I.	S2
Steinlechner, F.	S32
Swanson, A.	IS31
Şenadım Tüzemen, E.	S42, S44, S50, S52
Şirin, Ş.	S51
Tagiev, Z.H.	S19, FT2
Tanyeli, B.	S22
Timoshenko, V.Yu.	IS7
Torres, J.P.	S32
Trevisi, G.	S15
Tserkezis, Ch.	IS4
Turan, R.	IS23
Turchet, A.	IS17
Turgut, G.	IS29
Türkmen, M.	S12
Ulusoy, M.	S11
Ustinov, A.S.	IS7
Ünlütürk, S.S.	S16

Author's Name	Abstract No
Ünverdi, Ö.	S7
Vallés, A.	S32
Varlıklı, C.	IS5, S16, S18
Venkitesh, D.	IS11
Volyar, A.V.	IS15
Wang, J.	PS8
Wieser, P.A.	S13
Yağlıoğlu, H.G.	IS21
Yahya, M.F.O.	S47
Yakuphanoğlu, F.	IS18
Yergin, H.	S25
Yüksel Aldoğan, K.	S51, S53
Zabotnov, S.V.	IS7